



Republic of Iraq

Ministry of Higher Education and Scientific Research

University of Misan/College of Engineering

The Department of

Civil Engineering

**BEHAVIOR OF STEEL FIBER REINFORCED
CONCRETE (SFRC) SLABS WITH OPENINGS**

BY

Murtadha Diffar Abdulridha

B.Sc. in Civil Engineering, 2014

A thesis submitted in partial fulfillment
of the requirements for the Master of Science
degree in Civil Engineering

The University of Misan

May 2021

Thesis Supervisor

Assist. Prof. Dr. Samir Mohammed Chassib

بِسْمِ اللَّهِ الرَّحْمَنِ الرَّحِيمِ

اللَّهُ نُورُ السَّمَاوَاتِ وَالْأَرْضِ مِثْلُ نُورِهِ

كَمِشْكَاتٍ فِيهَا مِصْبَاحٌ الْمِصْبَاحُ فِي زُجَاجَةٍ الزُّجَاجَةُ

كَأَنَّهَا كَوْكَبٌ دُرِّيٌّ يُوقَدُ مِنْ شَجَرَةٍ مُبَارَكَةٍ زَيْتُونَةٍ لَا شَرْقِيَّةٍ وَلَا غَرْبِيَّةٍ

يَكَادُ زَيْتُهَا يُضِيءُ وَلَوْ لَمْ تَمْسَسْهُ نَارٌ نُورٌ عَلَى نُورٍ يَهْدِي

اللَّهُ لِنُورِهِ مَنْ يَشَاءُ وَيَضْرِبُ اللَّهُ الْأَمْثَالَ لِلنَّاسِ

وَاللَّهُ بِكُلِّ شَيْءٍ عَلِيمٌ

صدق الله العلي العظيم

DEDICATION

❖ I dedicate this work to the spirit of my father, who sacrificed himself for the sake of the nation. I ask God to dwell in paradise.

❖ To whom stood beside me and took care of me over the years,
to my sister,
my brother,
my wife
and close friends

ACKNOWLEDGEMENTS

First of all, all my thanks for Allah who led me during my way to complete this work.

I would like to express my sincere thanks, gratitude and appreciation to my Imam and great teacher AL-Hujjahu Ibn AL-Hassan (Aajal Allah Farajah AL-Sharif).

I would like to express my cordial thanks and deepest gratitude to my supervisor Asst. Prof. Dr. Samir Mohamed Chassib, whom I had the honor of being under his supervision, for his advice, help, and encouragement during the course of this study.

I would like to extend my thanks to Prof. Dr. Abbas Oda Dawood dean of the college of engineering, and Asst . Prof. Dr. Samir Mohamed Chassib, the Head of Civil Engineering Department.

I would like to express my thanks to Prof. Dr. Ahmad Khadim Al-Shara, Dr. Nasir hakeem, Dr. Hayder AL-Khazraji , Prof. Dr. Abdulkhaliq A. Jaafer Prof. Dr.saad Fahad , Dr. Fatin. Mussa and all the staffs of the Laboratory Concrete of the Technical Institute of Amara their technical support throughout the experimental program.

Special thanks also go to Dr.Hassn Bssel, Dr.Ghazwan and Assist lect. Abufadhel Munther and my friends in the master's stage and Mustafa Oda to help them in this work.

Special thanks go to, mother, my brother, my sister , and children's for their great efforts.

Special thanks and gratitude to my wife,for their care of it patience and encouragement ,throughout the research period.

Murtadha Difaar Abdulridha
2021

CERTIFICATION

I certify that the thesis titled (*Behavior of Steel Fiber Reinforced Concrete (SFRC) Slabs With Openings*) which is being submitted by **Murtadha Difaar Abdulridha** and prepared under my supervision at the University of Misan, Department of Civil Engineering, in partial fulfillment of the requirements for the Degree of Master of Science in Civil Engineering (Structures).

Signature:

Assist. Prof. Dr. Samir M. Chassib

Date:

In view of the available recommendations, I forward this thesis for discussion by the examining committee.

Signature:

Assist. Prof. Dr. Samir M. Chassib

(Head of Civil Eng. Department)

Date:

EXAMINING COMMITTEE'S REPORT

We certify that we, examining committee, have read this thesis titled *(Behavior of Steel Fiber Reinforced Concrete (SFRC) Slabs With Openings)* which is being submitted by **(Murtadha Difaar Abdulridha)** , and as Examining Committee, examined the student in its contents. In our opinion, the thesis is adequate for award of degree of Master of Science in Civil Engineering.

Signature:

Name: **Assist.Prof. Dr.Samir M .Chassib**
(Supervisor)

Signature:

Name: **Assist. Prof. Dr.Hayder Al Khazraji**
(Member)

Signature:

Name: **Assist. Prof. Dr. Ahmed A. Hassen**
(Member)

Signature:

Name: **Prof. Dr. Saad F. Rasan**
(Chairman)

Approval of the College of Engineering

Signature:

Name: **Prof. Dr. Abbas O. Dawood**
Dean, College of Engineering

ABSTRACT

One of the major requirements for strengthening or upgrading existing reinforced concrete structures is to increase their members' capacities to withstand larger expected loads. There are different techniques to increase existing slab capacities; however, such techniques differ in advantages and disadvantages. The main objective of the study is to investigate the efficiency of steel fibers reinforced concrete flat with openings near support. The main variables considered in the experimental study were steel fibers ratio, opening location, opening shape, location of the opening. Increase of hooked steel fiber ratio (0.5, 1, 1.5, and 2%) and effect of openings affect the load carrying capacity for both punching shear and flexural slabs. Regarding the punching shear flat slabs, the opening existence redistribute the stresses which show concentration in the corners of the opening and around the middle column. The openings existence affected the cracking load which decreased by (47.4%) which the cracks appeared at (27.3%) in the control solid slab when it decreased (13%) the group (A1), it contains the ratio steel fiber 1%, ($f_c=81.4$ MPa) and two openings near corner slab. Regarding the shape of the openings, the effect of the shapes of openings was not significant because of the locations of the openings which is far from the critical region. Concerning the openings' location and numbers, the effect of these two variables is the most effect on the general behavior of the concrete slab specially on the deflection. Group (A3), it contains the ratio steel fiber 2% ($f_c=91.7$ MPa), fabricated with four openings revealed a maximum displacement and load which was higher than the control slab by (61.42% and 11.1) respectively. The increment in the displacement seemed significant with fabrication of more openings which the difference between the two openings slabs (group A1) and four openings slab (group A3) is quite simply a slight difference in strength and a high difference in displacement. Concerning the slabs that included increase of the steel fibers from (0.5%) to (2%), which exposed compensation in the occurred loss on the stiffness, ductility, energy absorption and ultimate load.

Regarding the flexural specimens, the flexural behavior affected by use of steel fibers with several ratio and with existence of openings. The influence of openings existence was seemed on the behavior but this effect ranged from medium to high according the location and number of openings. The load at cracking stage appeared at (30.5%) approximately which raised to (88%) after increasing the steel fibers with making openings near corner slab (group B1) it contains the ratio steel fiber 1%, ($f_c=81.4$ MPa). Flexural strength of the slab specimens that fabricat with openings was higher than the solid one because of the steel fibers presence which these fibers recover the strength loss due to the presence of the openings. The difference between the opening's shapes in term of the load and deflection was not large due to the small size of the opening beside the location which placed far from the critical region. Concerning the openings' location and numbers, the effect of these two variables is the most effect on the flexural behavior of the concrete slab. Group (B3) fabricated with four openings and steel fibers of (2%). Ultimate load was obtained by (280) kN, which is higher than (61.5%) and deflected by (67%) higher than the control slab. The increment in steel fibers ratio from (0.5% to 2%), compensated the expected strength loss due to the openings existence and gained additional strength enhancement. More of steel fibers repay the happened loss with achieving of more upgrade in the flexural capacity. It should be noted that the variance in the shape of the openings has a small effect on the flexural capacity which was by (43.4%) but affect the displacement significantly. The most affect parameter is the number and location of openings which transmitting the two openings to the middle zone of the slab reduced the cracking load with average of (35.5%).

TABLE OF CONTENTS

TABLE OF CONTENTS	VIII
LIST OF TABLES	XII
LIST OF FIGURES.....	XIII
LIST OF SYMBOLS	XVI
LIST OF ABBREVIATIONS	XVII
CHAPTER ONE INTRODUCTION	1
1.1 General	1
1.2 Advantages and disadvantages of flat slab system	2
1.3 Punching shear failure.....	5
1.4 Flexural failure of flat slab.....	9
1.5 Slab with openings	9
1.6 Steel fiber-reinforced concrete.....	11
1.7 Objectives of research.....	14
1.8 Thesis layout	15
CHAPTER TWO LITERATURE REVIEW	16
2.1 General	16
2.2 Punching shear failure in slabs	16
2.3 Previous studies of flexural slabs.....	30
2.4 General summary and conclusion	38
CHAPTER THREE EXPERIMENTAL WORK.....	39
3.1 General	39
3.2 Details of two-way reinforced concrete slabs (Group A):.....	39
3.3 Details of two-way reinforced concrete slabs (Group B):	40
3.4 Test Variables.....	46
3.4.1 Volume fraction of fibers (V_f)	46

3.4.2 Openings shape	46
3.4.3. Opening size.....	46
3.4.4 Opening Location.....	46
3.5 Materials.....	46
3.5.1 Cement.....	47
3.5.2 Fine aggregate (Sand)	48
3.5.3 Coarse aggregate	50
3.5.4 Hooked-end steel wire fiber.....	51
3.5.5 Mixing water	53
3.5.6 Superplasticizer	53
3.5.7 Silica fume.....	54
3.5.8 Steel reinforcement	56
3.6 Control specimens	58
3.7 Molds.....	58
3.8 Concrete mix design.....	59
3.9 Mixing procedure	60
3.10 Casting procedure.....	61
3.11 Curing procedure.....	63
3.12 Tests on concrete mixture	64
3.12.1 Fresh concrete tests (Slump Test)	64
3.12.2 Hardened mechanical.....	65
3.12.2.1 Compressive strength	65
3.12.2.2 Splitting tensile strength (f_{sp}).....	66
3.12.2.3 Modulus of rupture (f_r).....	67
3.12.2.4 Static modulus of elasticity (E_c).....	68
3.13 Test Measurement and instrumentation	69
3.13.1 Load measurement	69
3.13.2 Support and loading conditions.....	70
3.13.3 Deflection measurement.....	72

3.13.4 Crack width measurement.....	72
3.14 Testing procedure	73
CHAPTER FOUR RESULTS AND DISSCUSION.....	76
4.1 General.....	76
4.2 Testing Slab Specimens under Monotonic Loads.....	76
4.3 Test Results	77
4.3.1 Series A (Punching Shear Models)	77
4.3.2 Load-Displacement Relationship	77
4.3.3 Openings Influence of on the Punching Shear Capacity	79
4.3.4 Influence of Steel Fibers	82
4.3.5 Number and Location of the Openings.....	83
4.3.6 Analyzed Slab Stiffness	86
4.3.7 Anlyzed Slabs Ductility	89
4.3.8 Analyzed slab Energy Absorption Index	92
4.3.9 Failure Mode and Crack width.....	95
4.4 Analyzing and Results Discussion	99
4.4.1 Flexural Models Results.....	99
4.4.2 Load-Displacement Relationship	99
4.4.3 Influence of Opening on the Flexural Behavior.....	101
4.4.4 Effect of Steel Fibers.....	104
4.4.5 Location and Numbers of the Openings	105
4.4.6 Stiffness of the Flexural Slabs.....	107
4.4.7 Ductility of theTested Slabs	110
4.4.8 Energy Absorption	112
4.4.9 Failure Mode and Crack Width.....	114
4.5 Effect of Steel Fibers.....	117
4.6 The Impact of Opening	118
4.7 The Openings' Location, Shape, and Number	119

CHAPTER FIVE CONCLUSIONS AND RECOMMENDATIONS.....	120
5.1 Conclusions.....	120
5.2 Recommendation for Future Works.....	121
Reference.....	122
Appendix –A :Data Sheets of Steel Fiber	
Appendix –B :Data Sheets of Superplastizer and Silica Fume	
Appendix –C : Design of Solid Slab	

LIST OF TABLES

Table 3.1 Details of slabs specimens group A.....	41
Table 3.2 Details of slabs specimens group B.....	43
Table 3.3 Chemical analysis of cement.....	47
Table 3.4 Main compounds (Bogue's equation) cement.....	47
Table 3.5 Physical properties of the cement.....	48
Table 3.6 Grading of the fine aggregate.....	49
Table 3.7 Physical properties of fine aggregate.....	49
Table 3.8 Grading of coarse aggregate.....	50
Table 3.9 Properties of coarse aggregate.....	50
Table 3.10 Properties of steel fibers.....	52
Table 3.11 Properties of superplasticizers (Sika ViscoCrete – 5930).....	54
Table 3.12 Physical composition of silica fume.....	55
Table 3.13 Chemical composition of silica fume.....	56
Table 3.14 Properties of steel reinforcement.....	57
Table 3.15 Details of control specimens.....	58
Table 3.16 Properties of different types of SFRC mixes.....	60
Table 3.17 Results of slump test results of various types of SFRC mix.....	64
Table 3.18 Average compressive results of various types of SFRC mix.....	65
Table 3.19 Average splitting results of various types of SFRC mix	66
Table 3.20 Average flexural results of various types of SFRC mix.....	67
Table 3.21 Average modulus of elasticity of various types SFRC mix.....	69
Table 4.1 Test results of punching shear series.....	78
Table 4.2 Crack width, failure angle, and failure area of punching models.....	96
Table 4.3 Test results of flexural series group B.....	100
Table 4.4 Crack width at the cracking and ultimate load of series two.....	115

LIST OF FIGURES

Fig 1.1 Analysis of punching shear mechanism (Halvonik& Fillo ,2013).....	4
Fig 1.2 Type of shear failure in flat slabs.....	6
Fig 1.3 Effect of flexural reinforcement on the punching shear (Ruiz, 2013).....	7
Fig 1.4 Different types of punching failure (Krüger,1999).....	8
Fig 1.5 Suggested opening size and location in flat slab (ACI318-14).....	11
Fig 1.6 Steel fiber reinforced concrete column(Atlantis,2021).....	13
Fig 1.7 Stress-strain curves for steel fiber reinforced (Muslim,2016).....	14
Fig 2.1 Failure shape and crack pattern of RC slabs (Hoang ,2011).....	19
Fig 2.2 Test details before and after the failure (Gouvia et al,2014).....	20
Fig 2.3 Crack pattern and failure mode of each specimen (Ha et al , 2015.....	21
Fig 2.4 Crack pattern after the failure of the slab (Silva et al,2017).....	23
Fig 2.5 Test setup : top and side view (Musse et al,2018).....	24
Fig 2.6 Crack pattern and failure mode the slab (Ismail,2018).....	25
Fig 2.7 Crack pattern and failure mode of tested slab (Liberti et al,2019).....	26
Fig 2.8 Crack pattern of the test slab (Abdel-Rahman et al,2019).....	27
Fig 2.9 Failure crack of test slab (Schmidt et al., 2020).....	29
Fig 2.10 Tested slab by (Kumari et,2013).....	30
Fig 2.11 Crack patterns at a bottom face of slab (Al-Hafiz et al,2013.....	31
Fig 2.12 Tested slab by (Baarimah & Mohsin, 2017).....	32
Fig 2.13 Crack pattern and failure mode of the slab(Shaheen et al., 2017).....	33
Fig 2.14 Crack pattern and failure mode slab (Chkheiwir &Abdullah,2017).....	34
Fig 2.15 Steel fiber crack of the test slab (McMahon and Birley,2018).....	36
Fig 2.16 Tested slab by(Qasim,2019).....	37
Fig 2.17 Scheme of crack development in the testing (Buracczewset al).....	38
Fig 3.1 Details of slabs specimens group A.....	42
Fig 3.2 Details of slabs specimens group B.....	44
Fig 3.3 Main details of the experimental program throughout this research.....	45

Fig 3.4 Gradation of sand sample.....	49
Fig 3.5 Gradation of gravel sample.....	51
Fig 3.6 Shape of hooked steel fiber.....	52
Fig 3.7 Sika ViscoCrete – 5930.....	53
Fig 3.8 Sags of silica fume used in present study.....	55
Fig 3.9 Stress-strain curve of steel bar.....	57
Fig 3.10 Testing machine of steel reinforcement.....	57
Fig 3.11 Molds of slabs.....	59
Fig 3.12 Casting of the specimens.....	62
Fig 3.13 Curing of the specimens.....	63
Fig 3.14 The slump cone used in the slump test.....	64
Fig 3.15 Compressive strength test	65
Fig 3.16 Splitting tensile strength test	66
Fig 3.17 Modulus of rupture test.....	67
Fig 3.18 Modulus of elasticity test.....	68
Fig 3.19 stress-strain curves for SFRC cylinders in compression.....	69
Fig 3.20 Testing mechanism.....	70
Fig 3.21 Steel frames group (A).....	71
Fig 3.22 Steel frames group (B).....	71
Fig 3.23 Dial gauge of deflection.....	72
Fig 3.24 Cracks Reader.....	72
Fig 3.25 Test procurer group (A).....	74
Fig 3.26 Test procurer group (A).....	75
Fig 4.1 Load-deflection relationship of solid slab and slab with opening.....	81
Fig 4.2 Load- deflection relationship between groupA1 and A2.....	83
Fig 4.3 Comparison between SP1 and SP9 ultimate load and deflection.....	85
Fig 4.4 Comparison between SP5 and SP8in term of the deflection.....	85
Fig 4.5 Comparison between SP6 and SP9 in term of the deflection.....	85
Fig 4.6 Comparison between SP7 and SP10 in term of the deflection nt.....	86

Fig 4.7 Comparison between SP8,SP9 and SP10 in term of the displacement.....	86
Fig 4.8 Determination of stiffness (evaluation of initial and secant stiffness).....	87
Fig 4.9 Comparison initial stiffness of the between SP1 and group(A1).....	88
Fig 4.10 Comparison initial stiffness of the between SP5 and SP2	89
Fig 4.11 Initial stiffness of the slabs with four openings (group A3).....	89
Fig 4.12 Determination of ductility index calculation (Sullivan et al., 2004).....	90
Fig 4.13 Comparison ductility index of the between SP1 and group(A1).....	90
Fig 4.14 Comparison ductility index of the between SP1 and group(A2).....	92
Fig 4.15 Comparison ductility index of the between SP1 and SP9.....	92
Fig 4.16 Determination of the energy absorption index (Husain et al, 2017).....	93
Fig 4.17 Comparison energy absorption of the between SP1 and group(A1).....	93
Fig 4.18 Comparison energy absorption of the between SP3 and SP6.....	94
Fig 4.19 Comparison energy absorption of the between SP2 and SP8..	95
Fig 4.20 Crack pattern and failure mode of series one models.....	98
Fig 4.21 Load-displacement relationship of flexural slabs.....	103
Fig 4.22 Comparison load-deflection between SF3 and SF4.....	103
Fig 4.23 Comparison load-deflection between group B2.....	104
Fig 4.24 SF6 and SF9 Load-displacement curve	106
Fig 4.25 SF7 and SF10 Load-displacement curve.....	106
Fig 4.26 SF8, SF9, and SF10 Load-displacement curve.....	107
Fig 4.27 Comparison stiffness between of the SF1 and group B1.....	109
Fig 4.28 Comparison stiffness between of the solid and opening slabs	109
Fig 4.29 Comparison ductility index between of the solid,slab with openings....	111
Fig 4.30 Ductility index of the solid and slab with four openings.....	112
Fig 4.31 Comparison energy absorption between of the SF1and group B1.....	113
Fig 4.32 Comparison energy absorption between of the SF1and group B2.....	113
Fig 4.33 Comparison energy absorption between of the SF1and group B3.....	113
Fig 4.34 Crack pattern and failure mode flexural slabs.....	117

LIST OF SYMBOLS

d	Effective depth of the slab (mm)
ρ	Reinforcement ratio
$\mu\Delta$	Ductility index
F_{sp}	Tensile strength (MPa)
F_r	Modulus of rupture (MPa)
F'_c	Cylinder concrete compressive strength (MPa)
F_{cu}	Cube compressive strength (MPa)
F_y	Yield stress of steel reinforcement (MPa)
K_i	Initial stiffness (kN/mm)
K_s	Secant stiffness (kN /mm)
P_{cr}	Crack load (kN)
P_u	Ultimate load (kN)
P_y	Yield load (Kn)
EAI	Energy absorption index
W_s	Width crack load (mm)
W_u	Width ultimate load (mm)
Δ_y	Yield deflection (mm)
Δ_u	Maximum deflection (mm)
V_f	Volume frication of fiber ratio
$V_{Rd,cs}$	Punching shear of concrete with shear reinforcement (MPa)
$V_{Rd,c}$	Punching shear of concrete without shear reinforcement (MPa)
A_{sw}	Total area of punching shear reinforcement (mm ²)
S_r	Distance between two concentric perimeters of reinforcement (mm)

LIST OF ABBREVIATIONS

ABAQUS	Finite Element Package
ACI	American Concrete Institute
ANSYS	Analysis System Program
ASTM	American Society for Testing and Materials
BS	British Standard
CEB-FIP	Euro-International Committee for Concrete - Federation International for Prestressing
CFRP	Carbon Fiber Reinforced Polymer
EC	Euro Code
FRP	Fiber Reinforced Polymer
HSC	High Strength Concrete
HESF	Hooked-End Steel Wire Fiber
HRWRA	High Range Water Reducing Admixture
IQS	The Iraqi Standards
IS	India Standards
RC	Reinforced Concrete
SFRC	Steel fiber reinforced concrete
SP	Superplasticizer
SF	Silica Fume
W/b	Water to binder ratio

CHAPTER ONE

INTRODUCTION

1.1 General

Flat slabs or flat panels should be described as a two way framed system consisting of slabs, which are directly supported by columns without capitals or drop panels. The benefits offered by this system include simpler shape, quick construction, reduction in height of stories and architectural versatility in a variety of applications in the construction industry. These slabs developed high shear stresses near the column and thus they were considered to the punching shear failure [1].

The dates of using reinforced concrete (RC) slabs braced directly on vertical members (columns) return to the last century [2], stated that the discovery of flat slabs was attributed to Robert Maillart, a well-known Swiss engineer. Maillart started the designing of flat slabs in 1900 then got a patent for his work in 1909, suggested that acknowledgement for developing this structure, George M. Hill must be granted, and C. Turner the American engineers who constructed many structures in US between 1899 and 1901 which they confirmed that flat slabs are dependable with many constructed buildings, the first of which was the “Johnson Bovey” constructions in Minneapolis city (1906). Turner’s slabs were contained capitals in the connection with the columns and reinforced by steel bars of 32 mm-diameter to work as shear heads [3].

In 1907, Arthur F. Loleit, Russian engineer designed and implemented a factory with slabs without beams in Russia. It was one of many buildings with slabs supported on columns made by him in that period [4]. The author also noted that in his presentations for construction "without beams" were registered at the cement specialists annual meeting in Moscow and the Russian society for material science (1913), and if world war I (1914-1918) did not exist, Loleit would definitely have presented his work to a wider audience. All designs employed large

capitals in order to move load from the slabs to the columns, while the flat plates had no particular form of shear reinforcement, including a certain variation in the flexural reinforcement. The First try to prevent punching by slab reinforcement was by install bent bars, then other shear reinforcements were developed, such as stirrups, shear heads, and headed shear stud that are now widely used [5].

After that, RC flat slabs became having an extensive application in buildings and bridges, but it lately becomes a source of worry for their weakness to damage or failure in many old structures. Some of these structures did not comply with shear and flexural reinforcement requirements. In addition, insufficient punching shear and flexural strength capacity of modern flat slab structures on a number of causes, such as changing their loading and use, adding new installations or design/construction mistakes (e.g., the relevant updated design codes) provides the necessity to upgrading existing structures. Over the past decade, many attempts to improve the punching shear and flexural strength capacity of existing slabs include; assigning steel plate in the tensile zone, adding steel bolts around the column, increasing column cross-section by adding a steel or concrete capital, and lately, using of steel fibers. The use steel fiber for strengthening RC structures has become very popular among the other strengthening techniques due to their favorable properties, namely: high strength, ductility, and ability resist loads, but it still has some disadvantages attributed to the usage of enhancer admixtures such as high cost and low workability [5].

1.2 Advantages and Disadvantages of Flat Slab System

There are many benefits of using RC flat plate systems .The formwork becomes simple and flat in case of beams, capitals, and drop panel absence .The flat plate has a pleasing architectural view, fast construction, and simple reinforcement details. For the architectural requirements, and in the absence of beams, there is no impediment on the column's location.

The flat plate can be built as thin as 125-mm in thickness. According to for every ten stores in a structure, an additional store may be inserted automatically with the same total height in flat plate structures as opposed to other systems of the same height. The savings in height of a building lead to savings in other structural members such as columns and walls in addition to the economist in the used materials [6]. Despite these advantages, there are many disadvantages of using this method. The most serious is failure by punching shear at the slab-column attachment, which is caused by shear transferring and the moment of the supporting columns. Punching shear failure is brittle in nature and can lead to building progressive collapse. In this failure, diagonal cracks in the form of truncated cone are formed due to the concentration of the stresses around the column. The failure surface extends diagonally from the bottom to the top of the slab. This phenomenon is related to the action of concentrated forces on the slabs, which may cause its punching. Figure 1.1 represents the surface of the shear with its cracks, which extends from the loaded area outline and extend at a specified angle to the other slab side [7]. Stated that the inclination of the shear surface was varied between 26° and 45° concerning the slab plan. The punching shear case exposed in Figure 1.1. It should be noted that there are two ways that the punching shear may occur; the first case when the concrete crushes at control perimeter of RC column (u), the second case is tension failure of concrete (u_1). The critical perimeter around the column is assumed at distance $2d$ from the column face where (d) is an effective depth of the slab[8]. The crushing at the periphery of the column is managed by decreased concrete strength compression, see formula:

$$V_{Rd,CS}=0,75V_{Rd}+1.5\left(\frac{d}{s_r}\right)A_{sw}\times f_{yw}\left(\frac{1}{u_1\times d}\right)\leq K_{max}\times V_{Rd} \quad \dots\dots 1.1$$

The current limit is based on the V_{Rdc} formula, which calculates the punching strength of concrete slab without shear reinforcement (1.2).The overall strength against the occurred punching at the basic control perimeter, including the

impact of shear reinforcement, must be less than $k_{max} V_{Rdc}$ (see formula) (1.3). As V_{Rdc} exceeds $k_{max} V_{Rdc}$, V_{Ed} must be less than $k_{max} V_{Rdc}$. In the EN1992-1-1, amendment, the k_{max} value will be added, with a suggested value of 1.5 [8].

$$V_{Rd,c} = \frac{0.18}{\gamma_c} \times K \times (100 \times \rho_1 \times f_{ck})^{1/3} \geq 0.035 K^{2/3} f_{ck}^{1/2} \quad \dots\dots\dots 1.2$$

$$V_{Rd,max} = \frac{\beta V_{Rd}}{u_o d} \leq V_{Rd} = 0.4 v f_{cd} \quad v = 0.6 \left[1 - \frac{f_{ck}}{250} \right], \quad f_{ck} (\text{MPa}) \quad \dots\dots\dots 1.3$$

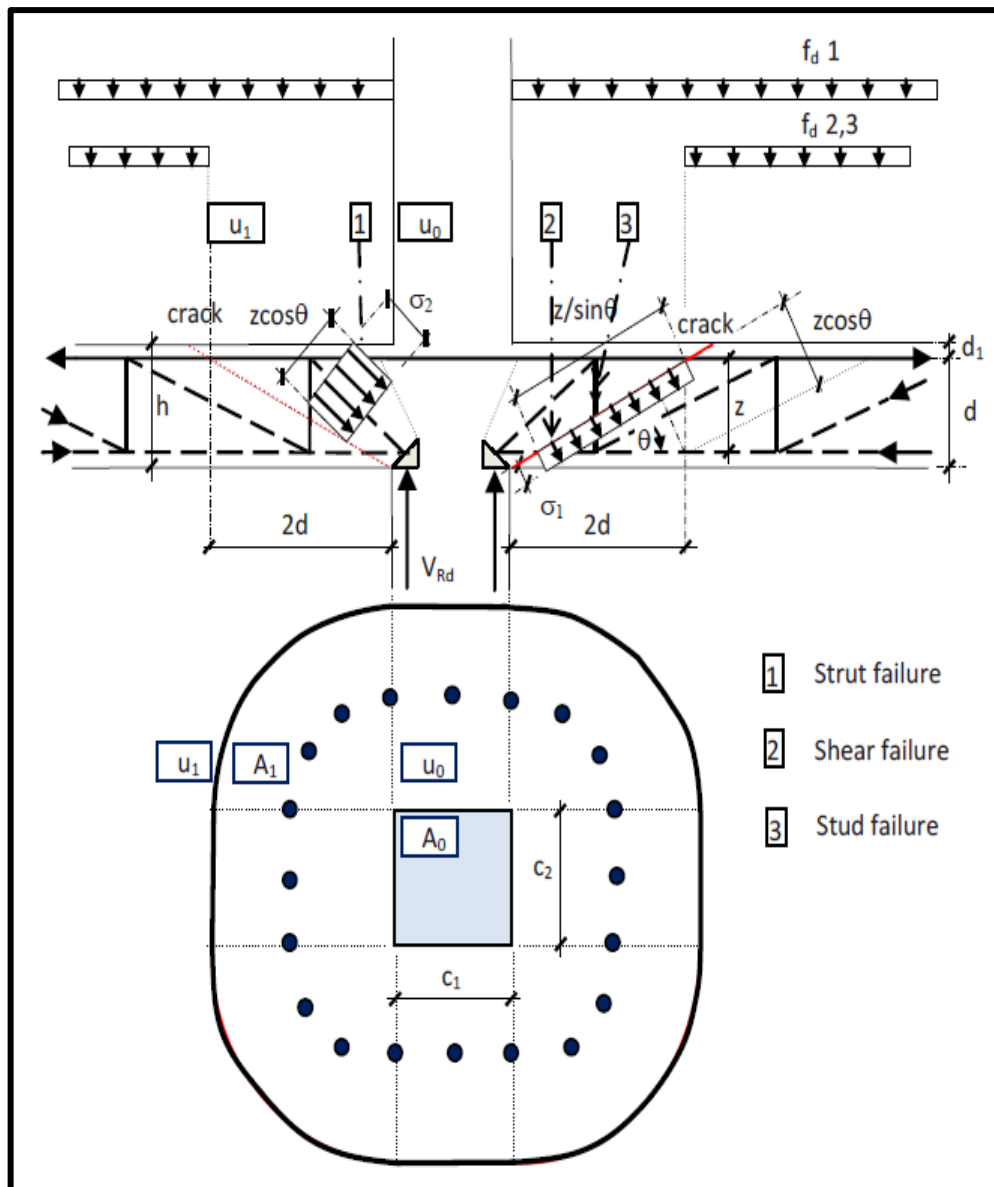
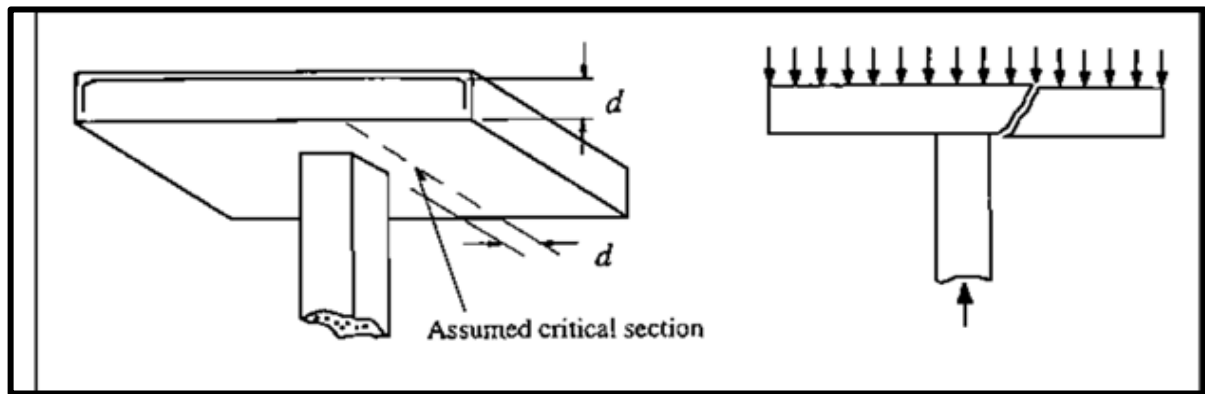


Figure 1.1 Analysis of Punching Shear Mechanism (Halvonik & Fillo ,2013).

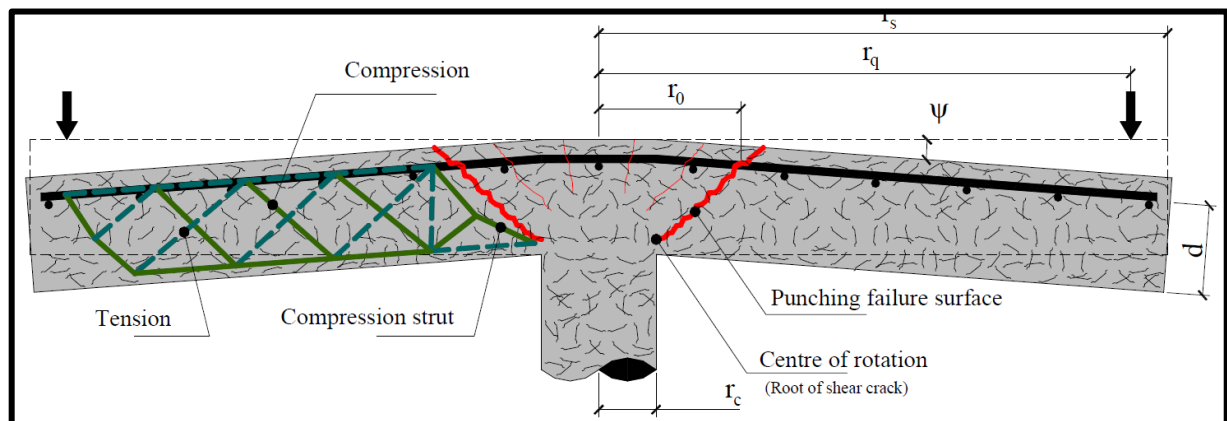
1.3 Punching Shear Failure

Two types of shear failure may be occurred in flat slab systems. The first one is the beam-type shear failure (one-way shear) which is similar to that of beams in terms of shear strength calculations and failure criteria, as illustrated in Figure (1.2.a) [9]. The second one is the punching shear failure (two-way shear) in which the failure may occurs in the vicinity of supported column or concentrated load by forming a truncated cone [6], as shown in Figure (1.2.b). Normally, the shear stresses which is causing by punching shear are much higher than those of beam-type shear. Punching shear failure may be happen by the actions of the gravity (vertical) load besides the unbalanced moment, which is resulting from unsymmetrical spans around the column or by the lateral loading (i.e. earthquake, wind etc.). Inhibition punching failure at the flat slab relies on its ability to resist the shear stresses, which caused by transferring shear forces and unbalanced moments to the columns.

Punching shear failure starts with radial cracks extending from the column, which is caused by a negative bending moment in the tangential direction and then followed by tangential cracks around the column perimeter (because of the negative bending moment at the radial direction). These radial tension cracks tends to form besides the slab mid-depth, which are more similar to web shear cracks than flexural shear cracks [10]. So that the slab stiffness surrounding the cracked area tends to preserve the shear transfer to the column by shear transfer mechanisms, which will be discuss in the next sections. When the applied load is high enough to overcome the slab stiffness, the slab starts to fail with the column penetrating through it. In general, punching shear failure in reinforced flat plates is sudden and brittle.



(a) Beam-type shear failure (Sayed .A,2015).



(b) 1.2 Punching shear failure (Park.R,2006).

Figure 1.2 Type of shear failure in flat slabs.

The flexural reinforcement contributes to resist the punching shear stresses as appeared in Figure 1.2,1.c. The role of steel reinforcement begins its effectiveness in resisting punching shear stresses immediately after the failure occurred, as these rods seek to keep the structural element stable or at least delay it. When the stresses reached to the maximum value that causing a rupture failure in the shear reinforcement, no rupture failure in tension occur in the flexural reinforcement. Contrary to the integrity reinforcement, where bars failed in tension by steel rupture, no ruptures in tension of the flexural reinforcement were reported in the tests performed in this paper. This shows that the strains in the steel have been mild (lower in any case to the ultimate strain).

On the contrary, the contribution of the bending arm was governed by the number of bars that had been enabled during the failure and their intensity of dowelling (because the cement cover had been spilled; see Figure 1.3 c. Figure 1.3, represent the role of steel flexural reinforcement to resist the punching shear stresses [11].

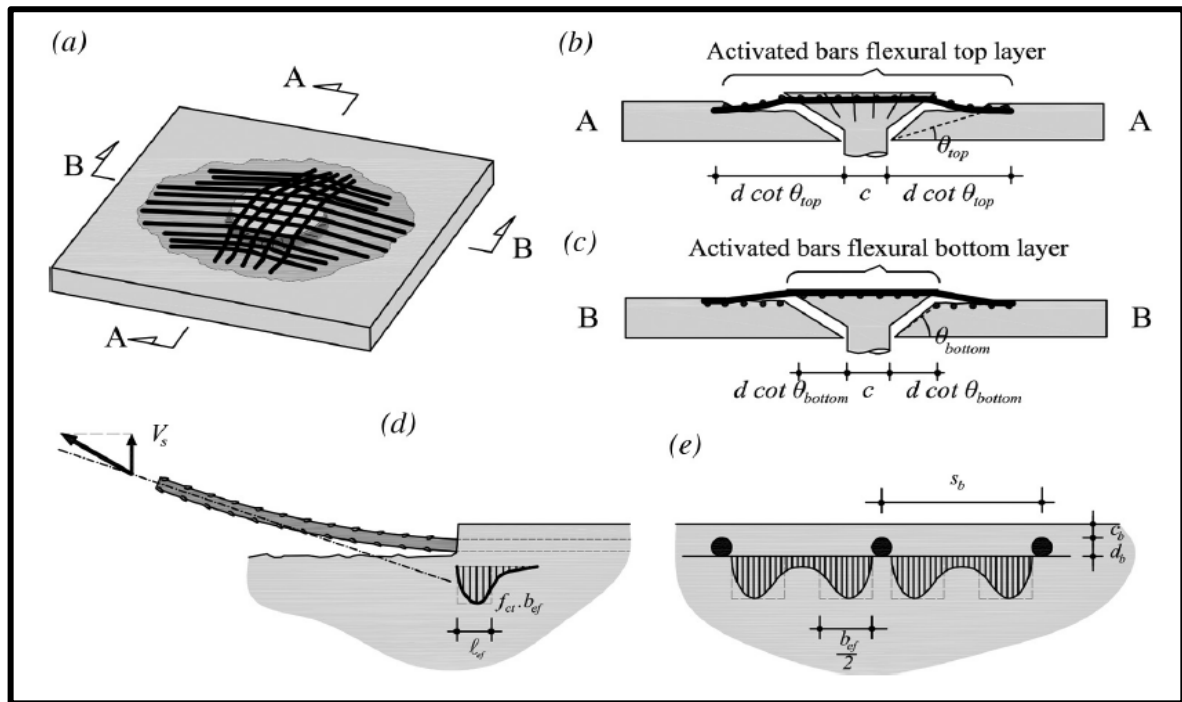


Figure 1.3 Effect of flexural reinforcement on the punching shear capacity
(Ruiz , 2013).

Punching can be divided into two types: symmetrical punching and non-symmetrical or asymmetrical punching. If the load, geometry, bearing conditions, and concrete member components (steel reinforcement, concrete, and another strengthening added materials) can be considered symmetrical with respect to the two axes of symmetry, the punching can be said to be symmetrical. as publicized in Figures 1.4 a, b. When the symmetry is relative to all the radial axes, the slab will be in a particular case of symmetrical punching (axis-symmetrical). If one of these criteria is not satisfied, the word "non-symmetrical boxing" will be used instead. It is still possible to differentiate between two forms in this case: punching that is asymmetrical but not eccentric, Figure 1.4 c, non-symmetrical punching

with eccentricity, Figure 1.4 d. The distinction between these two forms is that in the case of eccentric punching, non-symmetry caused bent moment moves from the slab to the column, which is referred to as the unbalanced moment [12].

One of the most difficult aspects of learning eccentric punching is the phenomenon of moment transmission between the slab and the column. Two effects are mainly generated by the combined action of the vertical load and the unbalanced moment, which have a larger effect on the punching shear resistance: the first is a concentration of the shear force per unit of length of the critical perimeter and the second is an increase of the critical crack width. The first increases the local stresses and the second decreases the resistance per unit length. These two effects result in a decrease in the carrying capacity.

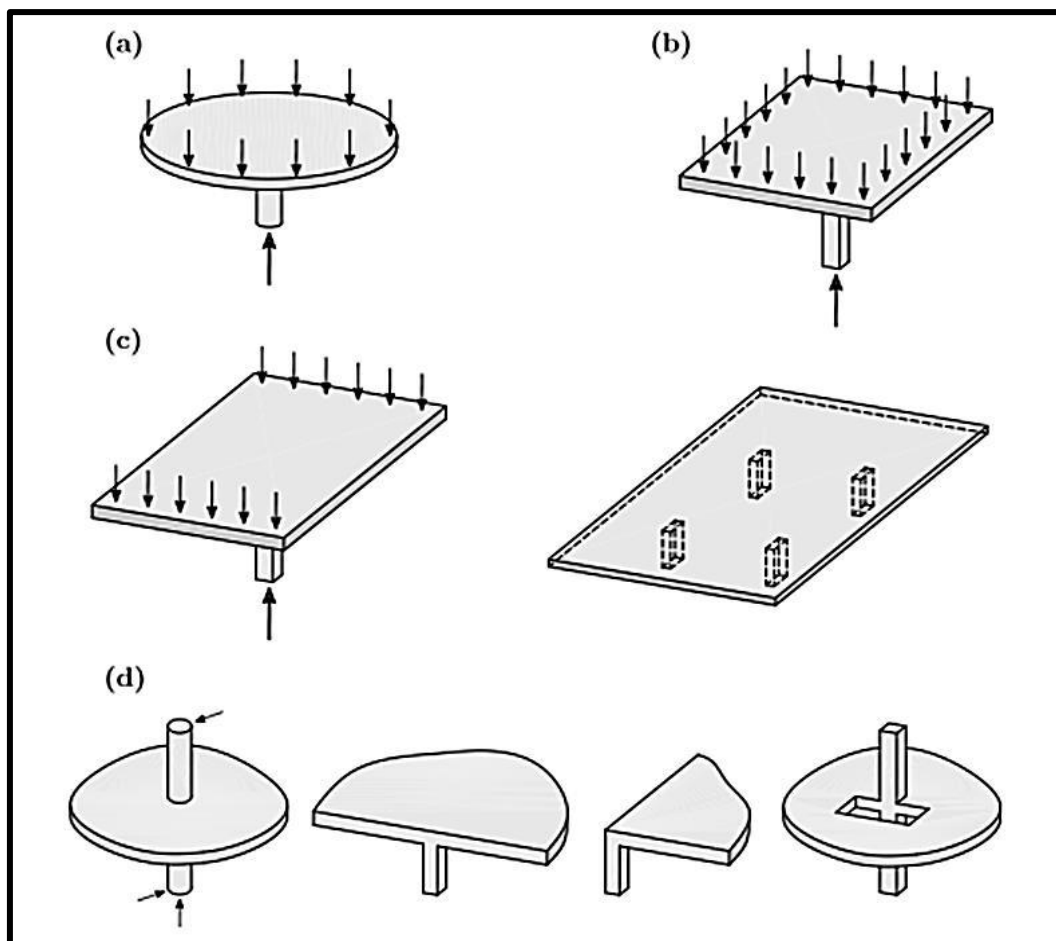


Figure 1.4 Different types of punching failure: (a) Axis-symmetrical punching, (b) Symmetrical punching, (c) Non-symmetrical punching (without eccentricity), and (d) Eccentric punching. (Kruger, 1999).

1.4 Flexural Failure of Flat Slab

The cracking patterns observed in slabs during bending were similar in all tests reviewed. Flexural cracking initiated and extending to the full width of slab as the deflection levels increased. As the cracks propagated in the transverse direction, they became inclined towards the transverse beams. The majority of cracks appeared concentrated in a region approximately equal to the effective depth of the beam from the face of the column. Inclined cracks, as continuation of the bottom slab flexural cracks, have been observed and extending. Measured strains in the slab varied transversely from the middle to the edge. Slab reinforcement yielded at approximately the same deflection level as did the main beam. At this deflection level the strain in the slab reinforcement close to the edge of the slab was very small.

At larger deflection levels, the slab reinforcement was reported to have high strains sometimes reaching values close to yield at the edge of the slab. Strains in the transverse reinforcement of the slab have been observed to increase with distance from the slab edges, reaching yielding at the edge of slab at high deformation levels. This particular observation is believed to be a result of the shear lag of the edges as compared to the center due to the reduction of longitudinal stresses with transverse distance. It may also be a reaction to the transverse contraction of the slab as it elongates longitudinally. (At large levels of longitudinal strains, the slab tends to contract due to Poisson's effect, where the Poisson's ratio of extensively cracked concrete may reach the value of unity [13].

1.5 Slab with Openings

Building codes recommend that concrete slabs with openings be constructed using traditional rules of thumb. However, those approaches have drawbacks in terms of the scale of the opening and the extent of the applied loads. Furthermore, this a scarcity of facts about the slab's load-bearing capability with openings [14].

In the slabs, openings are often wanted for electrical and mechanical services like fire protection pipes, plumbing, computer network and telephone, electrical wiring works, heating conditions, sewerage and water supply equipment, as well as ventilation. Meanwhile, substantial size openings are required by lift, staircases and elevator shafts. The structural effect of small openings is usually not considered due to ability of the structure to redistribute the stresses. However, in the case of a large slab openings they can hardly minimize the strength and load carrying capacity on account of cutting out of concrete and steel reinforcement together. This may lead to reducing the capacity of structures to resist the imposed loads and the structural need [15]. The design of reinforced concrete slabs with opening is not clearly indicated in the B.S 8110, 1997 [16] . Anyway, the ACI318-2014 [17], shows the openings allow in new slab system. The ACI code gives guidelines for different opening locations in reinforced concrete flat slab and flat plate. Figure 1.5, shows the size and location of the openings. In the area of the intersection of middle strip, The ACI code allows any size of openings.

The size of the opening allowed in the area common to intersecting column strip is $1/8$ the width of column strip in either span. Finally, the maximum permissible size in the region where one middle strip and one column strip meet is just $1/4$ the width of the middle or column strip in either span direction. The cumulative number of reinforcements for slabs without opening in both directions must be preserved in order to apply the ACI 318 guidelines. Hence, the reinforcement interrupted on the opening must be replaced on each side of the openings.

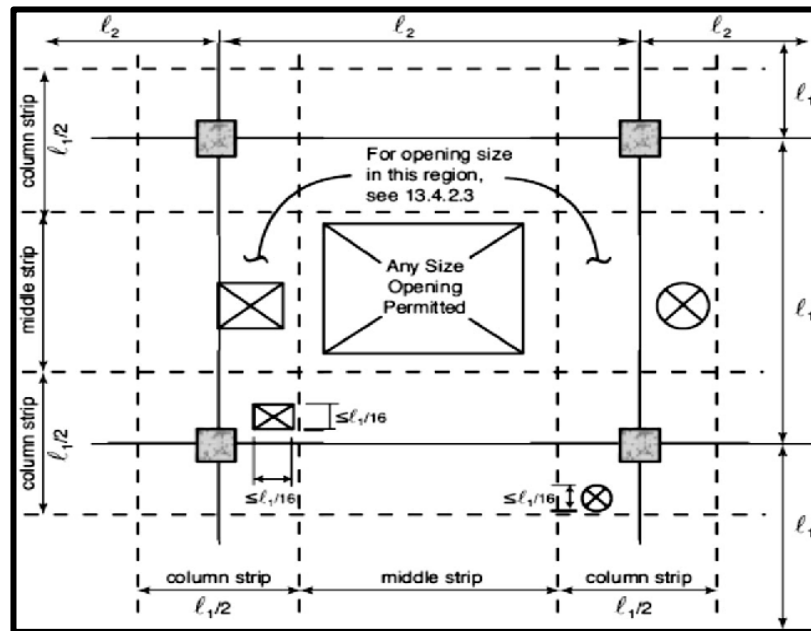


Figure 1.5 Suggested opening size and location in flat slab (ACI318-14).

1.6 Steel Fiber-Reinforced Concrete (SFRC)

Conventional concrete can be considered as a composite material in which the sand and aggregate are the dispersed particles in a multiphase matrix of cement paste. Concrete differs from most structural composites in that its strength is not greater than that of its components. The reason for this is that the interface between the components is the weak link in the composite and plays a major role in determining a number of properties of concrete. Usually, the aggregates are stiffer and stronger than the paste, and the non-linearity of the concrete stress-strain response is caused by the interaction between the paste and the aggregate [18]. Steel fibers intended for reinforcing concrete are defined as short, discrete lengths of steel having an aspect ratio in the range of 20-100, with any cross section and that are sufficiently small to be randomly dispersed in an unhardened concrete mixture using usual mixing procedures ACI 544-1R1996 [19]. The most significant improvement imparted by adding fibers to concrete is the increase in the energy absorption capacity. Toughness is a measure of the energy absorption capacity of a material and is used to characterize the material's ability to resist fracture when subjected to static strains or to dynamic or impact loads ACI 544.2R [20].

During the last four decades, fiber reinforced concrete has been increasingly used in structural applications, often in combination with reinforced concrete, and much research has been undertaken to more fully understand its mechanical properties. Steel fiber reinforced concrete (SFRC) is a concrete mix that contains discontinuous, discrete steel fibers that are randomly dispersed and uniformly distributed. The quality and quantity of steel fibers influence the mechanical properties of concrete. It is generally accepted that addition of steel fibers significantly increases tensile toughness and ductility, also slightly enhances the compressive strength. The benefits of using steel fibers become apparent after concrete cracking because the tensile stress is then redistributed to fibers [20].

Since that time, researchers made a widespread study on SFRC, motivated by formulas had exposed that increasing indication that concrete brittle behavior can be got by adding steel fibers. The addition of steel fibers to the concrete makes the construction of the airport, erosion resistance structures, building against the earthquakes, and explosive resistance structures [21]. The main purposes of using these fibers are:

- (a) To enhance the material's plastic cracking characteristics in the fresh state or up to about 6 hours after casting.
- (b) Upgrade the flexural and tensile strength.
- (c) Improve the toughness and impact strength of the structure.
- (d) Using these fibers reduce and control the cracks spread and failure mode.
- (e) Enhance durability.

The effect of steel fibers on the compressive strength of concrete is variable, typical stress-strain curves for steel fiber reinforced concrete in compression [22], in stress - strain curves for steel fiber reinforced slope of the descending

portion is less steep than that of control specimens without fibers. This is indicative of substantially higher toughness, where toughness is a measure of the ability to absorb energy during deformation, and it can be estimated from the area under the stress-strain curves or load-deformation curves [22]. The improved toughness in compression imparted by fibers is useful in preventing sudden and explosive failure under static loading, and in absorbing energy under dynamic loading. Under compression, HSC is significantly brittle. For this purpose, HSC has lacked in ductility. The steel fiber concrete mix has an improved ductility because of the elasticity in the steel material. Using of steel fiber in concrete constructions had become a very common and active way to upgrade the overall behavior, in addition to his ability to control the homogeneity of the mixture by spreading it [23]. Furthermore, adding the steel fibers in a concrete mix outcomes an increase in its ductility, cohesive between the concrete particles, and stops early cover spalling [24], as shown in Figure 1.6. Variation in tensile stress-strain curve of different types of steel fibers seems clear as demonstrated in Figure 1.7 [22].



Figure 1.6 Steel fiber reinforced concrete (Atlantis,2021).

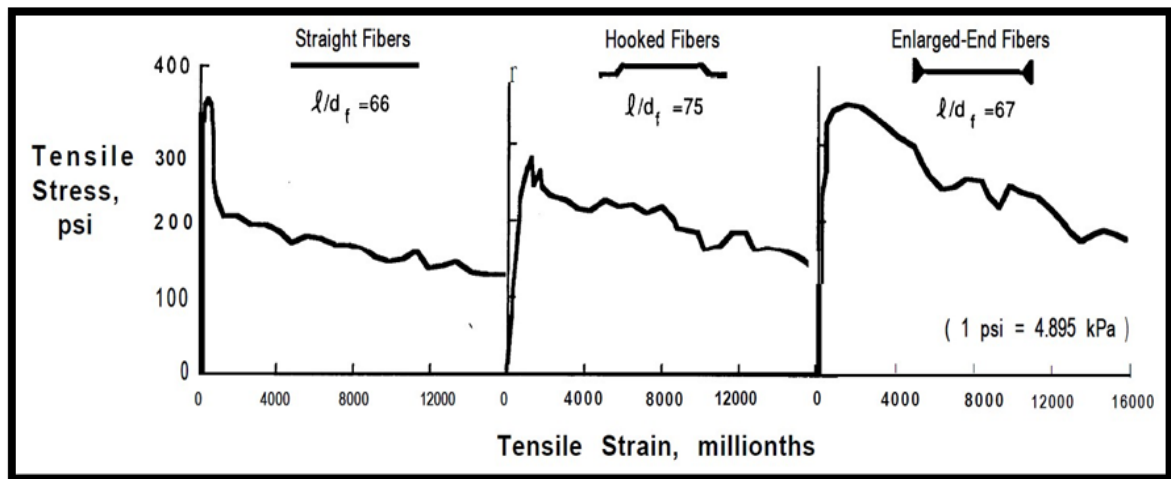


Figure 1.7 Stress-strain curves for steel fiber reinforced mortars in tension (Muslim , 2016).

1.7 Objectives of Research

The aim of this study is to investigate the behavior of fiber RC slab with and without openings and the effect of using steel fibers a technique. The primary goals of this work are as follows:

1. Checking the influences of varied parameters on the slab behavior, such as steel fibers ratio and openings.
2. Inspect the effect of opening's shape location, and number on the general behavior of the flat slab.
3. Check the possibility of punching shear and flexural capacity by steel fibers and compensate the loss that occurred due to the effect of the openings.

1.8 Thesis Layout

The analysis is divided into five chapters, which are as follows:

- [1] Chapter One: offers an introduction for flat slabs, punching shear and flexural failure, steel fibers, and slab with opening concept.
- [2] Chapter Two: offers previous experimental and numerical studies regarding use of strengthened of flat slabs and slab with openings
- [3] Chapter Three: deals with experimental program and test setup. Material properties , concrete mix design , details of slab with opening and test program are described also.
- [4] Chapter Four: Presents analysis and discusses the obtained results from the experimental work.
- [5] Chapter Five : summarized the conclusions and recommendations.

CHAPTER TWO

LITERATURE REVIEW

2.1 General

At the moment, the flat slab approach is widely used in construction. It enables architectural flexibility, clearer space, lower building height, simpler forming, and faster construction time. As a result, flat slab buildings must be devoted to public service connection requirements such as deflation pipes, gas pipes, or other requirements. These conditions necessitate the providing of larger space by removing the beam from the structural system or creation of an opening in the structure. However, the highest moments and punching shear remain which the shape of cracks created by these forces. Punching shear is a significant design problem for flat slab structures. One of the most common ways to strengthen concrete members to improve their mechanical properties and general behavior is to modify the concrete mix by adding reinforcing materials such as steel fibers. This addition provides cohesion forces between concrete particles and provides support to the concrete to resist the applied loads [25]. The percentage of addition of these fibers varies with different effects on the behavior of the structural component. In this chapter, experimental and numerical studies are presented for examining RC slabs subjected to a failure by punching shear and flexure.

2.2 Punching Shear Failure in Flat Slabs

In general, there are two phases to improve the punching behavior of a slab-column connection. First relates to newly constructed structure and the other to strengthen existing structure.

In the design of slab-column connections, there are many ways to enhance the punching shear strength, such as enlarging dimensions of the column, thickness of the slab, and the flexural reinforcement ratio, or by using high-

strength concrete, drop panels, and column capitals. Nevertheless, increasing of the column dimensions or using of drop panels and/or capitals are unacceptable for architectural reasons. In addition, they complicate the formwork and the construction process. It should be noted that they improve the punching shear capacity, but the behavior of the RC flat slabs remains brittle [25]. Increasing thickness of the slab may mean a considerable increase in the costs of the structure and foundations. At last, increasing the flexural reinforcement ratio or using high-strength concrete may have poor effectiveness, [26]. Consequently when it is necessary to improve the punching strength and to prevent a sudden brittle failure, the only practical solution may be the use of shear reinforcement, since it deals directly with the localized problem of punching [27]. Therefore, the focus in this section will be on using of punching shear reinforcement.

Since the last ten decades, shear reinforcements have been used to enhance the punching shear strength of flat slabs and to improve their deformation capacity (ductility), [28]. The major effect of shear reinforcement is crossing the inclined cracks to prevent punching shear failure. The effectiveness of the shear reinforcement concerning the punching behavior depends on several aspects, type, amount, distribution, and spacing of reinforcement used. Moreover, these aspects do not only influence the behavior but also describe the failure mode. It is necessary for their performance; shear reinforcements must should have a good tensile capacity, adequate ductility and enough anchorage. Since flat slabs are slender elements, anchoring is usually a critical point for most available types of shear reinforcement. Another essential aspect about using shear reinforcements in flat slabs is the practical application of their installation. The slab-column connection is usually subjected to high stresses (normal and shear), so it is common to concentrate flexural reinforcement in this area, which makes the distribution of the shear reinforcements so difficult [29].

Classified shear reinforcement for new-constructed slabs as follow:

1. Shear heads made of different forms of steel sections.
2. Headed Stud, shear studs, and shear bolts.
3. Stirrups, bent bars, double leg bar, and closed-ties.
4. Other type of reinforcements such as shear bands, lattice, UFO, etc.

In 2000, Broms [30] studied seven specimens, all of them was similar in geometry and approximately in flexural capacity but with different reinforcement. The main purpose of the study was to eliminate the punching failure mode of flat plate. According to the authors, this could happen by describing a reinforcement system that allows a flat plate to form plastic hinges at the columns and in the mid spans with no tendency for brittle punching failure. The described bent bar and stirrup combination is easy to fabricate and install in a stable way. The test results presented that effect of providing bent up bars on slab ductility and load carrying capacity was limited. For a typical flat plate structure, eight stirrup cages at each column are normally sufficient. The extra cost (including labor cost) as compared to a conventional brittle flat plate without any shear reinforcement is assessed at less than 1.5% of the total cost for the slab.

In 2011, Hong [31], offer an experimental study about the effect of the initial cracking on the behavior of RC flat slab under punching shear load. This study involved of six specimens with dimensions of 120 x 120 x 15 cm reinforced with diameter(15mm) steel rebar at 120 mm spacing in both directions. Yield strength of the steel reinforcement was 900 MPa to ensure that the failure will occur in the punching shear. The procedure included pre-cracking the concrete slab by 0.55 mm. The axial loads were withdrawn after cracking and before the punching tests. The gotten results revealed that comparing to the strength of originally uncracked slabs, no noticeable load carrying capacity- reduction. This shows that no care should be taken for axial

cracking plaques in respect of punching ability, see Figure 2.1 Failure and crack pattern .

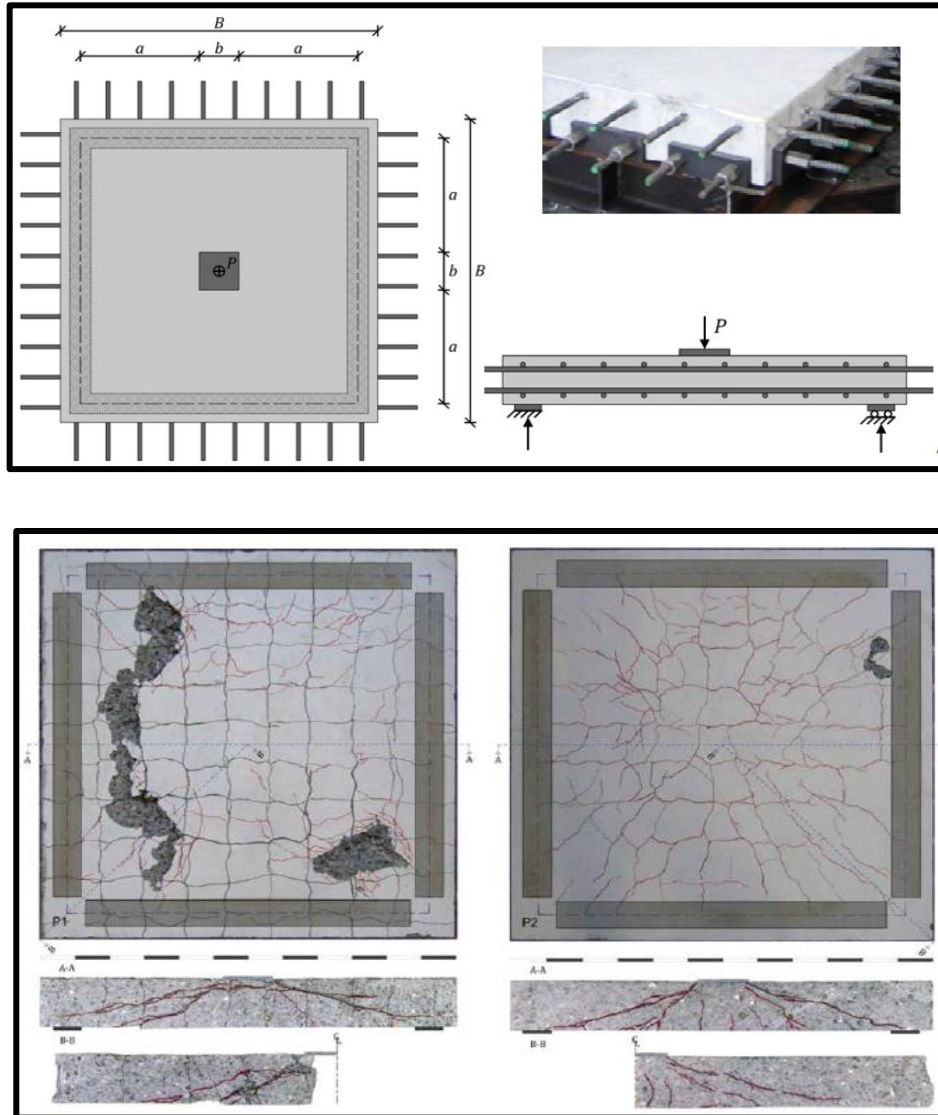


Figure 2.1 Failure shape and crack pattern of RC slabs (Hoang ,2011).

In 2014, Gouveia et al. [32] investigate the punching behavior of steel fibers reinforced concrete (SFRC). This investigation consisted of six flat slabs reinforced with five ratios of steel fibers tested under concentrated load as shown in Figure 2.2. The outcomes revealed that fibers included could have a positive effect on the slabs' behavior, namely in terms of response rigidity .The addition of steel fiber increased the slab load capacity and increased the slab deformation capacity which increased to 64% as compared with the slab

without fiber was observed for the slab with 1.25 percent fiber volume content. For slabs with higher fiber ratios the expected load capacity is more conservative.



Figure 2.2 Test details before and after the failure (Gouvia et al., 2014).

In 2015, Ha et al. [33] search for the effect of the opening on the punching shear strength of concrete flat slabs. Eight flat slabs were tested contained several openings with varied locations. Each test investigated the failure characteristics of specimen. Compared to many specific design codes, such as the beton and federation International (CEB-FIP), American Concrete Institute (ACI Code), Commit Euro International du model and model codes. the measured punching shearing forces of the test specimens are measured. Shear failures of Brittle punching in all test specimens were observed. The results of the test showed that the ratios of effective critical perimeter lengths usually correspond well to the failure loads ratios. The validity of the statement is therefore confirmed that the decrease in punching shear strength due to openings is comparable to the loss of a critical section perimeter, see Figure 2.3 crack pattern and failure mode.

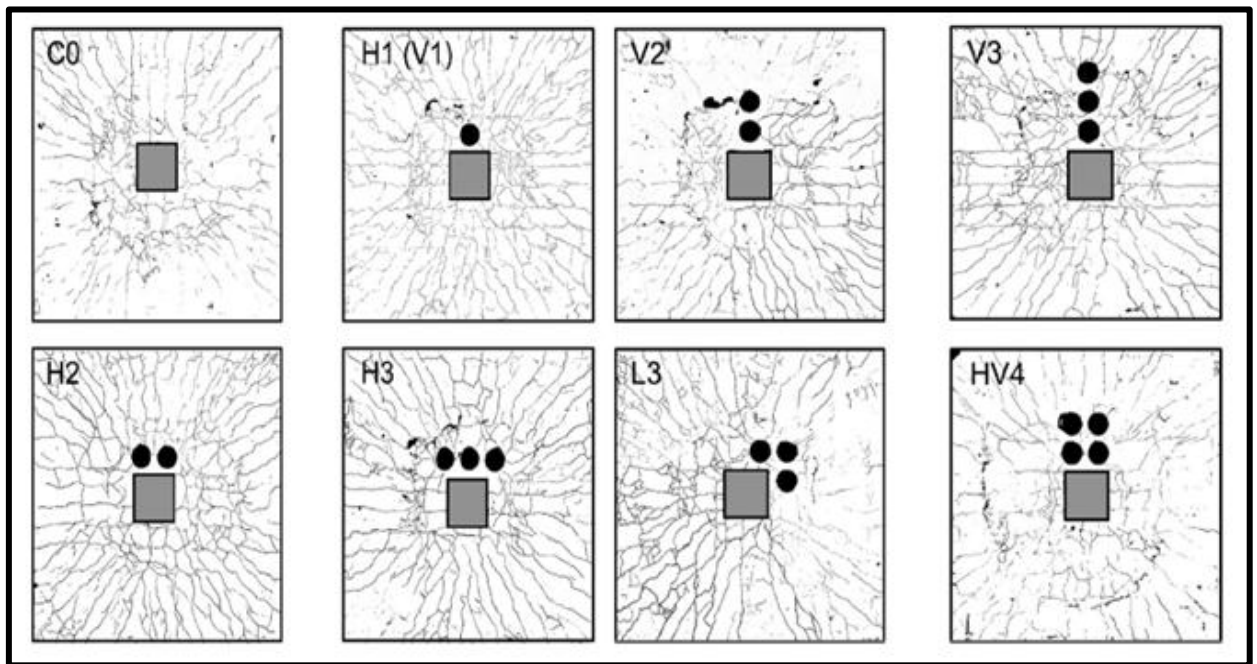
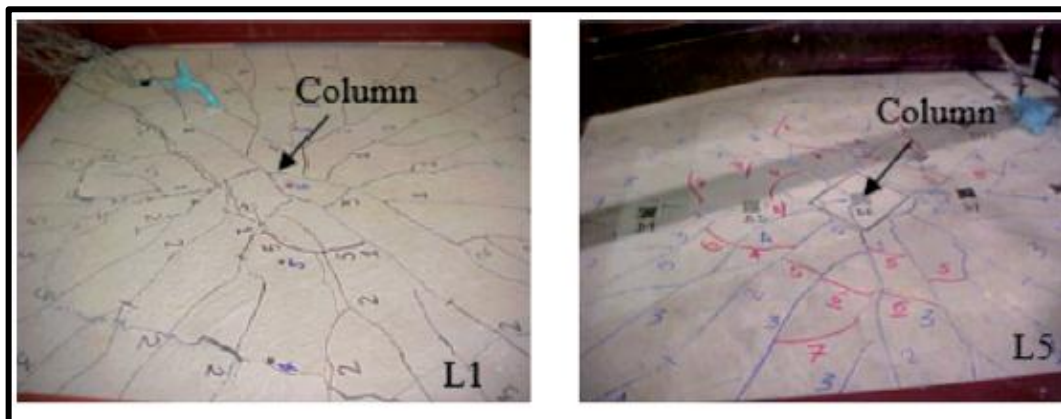


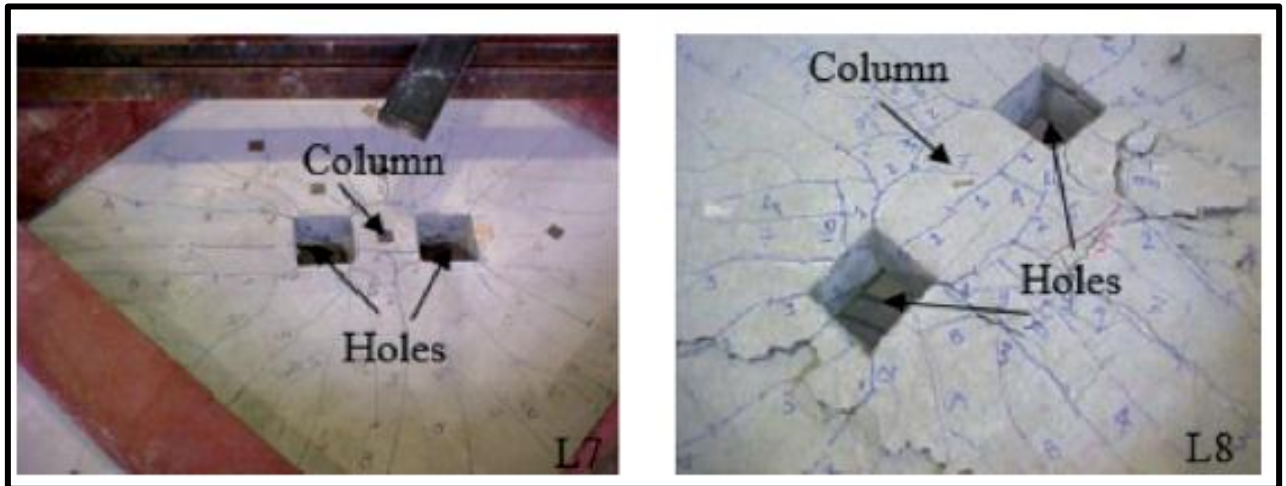
Figure 2.3 Crack pattern and failure mode of each specimen (Ha et al. , 2015).

In 2015, Bartolac et al. [5] tested six slabs had similar dimensions and concrete composition. The slab dimensions was 1500 x 1500 x 125 mm with different parameters. Models were represented on a 1/2 scale in relation to a real flat slab structure. Three models reinforced against punching shear (serving as reference specimens), while the remaining three slabs were without steel reinforcement against punching shear .As punching shear reinforcement, a system of three vertical reinforcing bars (D6 mm) with hooks (30 mm) in length at a 90° angle was used. These three bars were then hooked onto a metal strip with dimensions of (16 x 3) mm and spaced at 70 mm. This reinforcement method was used in this study to try to replicate headed shear studs, which are not manufactured for such thin slabs. According to the test results, applying shear reinforcement around the column increases the punching shear enhancement by an average of 17% as compared to the reference specimen. Furthermore, the deformation capability of slabs was found to have increased by 36%.

In 2017, Silva et al. [34] offered an investigation about the strengthening of concrete flat slab with opening by steel fibers and shear reinforcement. This paper provided an experimental study of the concentrated loading of nine flat reinforced concrete slabs (1800x130 mm). The principal parameters were two square openings (150 mm) near the central column. The use of three layers of shear reinforcement with six or eight elements per sheet, distributed radially along the column. The study concluded that presence of opening near the column had an impact on the punching shear's intensity, but that proper shear strengthening by steel fibers could reduce and compensate the occurred loss. In comparison with the flexural strength, the punching shear strength could be less than the flexural strength by a large percentage. External failures occurred in the slabs of shear reinforcement, with the failure surface appearing after the last layer of shear reinforcement. Regarding the openings effect, the existence of openings near the central column reduced the load carrying capacity by 13%. Concerning the cracking load, the slabs without shear reinforcement revealed that the circumferential crack occurred at (26%-48%) of the ultimate load for slabs the slab that containing shear reinforcement exposed a crack at 33-86% as shown in Figure 2.4. The findings also suggest that using this shear reinforcement to improve the punching strength of flat slabs with holes is a viable option. As compared to a slab without shear reinforcement and gaps, this increase may be even greater than (19%).



(a)



(b)

Figure 2.4 Crack pattern after the failure of slab (Silva et al. , 2017).

In 2018, Musse et al. [35] presented an extensive experimental study about the strengthening the flat slab by steel fibers and shear reinforcement against the punching shear loads. The study included testing of eight models of flat slabs with dimensions of (180 x 180 x13) cm had been loaded see Figure 2.5. The models were classified into two classes based on the form of concrete used (with and without steel fibers). The amount of steel fiber used in the slabs of the second category was 0.9 percent. Each series involved of four slab specimens: the first one was without shear reinforcement and other three ones were with shear reinforcement (studs) spread radially around the column. Steel fibers improved the ultimate strength shifted the failure surface from outside to inside the punching shear reinforcement area. The use of shear stud reinforcement and steel fibers in the concrete were the two key variables in this analysis. The shear reinforcement was made up of three, five, or seven studs' layers with diameters of 5 or 10 mm and spacing of 43 or 63 mm. according to the obtained outcomes, the conclusions of this study were; the usage of steel fibers can increase the load carrying capacity of the tested concrete slab which the average upgrade was 75%. Regarding the slabs without shear reinforcement, the upgrade in the punching shear strength was 12%. The failure mode affected

by the steel fibers existence which changed from the outside to the inside which produced a large-cracks. As compared to slabs without fibers, vertical displacements were up to 74% higher in slabs with fibers. Radial cracking occurred at about the same loading stage in all slabs, regardless of shear reinforcement or fiber usage in concrete. The fiber-enhanced slabs had a greater number of radial cracks with smaller thicknesses.

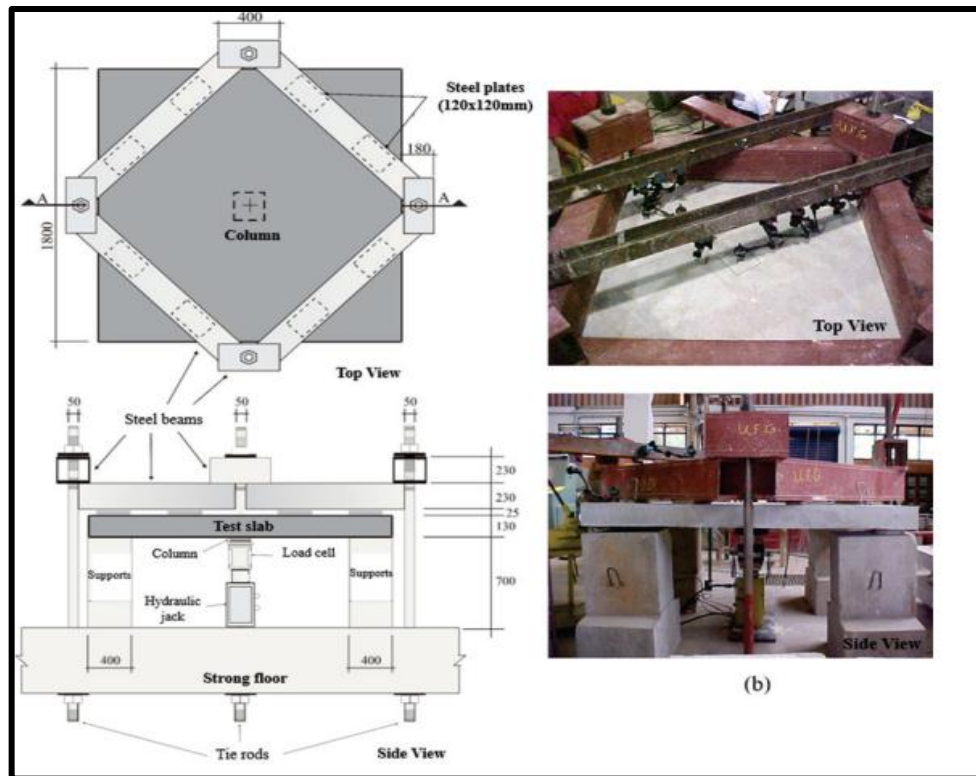


Figure 2.5 Test setup : top and side view (Musse et al. ,2018).

In 2018, Ismail [36] present an extensive numerical study about the the punching shear behavior of concrete flat slabs with opening under eccentric loading. Nonlinear finite element analysis was performed on 27-interior flat slabs with large scale with dimesnions of (200 x 200 x 15.5 cm) which subjected to the concentric and eccentric punching load. The variables of this study were the size and location of openings, and configuration of the reinforcement near to the opening. The verification process between the experimental and numerical models showed a good agreement. The comparison between the results occurred with the experimental previous studies. The numerical outcomes revealed that

the existence of opening near the column decreased the ultimate strength and this reduction increase with increasing in the size of the openings. The ultimate shear strength was reduced by 35% for specimens with openings of (250 x 250) mm, and specimens with openings of (250 x 450) mm by 45%. The load eccentricities by 112.5 mm and 225 mm led the capacity to reduce by 18% and 28% respectively. The continuous bars around the opening for the reinforcing cutting areas led to an enhancement of serviceability, representing an upgrade in the stiffness and no noticeable impact on the punching potential for concentric loads. The strengthening of the reinforcing reinforcement surface can be considerably increased. Finite element analysis carried out in the case of the opening in line with the direction of the principal moment is consistent with the provisions of the Building Code (e.g. ACI-318) and provides conservatory values when the opening is in the upside of the curvature moment, see Figure2.6 crack pattern and failure mode .

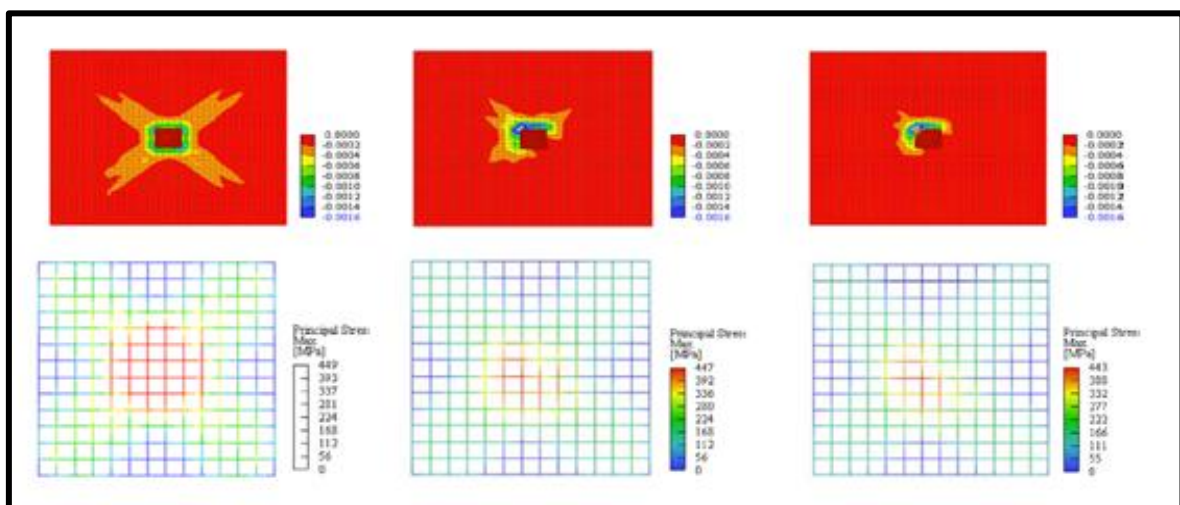


Figure 2.6 Crack pattern and failure mode the slab (Ismail , 2018).

In 2019, Liberti et al. [37] analyzed the failure by punching shear in reinforced concrete flat slabs containing an opening near a central column. In this experiment, 12 slab specimens with dimensions of (180x180x13) cm with no shear reinforcement were subjected to symmetrical loading. According to the number of openings adjacent to the column, these slabs were divided into three

classes. The failure modes and collapse load values were investigated. The experimental findings were compared to those found in the literature as well as the responses expected by the normative instructions. The slab specimens divided into three series according to the number of openings. The test results were compared with previous studies which showed a compatibility in the structural response in term of load-displacement. In comparison to the ultimate strength of the control slabs, the ultimate strength of the flat slabs with two openings decreased by 16 percent. Maximum loss in the strength occurred by 23.2 percent. The maximum displacements in the slabs with openings were lower than those in the reference slabs. Slabs with openings, on the other hand, are less rigid than slabs without openings. The ability of flat slabs to dissipate energy decreases as the opening dimensions become larger, see Figure 2.7 crack pattern and failure mode.

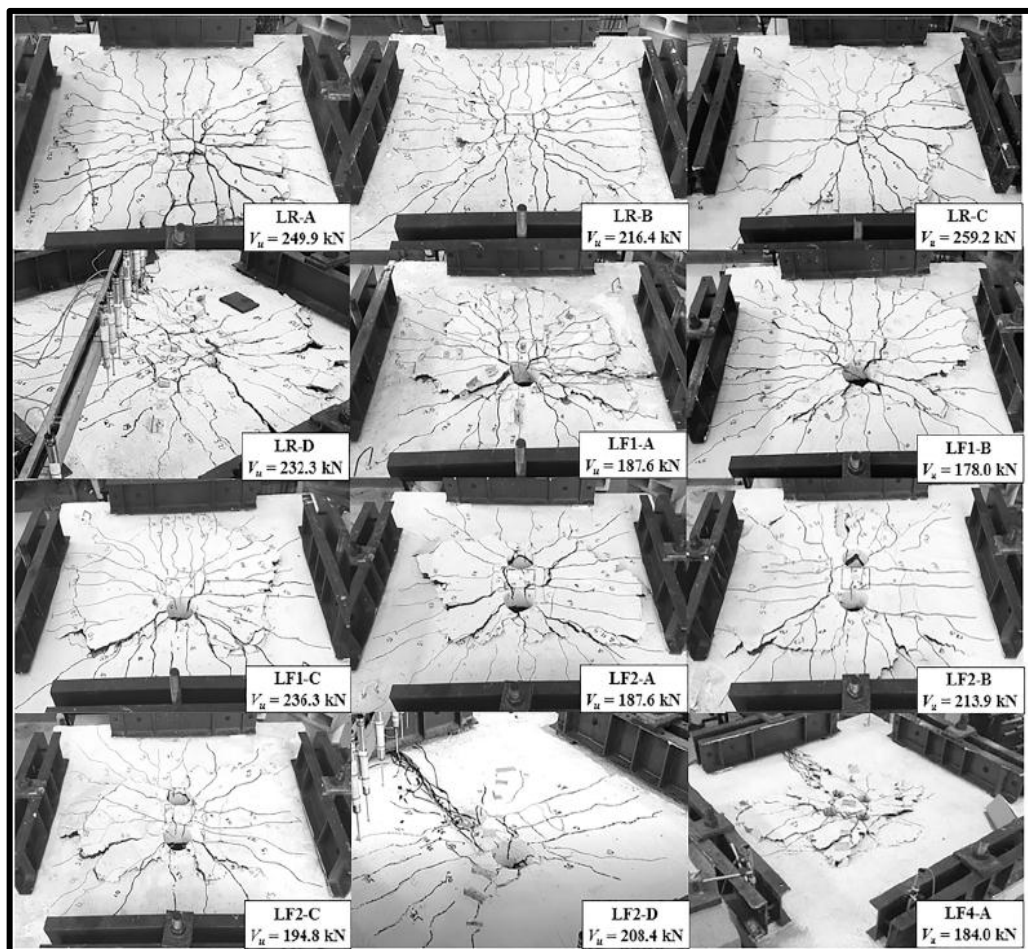
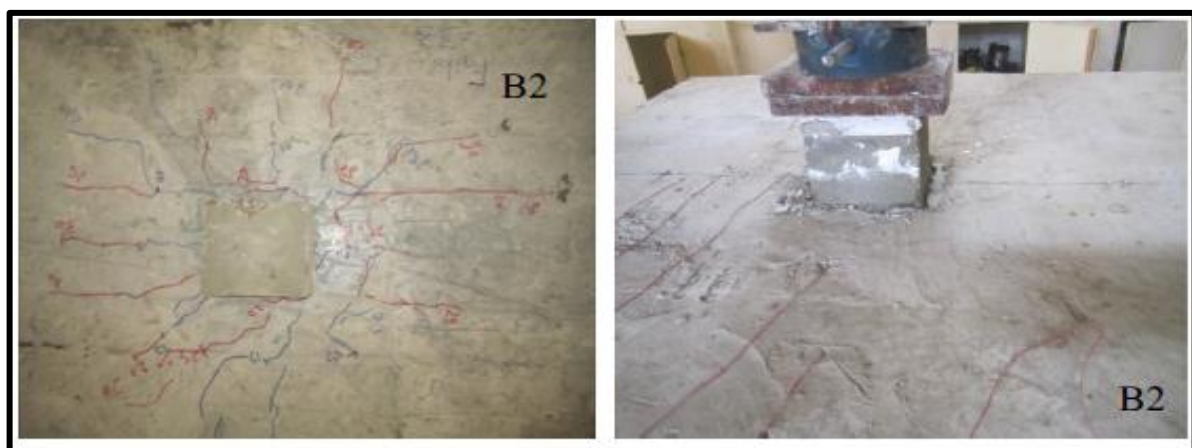


Figure 2.7 Crack pattern and failure mode of tested slab (Liberti et al. , 2019).

In 2019, Abdel-Rahman et al. [38] presented a numerical and experimental study about the behavior of fiber reinforced concrete flat slab subjected to punching shear load. Total of 14 slabs were divided into two series, the first one included 10 specimens with square cross section and tested under axial loads. The second series involved four slab specimens to explore the effect of moment transfer when subjected to eccentric loading. The main variables were the ratio of steel fibers (0.5, 1, and 1.5%), area dimensions of the punching zone, in addition to the column dimensions. It should be noted that all tested models were with dimensions of (170 x 170 x 15) cm and steel ratio of 1.2%. The obtained results showed an increment in the load carrying capacity and energy absorption by increasing the steel fibers. It should be noted that the optimum ratio of steel fibers was 1.5% which got the higher upgrade in the load carrying capacity. The analysis outcomes indicated that the use of steel fiber in a section of the slab equal to the thickness of the slab from the column face was sufficient to achieve the best results in terms of both failure load and ductility behavior. Regarding the numerical side, the test performed analytically by use of nonlinear finite element method by ANSYS software to simulate the flat slab specimens which showed good agreement with the experimental work in term of crack pattern, failure mode, and load and displacement, see Figure 2.8 crack pattern and failure mode.



(a) Bottom View

(b) Top View

Figure 2.8 Crack pattern of the test slab (Abdel-Rahman et al, 2019).

In 2020, Mostofinejad et al. [39] offered a numerical investigation on the behavior of slab column with openings under punching shear load. The aim of this study was to examine the effect of openings on the punching shear behavior of this member. The main parameter were the size and location of the openings. The first step of the investigation was modeling an experimental slab specimen and making a validation with the experimental results which exposed a good matching. The parametric models were eight slabs represent the interior connection and another 8 edge connection. Each model had a dimension of 150 x 150 cm and 250 ×250 cm placed at 0, 7.5, 15, and 30 cm away from the column. The outcomes revealed that the increasing of the dimensions of the opening increased the shear stresses around the column and reduce the punching shear capacity. The location of the opening had a significant effect on the punching shear capacity which the reducing of the distance between the opening and column cause decreasing in the shear strength of the concrete flat slab.

In 2020, Schmidt et al. [40] investigated the role of concrete member component (steel reinforcement and concrete) for shear to resist the punching shear forces in flat slabs. Total of 22 flat slab specimens were divided into two series which the first series consisted of eleven tests for punching shear on flat slabs and another eleven extra models on footings were performed. The study investigated the contribution of steel and concrete against punching shear and compare with the limitation of the several design codes such as Model Code 2010, and Euro code 2. The outcomes showed that the amount of steel rebar of shear affected the contribution of the concrete against the punching shear. The EC2 semi-empirical design theorem provides a constant concrete influence and linear increase in shear steel reinforcement contribution in proportion to the shear refurbishment per stroke design and that applies with the results obtained with this study, see Figure2.9 crack pattern and failure mode

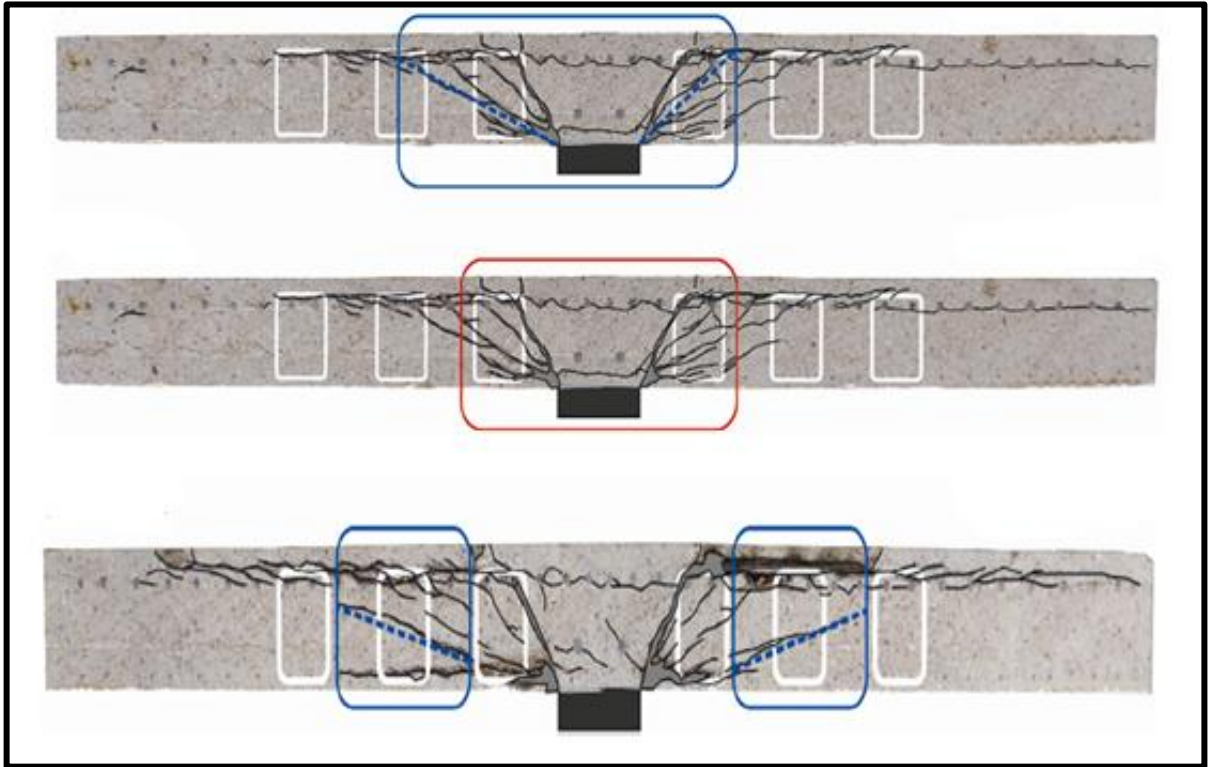


Figure 2.9 Failure crack of test slab (Schmidt et al., 2020).

2.3 Previous Studies Flexural Behavior of Slabs

In 2013, Kumari et al. [41] examine the flexural characteristics of steel fibers reinforced concrete one-way slab. Twenty slab specimens with 1% steel fibers with dimensions of (110 x 50 x 6.5) cm reinforced with 8 and 6 mm. the test results showed that the researchers used available codes equations to evaluate the load-deflection relationship, ultimate load, maximum deflection, and stress and strain in concrete member component. In the deflection trials, the codes expect a 20% variance. The estimated deflection to experimental one ratio according to IS 456:2000 was 1.15. But for EN 1992:2002 codes it was 1.26, for ACI 318 it was 0.94, and for the Bilinear system it is 1.04. With the exception of the ACI 318 codes, all of the other codes predict a greater deflection than the experimental deflection. All of the codes predict lower ultimate loads than the experimental ultimate load. In comparison to the experimental crack width, IS 456:2000 predicts a 28% increase in crack width. The tension test achieved by the strain gage installation in the steel reinforcement of steel is almost three times higher than the measured strain in steel using the IS 456:2000 process, see Figure 2.10, crack pattern and failure mode.

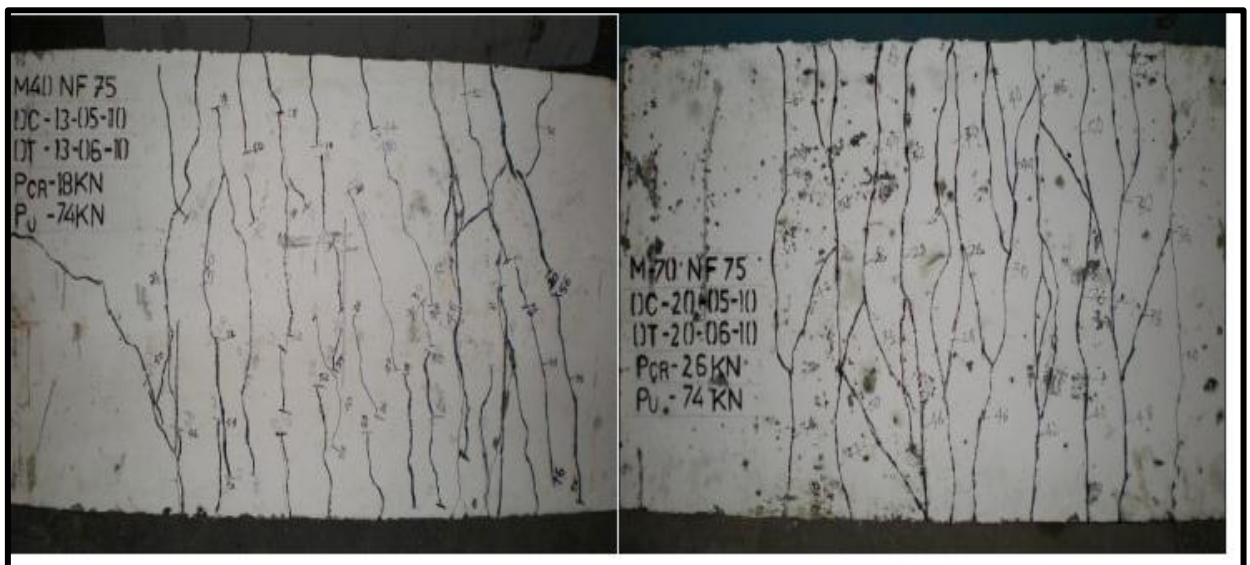


Figure 2.10 Tested slab by (Kumari et al., 2013).

In 2013, Al-Hafiz et al. [42] presented an experimental study about strengthening of RC slabs with openings under flexural loading. New techniques were used to reinforcing the opening in the slab and strengthening the concrete slab by use of steel plates and steel connectors. Total of fifteen slab specimens were fabricated with dimensions of (110 x 110 x 4) cm with a middle square opening (7.5 cm side length). The studies variables were the slab thickness (4, 6, and 8 cm), steel plate thickness (2, 4, and 6 mm). the obtained results exposed that existence of openings decreased the strength capacity of the concrete slab by (25%) when compared with the solid slab. The strengthening by steel plates revealed compensate the occurred loss due to the opening's presence. The thicknesses of the used plated were more efficient which the increase in steel plates thickness led to an upgrade in the ultimate flexural strength which the maximum enhancement occurred with the plate of 6 mm. regarding the slab thickness, increase the slab thickness weaken the flexural strength of the slab which decreased by (16%, 10%, and 23%) for the thicknesses (4, 6, and 8 cm) respectively. see Figure2.11 crack pattern and failure mode

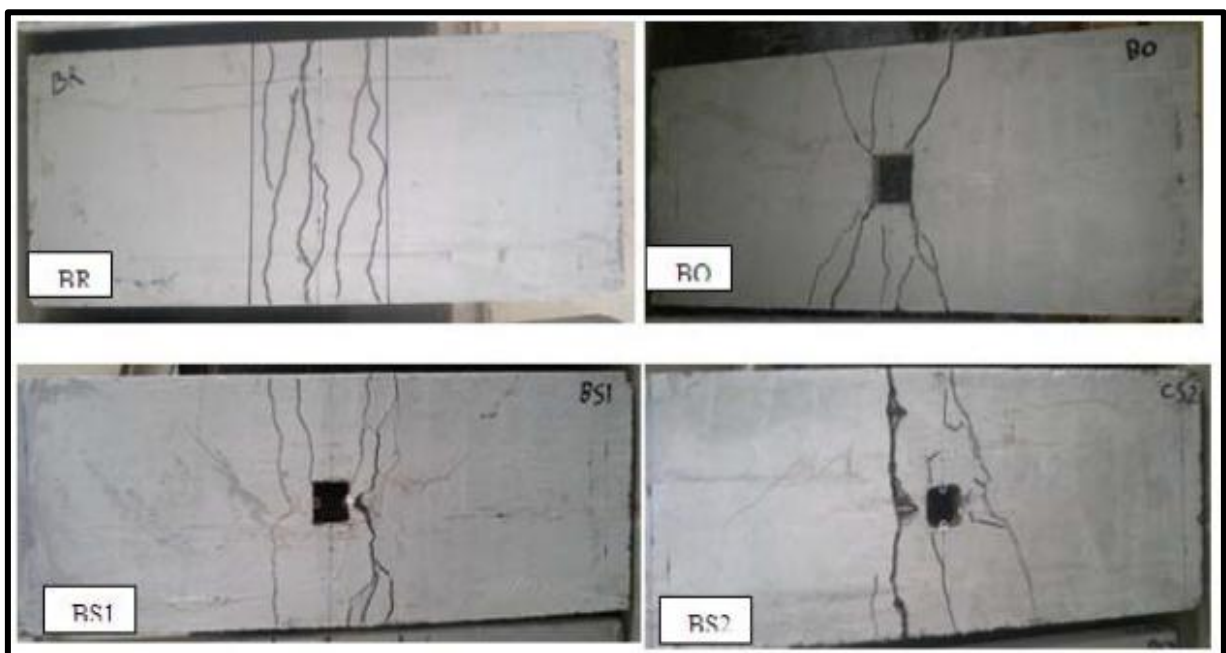


Figure 2.11 Crack patterns at a bottom face of slab (Al-Hafiz et al., 2013).

In 2017, Baarimah & Mohsin [43] offered an investigation regarding the effect of steel fibers on the flexural behavior of reinforced concrete slab. Six slabs were fabricated in which three of them were designed according to the Euro code 2 to satisfy the design requirement whereas the remaining specimens designed with 17% less thickness to insure that the failure will occur in the flexure. Three ratios of fibers were added to the concrete mix of the slab which were (0, 1, and 2%). The slab specimen was with zero steel fibers ration with no reduction in the thickness. The experimental results showed that the steel fibers upgraded the mechanical properties of the concrete, as shown in Figure 2.12. The best ratio of the steel fibers was (2%) which upgraded the load carrying capacity by (32%) and ductility by (87%) in addition to the delaying the crack propagation. Also, the steel fibers could compensate the occurred loss in the strength due to the reduction in slab thickness as well as made the failure of the slab in ductile manner.

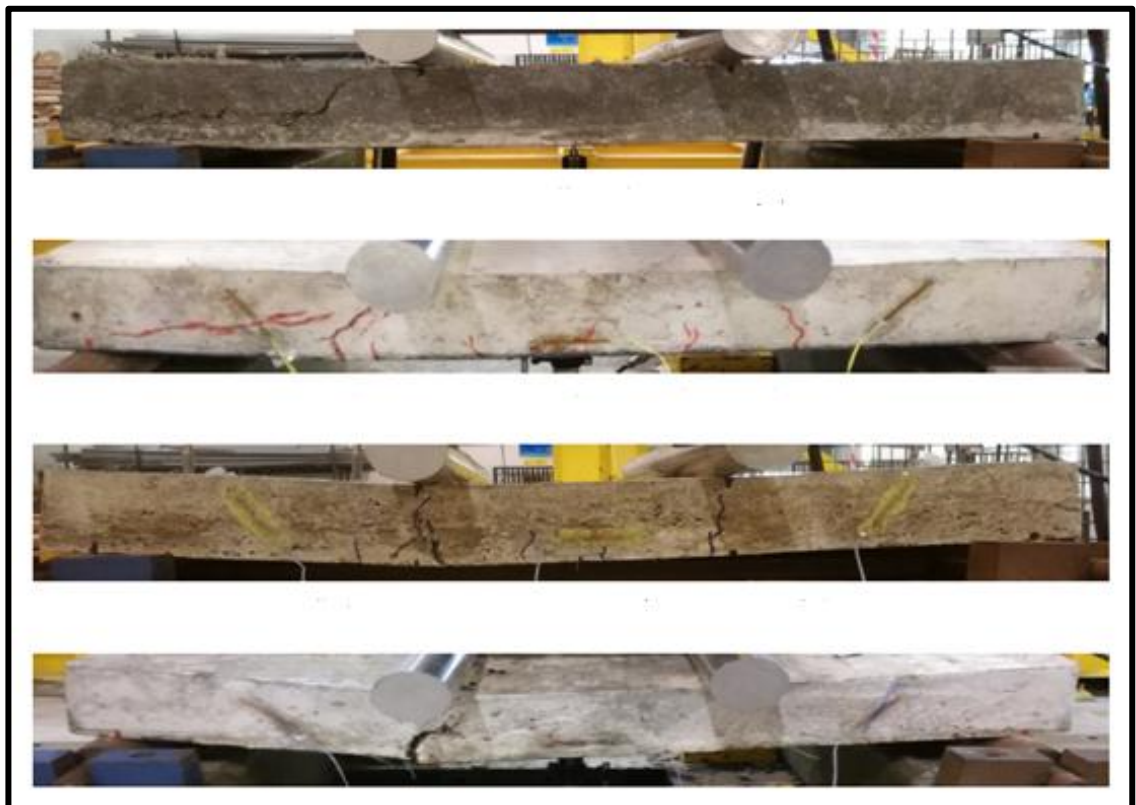


Figure 2.12 Tested slab by (Baarimah & Mohsin, 2017).

In 2017 Shaheen et al. [44] investigated the flexural behavior of reinforced concrete slab with openings. The theoretical examination was performed by use of ABAQUS by validate the models with previous studies to ensure that the followed procedure is correct. The main parameters included the openings' location and shape. According to the obtained results, its revealed that affected the stresses distribution but this effect seemed less effectiveness with the circular openings. The location if the openings controlled the failure and behavior of the concrete slab which shifting the opening to the center of span caused more deflection and deformation, as shown in Figure 2.13.

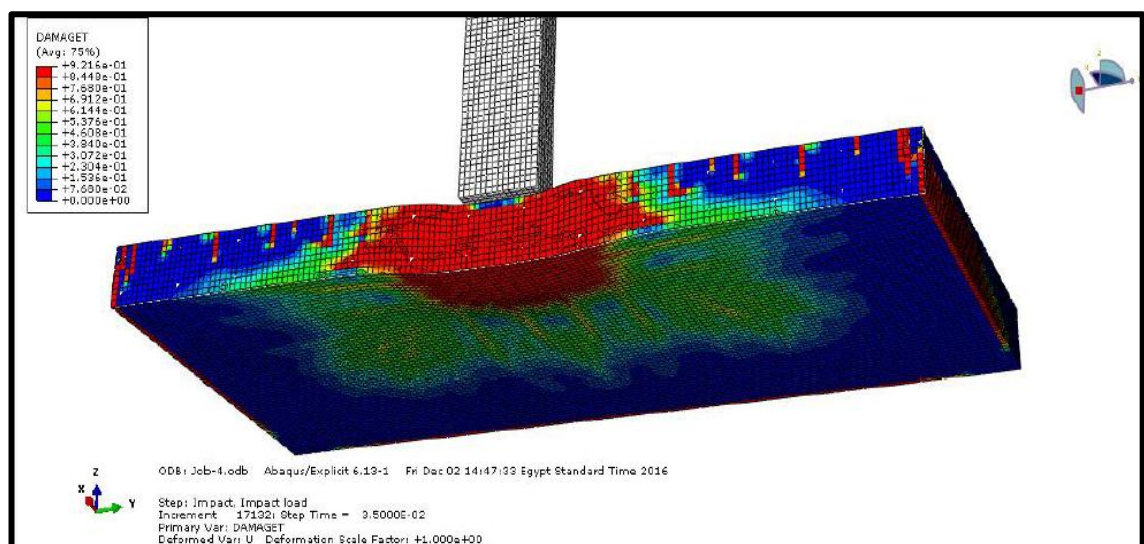


Figure 2.13 Crack pattern and failure mode of the tested slab
(Shaheen et al., 2017).

In 2017, Chkheiwir & Abdullah [45] presented an experimental study to explore the possibility of use steel fibers and wire mesh to strengthening the concrete flat slab after making an opening. Total of fifteen specimens were fabricated with dimensions (80 x 80 x 9.5) cm from the high strength concrete. The specimens divided into two series which each series have one type of opening. The first series had a square opening while the second one had rectangular opening. Each series strengthened with steel fibers with varied ratios (0, 0.5, and 1%) and wire mesh with several layers and widths. The obtained

results revealed that both strengthened techniques upgraded the flexural capacity of slabs with openings. Regarding the upgrade percentages, the strengthening by wire mesh was more efficient than steel fibers in strengthening the openings. Both techniques reduced the stress concentration at the openings corner so led to less crack at the opening, see Figure 2.14 crack pattern and failure mode.

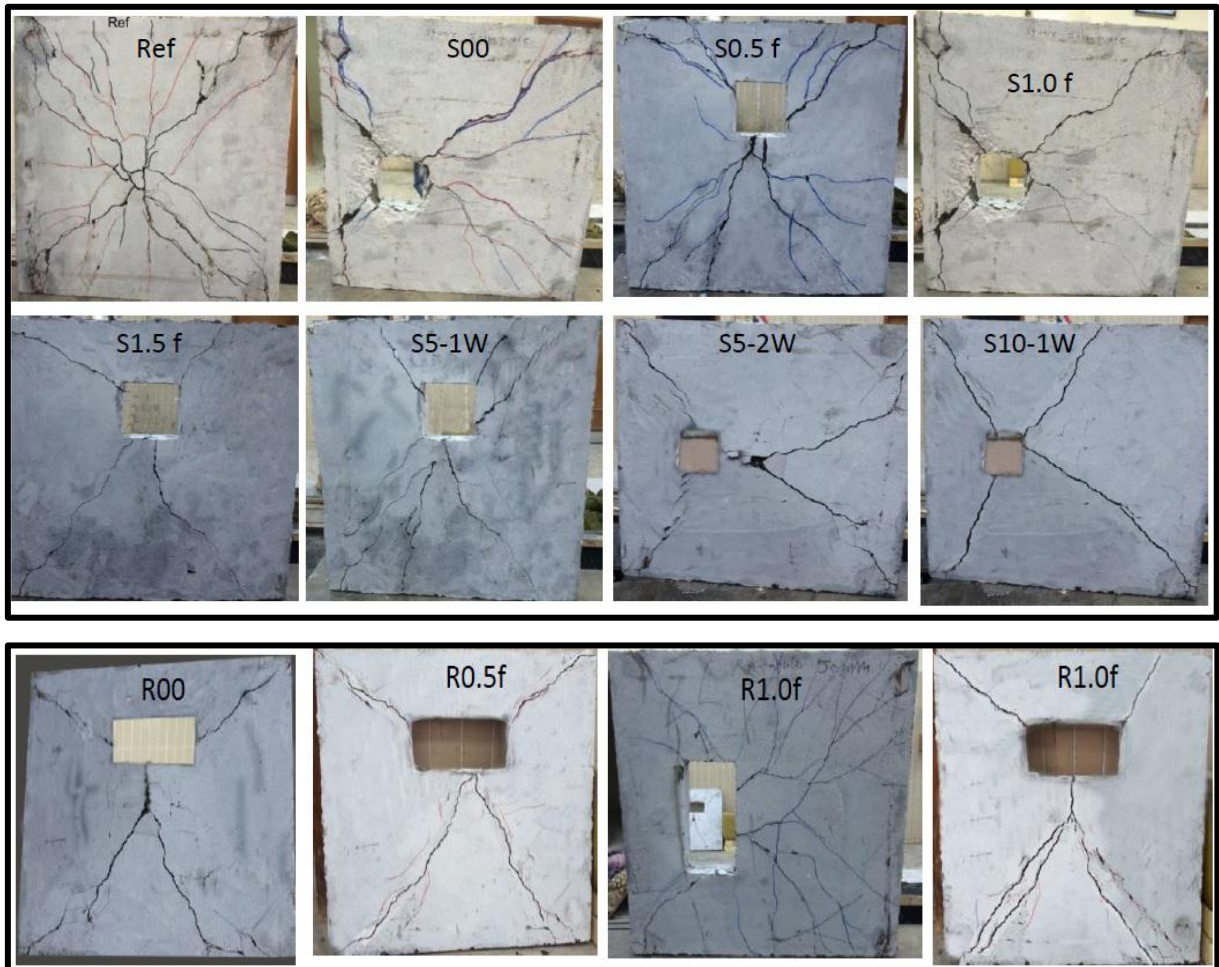


Figure 2.14 Crack pattern and failure mode of control slab and slab with openings (Chkheiwir & Abdullah, 2017).

In 2018, McMahon & Birley [46] presented an experimental study about the service performance of steel fibers reinforced concrete slabs. Total of the ten full-scale strip slabs strengthened with 0.5% hooked ends steel fibers tested under static loading. The main parameters were the slab thickness, amount of steel reinforcement, in addition to steel location. The results showed the

effectiveness of the steel fibers used to strengthen concrete slabs while improving their efficiency in terms of stiffness, energy absorption, and ductility. The presence of steel fibers dominated the pattern of failure and the spread of cracks, as the difference between the presence of the fiber or not was in the spread of the fiber, as the cracks visible in the case of the fiber were more numerous and smaller in size compared to their counterpart, where large cracks appeared led to earlier failure. Steel reinforcement located in the middle of the specimens behaved similarly to steel reinforcement located in, with localization of single cracks. Regarding the crack pattern, slabs with steel in the middle had less cracks than those found in the bottom-slab and the average crack widths were wider as shown in Figure 2.15. With a reduction in steel area, the overall number of cracks decreased. For slabs with steel at the bottom and middle, there were no significant variations in the displacement at which the crucial crack width was reached. Owing to the increased flexibility of the slabs, larger cracks were found in the slabs with steel at the middle at small displacements.



(a) Spalling at surface of concrete

(b) Steel fiber anchorage failure

Figure 2.15 Steel fiber crack behavior of the test slab

(McMahon & Birley, 2018).

In 2019, Holy et al. [47] examined the flexural strength of ultra-high-performance fiber reinforced concrete thin slab experimentally and numerically. Total of eight models were fabricated with several parameters such as the slab thickness (4, 5, 6, 7, and 8) cm and different slab sizes and tested under four and three-point loads for models with span (190 and 60) cm respectively. The flexural strength of the slabs with dimensions of 4 x 4 x 16 cm is about 2.4 times that of specimens with dimensions of 15 x 15 x 70 cm. The 4-point bending tests revealed a lower flexural strength than the 3-point bending tests. In the case of normal test specimens, the disparity between 3-point and 4-point bending tests was about 8-9%, and in the case of special test specimens, it was about 25%, the disparity becomes more pronounced as the test specimens' length increases. Concerning the numerical side, the matching between the outcomes of the experimental and numerical results were good.

In 2019, Qasim [48] offer an experimental examination concerning the flexural behavior of steel fibers reinforced concrete slabs with openings. Reactive powder concrete used to fabricate 10 slab specimens with dimension of (66 x 66 x 4) cm and tested under four symmetrical concentrated point loads, as shown in Figure 2.16. The models manufactured with many variables such as opening shape and size, opening location, in addition to the steel fibers ratio (0, 0.5, 1, 1.5 and 2)%. Based on pore size and grain size refining methods, which improve the transitions zone and minimize interfaced microscopy, reactive powder concrete improves the concrete strength. Increment occurred by (8.3%, 16.7%, 25% and 33%) in cracking loads, and (9, 18, 30 and 42.4) % in ultimate load, due to fiber ratio (0.5, 1, 1.5 and 2) %. In other words, the cracking load and the deflection increase with the material of the steel fiber. Presence of opening affected the load carrying capacity which reduced by (49.5%) approximately. The location of openings had a significant effect on the ultimate flexural strength which shifting the opening form the edge to the center decreased the flexural strength by (17%). The shape of the opening also affected

the behavior of concrete slab which the transfer from the square to circular shape decreased the cracking load by (6.3%) and failure load by (2.1%). Steel fibers affected the propagation of the cracks which reduced the crack width and increased the propagation due to the increase in the strain at both compression and tension regions.

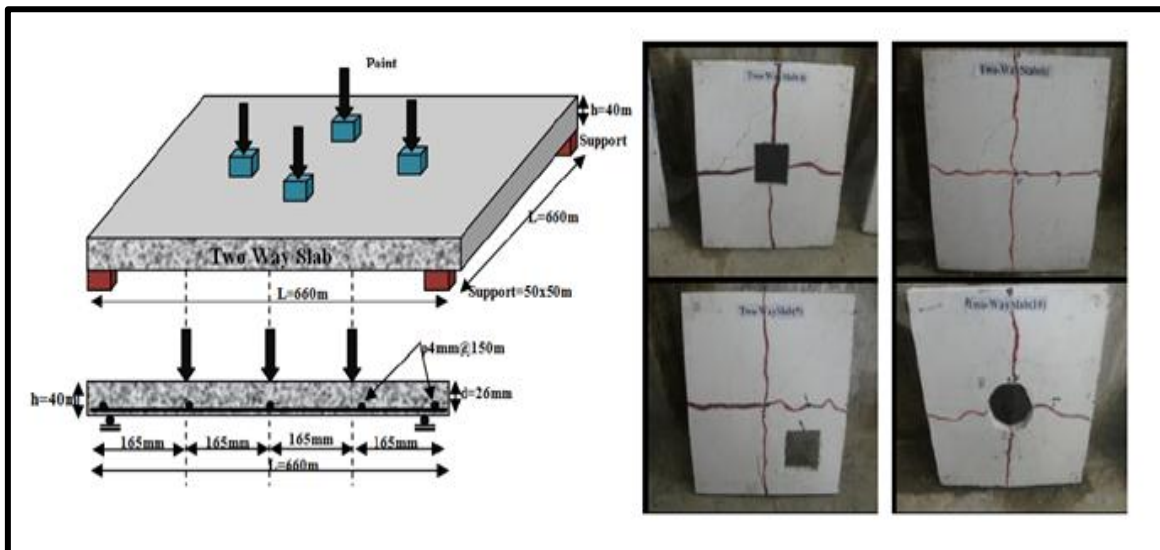


Figure 2.16 Tested slab by (Qasim ,2019).

In 2020, Buraczewska et al. [49] explored the effect of steel fibers and polypropylene on the flexural behavior of concrete slab. The experimental study included testing of three slabs strengthened with 1% steel and polypropylene fibers. The parameters of this study included compare between two material which showed that the compressive strength of the concrete with steel fibers was higher than those in polypropylene by 23%. The results of the study exposed that the ultimate flexural strength upgraded by 12% in comparison with the control slab. The reduction in the specimen with polypropylene is lower than steel fibers one due to the excessive amount of fibers. Regarding the flexural strength, the normal concrete was lower than concrete with steel and polypropylene fibers by 15% and 27% respectively. Combining the two-material provided higher upgrade in the compressive strength. Crack propagation affected by existence of steel and polypropylene fibers which showed less crack

width and more propagation when compared with reference slabs as shown in Figure 2.17 .

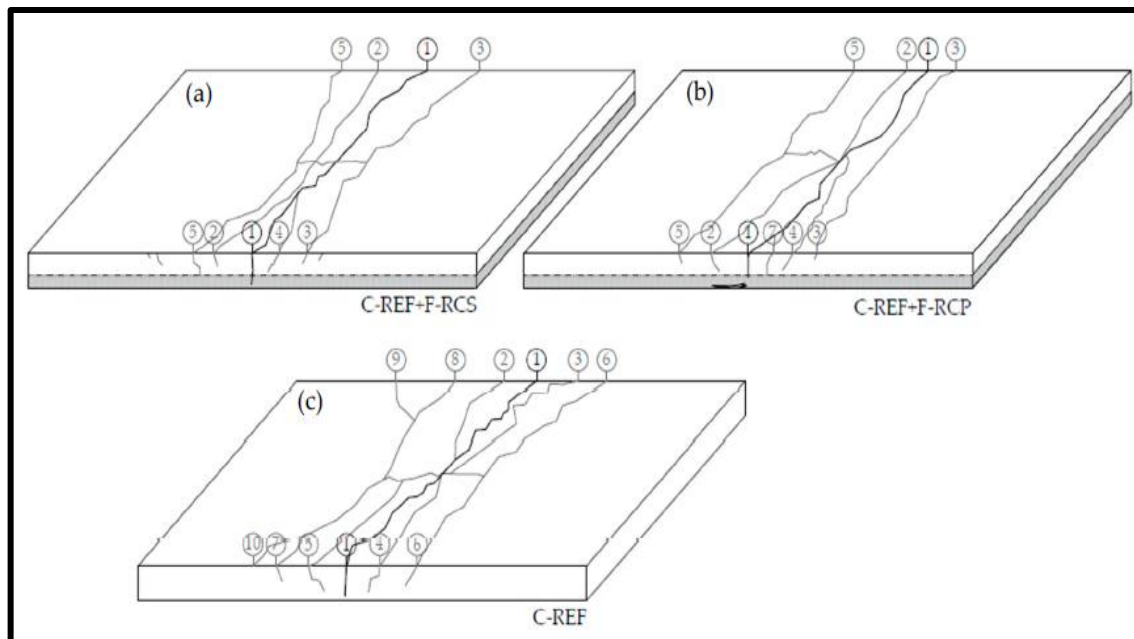


Figure 2.17 Scheme of crack development in the final testing phase of the slab (Buraczewska et al., 2020).

2.4 General Summary and Conclusion

From the previous literature review, the following points may be noted:

- This chapter has reviewed many experimental and theoretical studies concerning the behavior of concrete slabs. It is apparent that a few studies concerning of slabs with many parameters concerning the opening location, number, and shape in both flexural and punching shear loads.
- Strengthening the RC slabs by steel fiber reinforced concrete are one of the performances improving technique that increases the ultimate capacity and improved other characteristics of RC slabs.
- This thesis will investigate the behavior of the RC slabs strengthened by steel fiber reinforced concrete using variables are not available in the literature review in former researches .

CHAPTER THREE

EXPERIMENTAL WORK

3.1 General

The main target of the experimental program is to study the effect of the of steel fiber reinforced concrete on the behavior of reinforced concrete two-way slabs with openings (punching shear and flexural strength) and this chapter illustrates the main detailed information regarding the material and methods of the experimental program, materials component used and their characteristics, the mix proportion, mix design, mixing procedure, placing, curing of specimens, preparation, fresh and hardened properties and instrumentation used. The main details of the experimental program throughout this research are illustrated in Figure 3.3. Fabricating and testing of full-scale model is an illogical choice for researchers. The fact that it includes many obstacles, especially the laboratory equipment needed to conduct the examination, as well as the total cost of the research process. The engineer must have the ability to estimate the resistance and precipitation of the structural elements while finding the difference in structural behavior between the full and reduced scale. Through the literature reviews and previous studies, it was found that there are all related studies deals with reduced scale [50]. All the specimens have been prepared and casted then cured for 28 days and testing at the structural laboratory of the Technical Institute in Misan. The experimental program includes a test of 20 specimens to study the behavior of high performance concrete two-way slab with openings. The specimens were divided into two group(A,B) Shown in Table 3.1 and Table 3.2 . More details on the slabs considered in the analysis are as follow:

3.2 Details of Two-Way Reinforced Concrete Slabs (Group A)

Ten two-way-reinforced concrete slabs with dimension of(1500x1100x100) mm and a square column with dimensions (150×150) mm in the middle, were

cast in laboratory concrete of the technical institute of Amara and tested the all specimens were tested under concentrated load the load was transmitted to column. The slabs were designed to have punching failure. All slabs were identical in size but different in opening shapes, number and location as shown in Figure 3.1. Shows isometric view of the slabs and the geometry and reinforcement details. The slabs were placed on four (1350×950) mm lines which were simply supported on all four sides. The slabs were internally reinforced isotopically with steel bars having reinforcement ratio of ($\rho=0.0105$) at the bottom in each direction (the flexural reinforcement was provided on the tension side only), with bars of (10mm) diameter and spaced at (100mm) in each direction. The columns for all specimens were reinforced with (4Ø12) steel bars and closed stirrups (Ø 10 @ 50mm) to prevent primary failure. A clear cover of 20 mm at bottom and sides of the slab and column. as concrete cover with effective depth of (75mm) average of the two directions.

3.3 Details of Two-Way Reinforced Concrete Slabs (Group B)

Ten two-way reinforced concrete slabs with dimension of (1800×1100×100) mm, were cast in laboratory concrete of the technical institute of Amara and tested the all specimens were tested under four-point load. The load was transmitted to four points using frame which consisted of cross arm steel members with I section (320×80) mm and length 550mm. The slabs were designed to have flexural failure. All slab were identical in size but different in opening shapes, number and location as shown in Figure 3.2. isometric view of the slabs and the geometry and reinforcement details. the slabs were placed on two (1650×950) mm lines which were edge simply supported (supported on two opposite sides only). The slabs were internally reinforced isotopically with steel bars having reinforcement ratio of ($\rho=0.0105$) at the bottom in each direction (the flexural reinforcement was provided on the tension side only), with bars of (10mm) diameter and spaced at (100mm) in each direction. A clear cover of 20

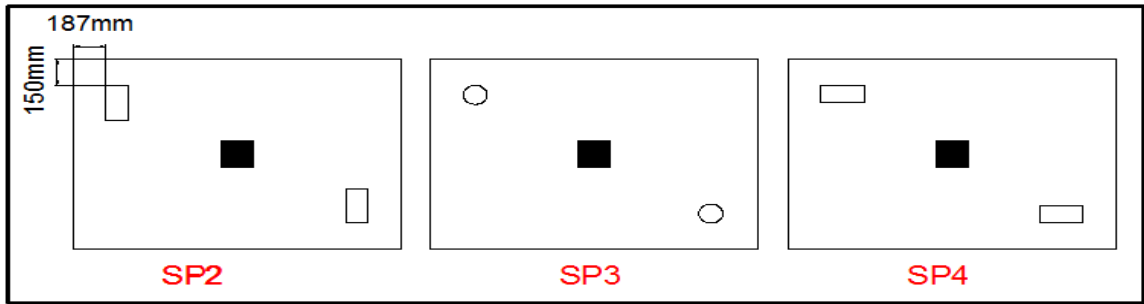
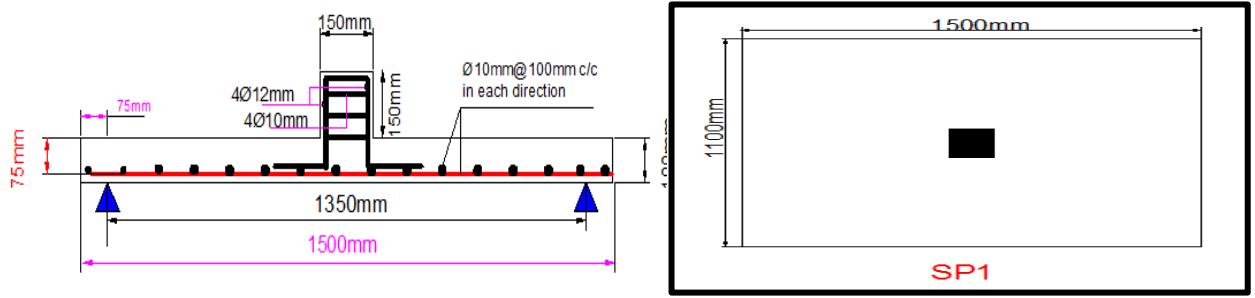
mm was delivered at bottom and sides of the slab as concrete cover with effective depth of (75mm) average of the two directions.

Table 3.1 Details of slabs specimens group A.

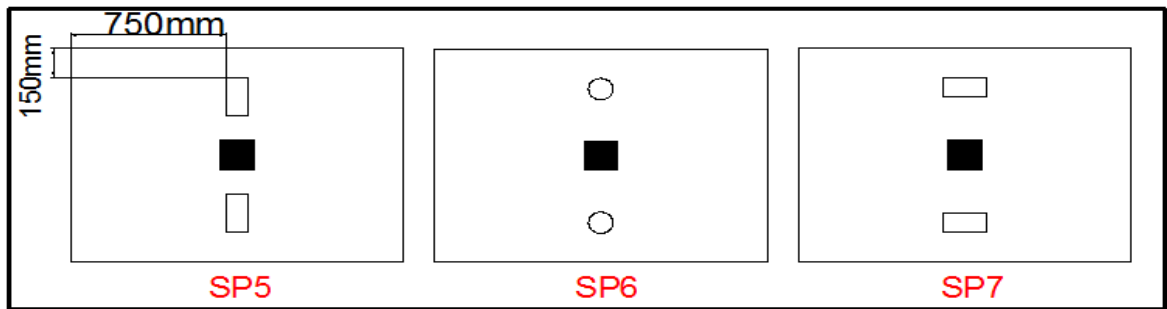
Group No	Slab	Dimensions (cm)			Column side Length cm	ρ	Opening shape	Opening size respectively (x,y) mm	Number of opening	opening Location in X-Y directions mm	V_f %	SF%
		Length	Width	Depth								
control	SP1	150	110	10	15	0.0105	without	---	0	---	0.5	20
A1	SP2	150	110	10	15	0.0105	rectangular	10×20	2	187-150	1	20
	SP3	150	110	10	15	0.0105	circle	11	2	187-150	1	20
	SP4	150	110	10	15	0.0105	rectangular	20×10	2	187-150	1	20
A2	SP5	150	110	10	15	0.0105	rectangular	10×20	2	750-150	1.5	20
	SP6	150	110	10	15	0.0105	circle	11	2	750-150	1.5	20
	SP7	150	110	10		0.0105	rectangular	20×10	2	750-150	1.5	20
A3	SP8	150	110	10	15	0.0105	rectangular	10×20	4	375-150	2	20
	SP9	150	110	10	15	0.0105	circle	11	4	375-150	2	20
	SP10	150	110	10	15	0.0105	rectangular	20×10	4	375-150	2	20

V_f = Volume fraction of fibers

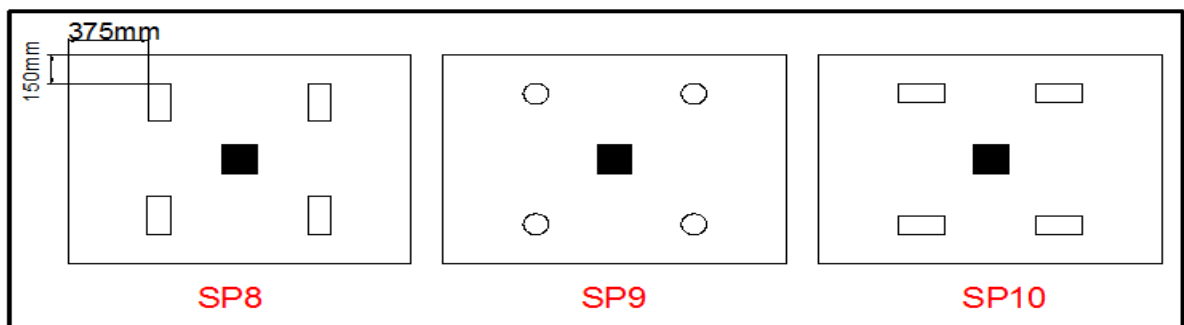
SF= Silica fume



Group A1



Group A2



Group A3

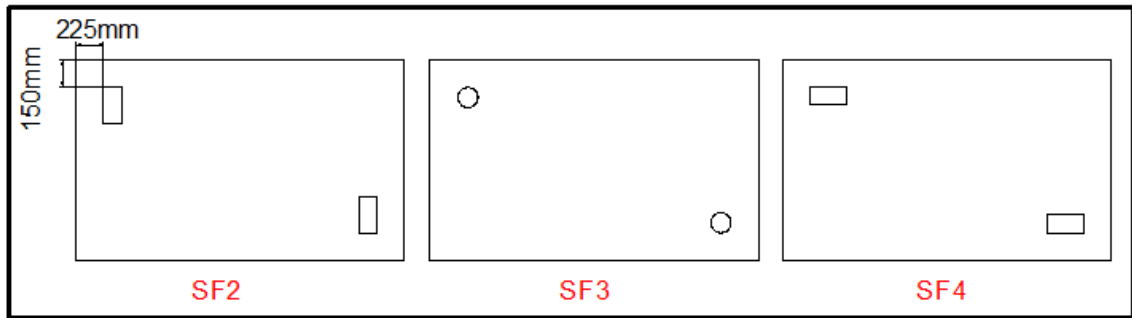
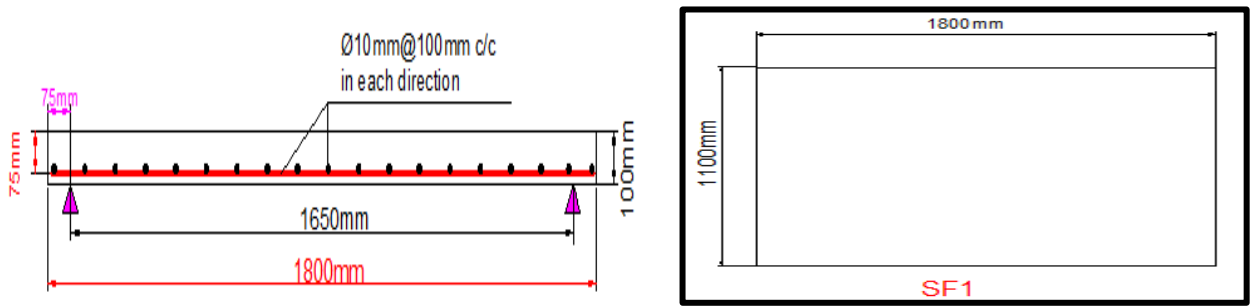
Figure 3.1 Details of slabs specimens group A.

Table 3.2 Details of slabs specimens group B.

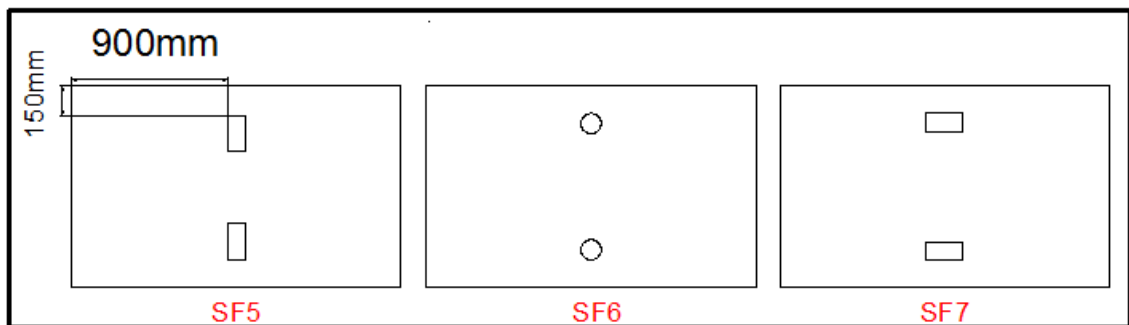
Group No	Slab	Dimensions (cm)			ρ	Opening shape	Opening size respectively (x, y) mm	Number of opening	opening Location in X-Y directions mm	V_f %	SF%
		Length	Width	Depth							
control	SF1	180	110	10	0.0105	without	---	0	---	0.5	20
B1	SF2	180	110	10	0.0105	rectangular	10×20	2	225-150	1	20
	SF3	180	110	10	0.0105	circle	11	2	225-150	1	20
	SF4	180	110	10	0.0105	rectangular	20×10	2	225-150	1	20
B2	SF5	180	110	10	0.0105	rectangular	10×20	2	900-150	1.5	20
	SF6	180	110	10	0.0105	circle	11	2	900-150	1.5	20
	SF7	180	110	10	0.0105	rectangular	20×10	2	900-150	1.5	20
B3	SF8	180	110	10	0.0105	rectangular	10×20	4	450-150	2	20
	SF9	180	110	10	0.0105	circle	11	4	450-150	2	20
	SF10	180	110	10	0.0105	rectangular	20×10	4	450-150	2	20

V_f = Volume fraction of fibers

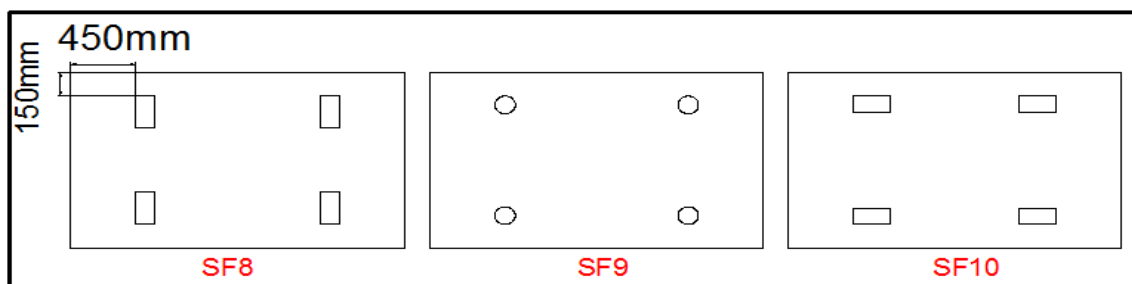
SF= Silica fume



Group B1



Group B2



Group B3

Figure 3.2 Details of slabs specimens group B.

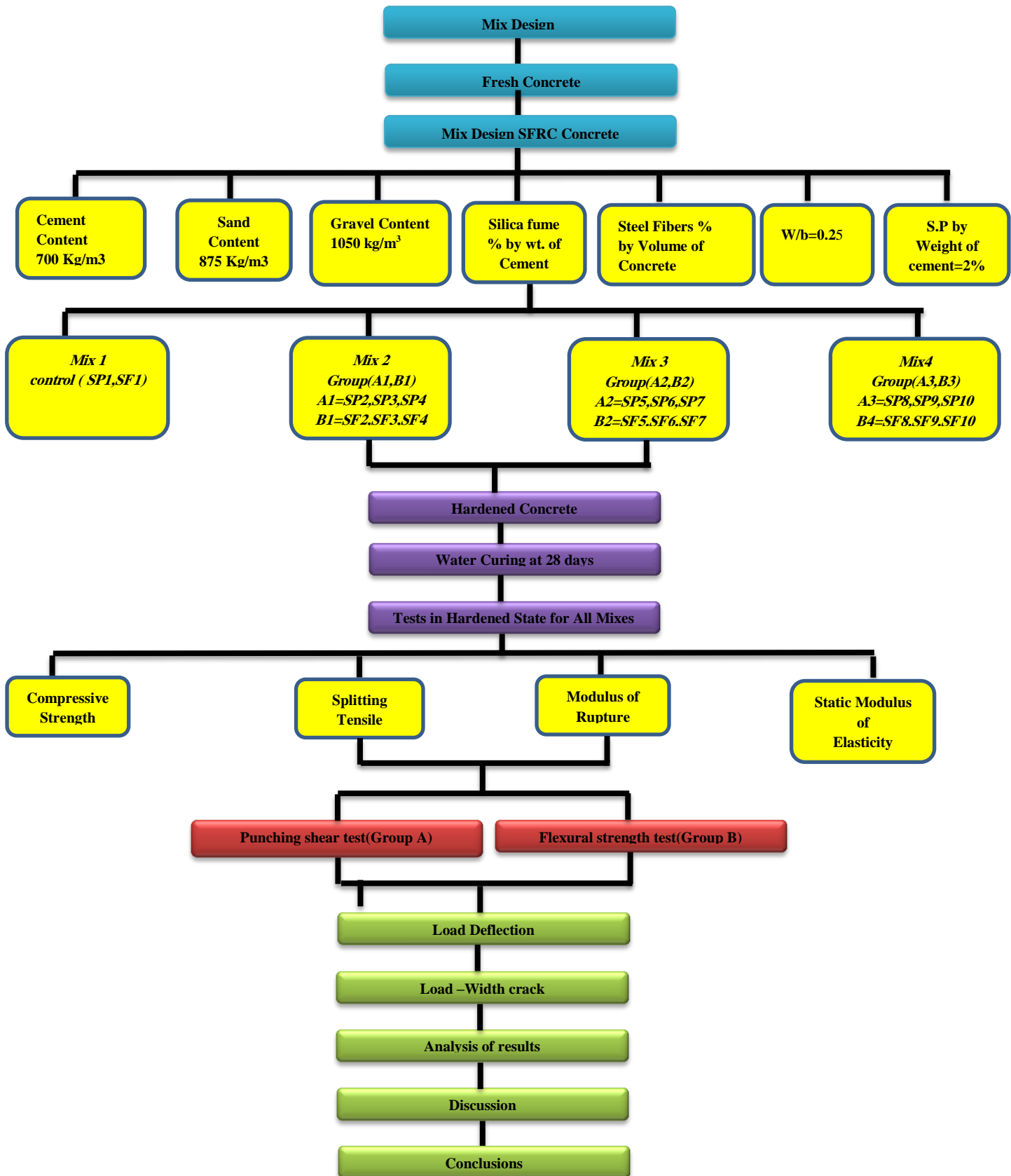


Figure 3.3 Main details of the followed experimental program throughout this research.

3.4 Test Variables

In this study five variables are investigated, openings shape, size, number and location and volume fraction of fibers (V_f). The specimens were cast, water cured for 28 days, air dried in the laboratory and then were tested to failure. The main purpose behind the project is to study the behavior of steel fiber reinforced concrete(SFRC) slabs with openings. To this aim the experimental program examined the effect of the following variables on the strength of SFRC slabs:

3.4.1 Volume Fraction of Fibers (V_f)

Four values of steel fibers with volume fractions of (0.5%,1%, 1.5%, and 2.0%), were used in casting the slabs, in order to study the effect of steel fiber content on the flexural strength and punching shear.

3.4.2 Openings Shape

Slabs may include different shapes of openings like (rectangular openings and circular openings). Therefore, a study was carried out to determine the effect of opening shape on the ultimate load capacity.

3.4.3 Openings Size

Two type opening sizes (rectangular (200×100) mm and (circular $D=110$) mm were selected to study its effect on the ultimate load capacity of slab.

3.4.4 Opening Location

The different opening locations and numbers were chosen to study their effect on the maximum load capacity slabs. The location of openings support from line.

3.5 Materials

General description and specification of the materials used in the test program are listed below:

3.5.1 Cement

Ordinary Portland cement (type I) was used in this work. It was stored in suitable conditions to avoid any exposure to the moisture. The chemical analysis and physical test results of the used cement are given in Tables 3.3, 3.4 and Table 3.5 respectively. The tests are done in the laboratory of the Technical Institute of Amara according to the Iraqi Specification No.5/1984 [51] and ASTM C150 [52].

Table 3.3 Chemical analysis of cement.

Compound Composition	Chemical composition	Content %	Limits of IQS 5:1984 (%)	ASTM C150 max %
Lime	(CaO)	60.4	-----	-----
Alumina	(Al ₂ O ₃)	5.32	-----	6
Magnesia	MgO	2.62	<5	----
Iron oxide	(Fe ₂ O ₃)	2.58	-----	6
Sulphate	(SO ₃)	2.5	<2.8	3
Loss on ignition	(L.O.I)	2.6	<4	3
Insoluble residue	I.R	<1.5	0.8	0.75
Lime saturation	(L.S.F)	0.89	0.66 -1.022	-
Silicone oxide	(SiO ₂)	27.21	-----	-----

Table 3.4 Main Compounds (Bogue's equation) percentage by weight of cement

Tri Calcium Silicate (C ₃ S)	48.10
Di Calcium Silicate (C ₂ S)	20.82
Tri Calcium Aluminate (C ₃ A)	12
Tetra Calcium Alumina Ferrite (C ₄ AF)	8

Table 3.5 Physical properties of the cement.

Physical Properties	Test result	Limit of IQS 5:1984	ASTM C150
Fineness utilizing Blain-air permeability apparatus (m ² / kg)	310	≥230	(280)Minimum
Soundenes	0.19%	<0.8	≥5%
Setting-time utilizing Vicat's instrument			
Initial (min)	90	≥ 45min	≥ 45min
Final (hr)	4	≤10 hrs	≤10 hrs
Compressive strength at:			
3 days (MPa)	15.2		
7 days (MPa)	19.5	≥15	≥12
28 days(MPa)	35	≥23	≥10

3.5.2 Fine Aggregate (Sand)

Natural graded sand with modulus of fineness 2.8 was supplied from Al-Basra Province in order to use it in all types of concrete mixes within this research for pouring the specimens. Sieve analysis was carried out on sand sample to check its limits (gradation zone II) according to the Iraqi specifications No. 45/1984 [53] and ASTM C33 [54]. The results of these tests have been listed in Table 3.6 and Table 3.7. Figure 3.4 shows the gradation of the sand according to the IQS No. 45/1984.

Table 3.6 Grading of the fine aggregate.

NO	Sieve size mm	Passing(%) by weight		
		Percentage finer	Limits of IQS No. -45/1984 zone II	ASTM C33-03
1	10	100.00	100	100
2	4.75	96.80	90-100	95-100
3	2.36	85.60	75-100	80-100
4	1.18	73.60	55-90	50-85
5	0.60	36.00	35-59	25-60
6	0.30	17.60	8-30	5-30
7	0.15	1.40	0-10	0-10

Table 3.7 Physical properties of fine aggregate.

Physical properties	Test results	Limits of Iraqi specification No.45/1984
Specific gravity	2.65	----
Fineness modulus	2.8	----
Sulfate content %	0.33%	$\leq 0.5\%$
Absorption %	1.5	----
Chloride content(CI)	0.072%	$\leq 0.1\%$
Loose bulk density kg/m^3	1645	----

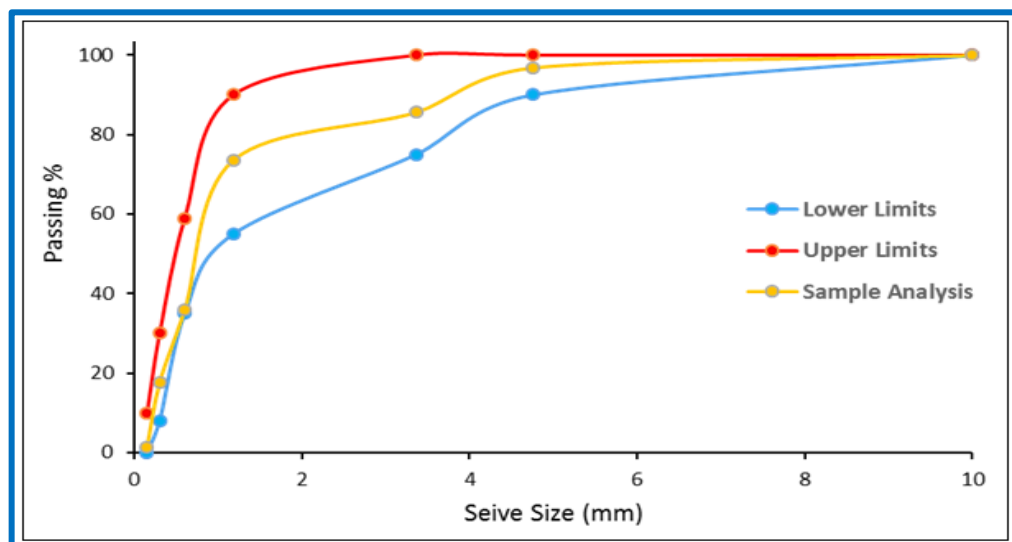


Figure 3.4 Gradation of sand sample

3.5.3 Coarse Aggregate

Crushed gravel of 10 mm maximum size was supplied from north of Misan Province to be use in all types of concrete mixes. The results indicate that, the coarse aggregate grading is within the requirements of Iraqi specification No. 45/1984 [53]and ASTM C33 [54]. The coarse aggregate was washed to remove the dust, then exposed to air to dry the surface, and then stored in a saturated-surface dry state before use. Grading and properties of the aggregate are presented in Tables 3.8 and 3.9 and represented in the Figure 3.5.

Table 3.8 Grading of coarse aggregate.

NO	Sieve size (mm)	Passing(%)		
		Percentage Finer	Limits of IQS No.45/1984	ASTM C33-03
1	12	100	90-100	90-100
2	10	95	85-100	85-100
3	4.75	8	0-25	10-30
4	2.36	3	0-5	0-10

Table 3.9 Properties of coarse aggregate.

Physical properties	Test results	Limits of IOS No.45/1984
Specific gravity	2.63	-
Sulfate content(SO ₃)	0.073%	≤ 0.1 %
Absorption	0.65%	-
Chloride content(Cl)	0.092%	≤ 0.1 %
Loose bulk density kg/m ³	1548	-

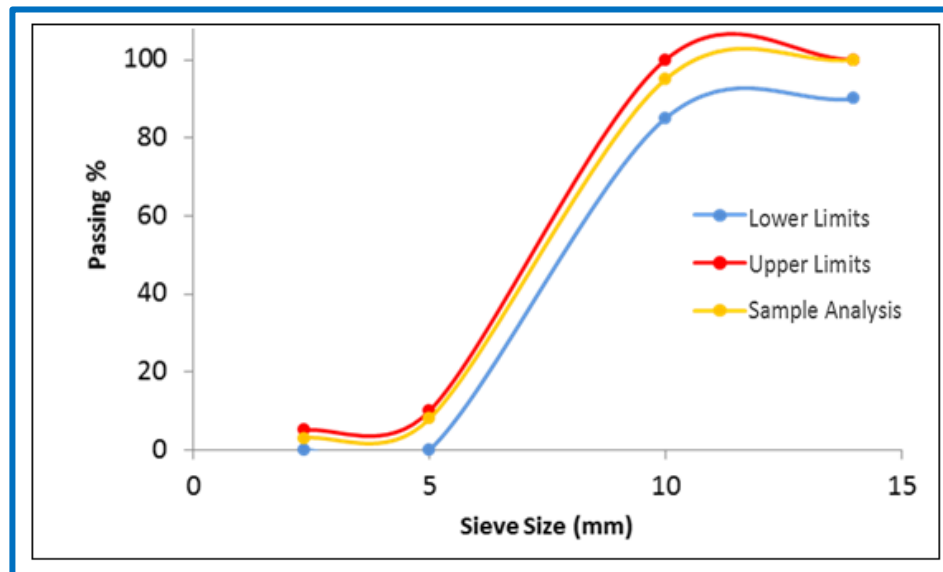


Figure 3.5 Gradation of gravel sample

3.5.4 Hooked-End Steel Wire Fiber (HESF)

Steel fibers are generally made from carbon steel or stainless steel the latter is used in facilities that require the use of corrosion resistance. Steel fibers is used in many kinds of concrete due to its ability to improve the mechanical properties of concrete. Benefits of steel fiber reinforced concrete [55]:

- 1-Increases tensile strength and toughness.
- 2- Resistance to impact.
- 3-Resistance to freezing and thawing.
- 4- Shrinkage reduction.
- 5-Reduced cracking.
- 6-Reduced tiling thickness.

Steel fibers are used in this study (hooked-end).This type of steel fiber is manufactured by (Hebei Yusen Metal Wire Mesh Company ltd. Company, China), were used as shown in Figure 3.6.The steel fiber used throughout this investigation conformed to the requirements of ASTM A820 [56].This type of steel fiber is classified as (Type II). The properties of the steel fibers are presented in Table 3.10. According to [57], the steel fibers usually range from

0.25 to 2 percent by volume. Random propagation was used to the steel fibers. The addition of steel fibers to high performance concrete does not have an effective impact on compression strength , while it has a noticeable effect on tensile and bending resistance also reduce the width of cracks during the bending check [23].



Figure 3.6 Shape of hooked steel fiber.

Table 3.10 Properties of steel fibers.

Property	Specifications
Density	7800 kg/m ³
Ultimate strength	1200 MPa
Modulus of Elasticity	210 x 10 ³ MPa
Strain at proportion limit	5650 x 10 ⁻⁶
Poisson's ratio	0.28
Average length(L_f)	30mm
Nominal diameter(D_f)	0.50mm
Aspect ratio (L_f/D_f)	60

3.5.5 Mixing Water

Reverse osmosis (R.O.) water is used for mixing all concrete mixes and also for curing purpose.

3.5.6 Superplasticizer

The water cement ratio affects many characteristics of the concrete mix, so, using a high range water reducer (HRWR) admixture works to improve the fresh concrete properties by reducing the quantity of water added to the mix and increasing the workability without segregation or bleeding. The properties of the concrete mix will be improved by using HRWR such as the concrete compressive strength, density, permeability, the cracks due to shrinkage, less vibration required and Improved surface finish. In this study Sika ViscoCrete - 5930 superplasticizer type was used as shown in Figure 3.7. It's met the requirements of ASTM C494[58]. Type was used for the present study. The properties of the are presented Sika ViscoCrete - 5930 in Table 3.11.



Figure 3.7 Sika ViscoCrete – 5930.

Table 3.11 Properties of superplasticizers (Sika ViscoCrete – 5930).

Appearance	Turbid liquid
Density	1.095kg/lt
Chloride content	NIL
Colour	Turbid
Basis	Aqueous solution of modified Polycarboxylate
Storage condition /shelf life	12 months if stored at temperatures between 5°C and 35°C

3.5.7 Silica Fume

Natural pozzolanic materials have become a significant source in the production of essential materials that enter in the composition of high performance concrete mixtures, including micro-silica and fly ash, but the micro-silica is more effective than fly ash. Micro silica is one of the necessary materials production of high density concrete ,which is commercially called as silica fume or micro-silica or condensed Silica Fume and others.

Silica fume is an ultrafine material with spherical particles less than (0.1 μm) in diameter, the average being about (0.15 μm), this makes it approximately 100 times smaller than the average cement particle. The microsilica used in this work conforms to the chemical and physical requirements of ASTM C1240 [59], as shown in Figure 3.8. Tables 3.12 and 3.13 show the chemical and physical test.

The American concrete Institute ACI 234R [60], define silica fume as "very fine non-crystalline silica produced in electric arc furnaces as a by production of elemental silicon or alloys containing silicon. Silica fume was added to Portland cement concrete to improve its properties such as its compressive strength, bond strength and abrasion resistance. These improvements stem from both the mechanical improvements resulting from the

addition of very fine powder to the cement paste mix as well as from the pozzolanic reactions between the silica fume and free calcium hydroxide in the paste. Addition of silica fume also reduces the permeability of concrete to chloride ions, which protects the reinforcing steel of concrete from corrosion. Especially in chloride-rich environments such as coastal regions and those of humid continental roadways and runways (because of the use of deicing salts) and saltwater bridges [61].



Figure 3.8 Sags of silica fume used in present study.

Table3.12 Physical composition of silica fume.

Requirement	Analysis%	Limit of Specification Requirement ASTM C1240
SiO ₂	88.21	Min 85%
Moisture content	0.72	Max 3%
Loose on ignition	4.32	Max 6%
Percent Retained on 45µm (No.325) Sieve, Max	8	Max 5%
Accelerated Pozzolanic Strength Index with Portland cement at 7 days, Min. percent of control	129.1	Min 105
Specific Surface, Min, m ² /g	21	Min 15

Table 3.13 Chemical Composition of Silica Fume.

Compound composition	Chemical Composition	Oxide Content (%)	Limit of Specification Requirement ASTM C1240
Lime	CaO	0.5	---
Iron Oxide	Fe ₂ O ₃	1.4	---
Alumina	AL ₂ O ₃	0.5	---
Silica	SiO ₂	92.1	85(min)
Magnesia	MgO	0.3	---
Sulphate	SO ₃	0.1	---
Potassium oxide	K ₂ O	0.7	---
Sodium oxide	Na ₂ O	0.3	---
Loss on ignition	L.O.I	2.8	6(max)

3.5.8 Steel Reinforcement

In this research, two sizes of the deformed steel reinforcement were used ($\phi 10$, $\phi 12$) mm, a square mesh of with a 10mm diameter bar spaced at 100 mm in two directions in the tension face of the slab group (A,B) as shown in Figure 3.7, a clear cover of 20mm was provided below the mesh all specimens. In the group (A) use 4 deformed bar $\phi 12$ mm were used for column stub to prevent the crushing of the column during loading, and use 4 deformed $\phi 10$ mm steel reinforcement (stirrups). Three samples were tested for each bar diameter and the average of the results was used. According to ASTM A615[62], Figure 3.9 shows stress-strain curve of steel bar and Figure 3.10 shows the tensile strength of reinforcement test bars and tested until ruptures. The recording data is listed in Table 3.14. The tests were carried out in the accomplished in the Technical Institute of Amarah laboratory using the testing machine SANS (1000 kN). All the steel rebar were Ukrainian origins.

Table 3.14 Properties of steel reinforcement.

Nominal diameter (mm)	Actual diameter (mm)	Area (mm ²)	Yielding Stress (MPa)	Ultimate Strength (MPa)	Elongation %
10	9.68	78.5	488	610	16
12	11.77	113.04	562	665	15

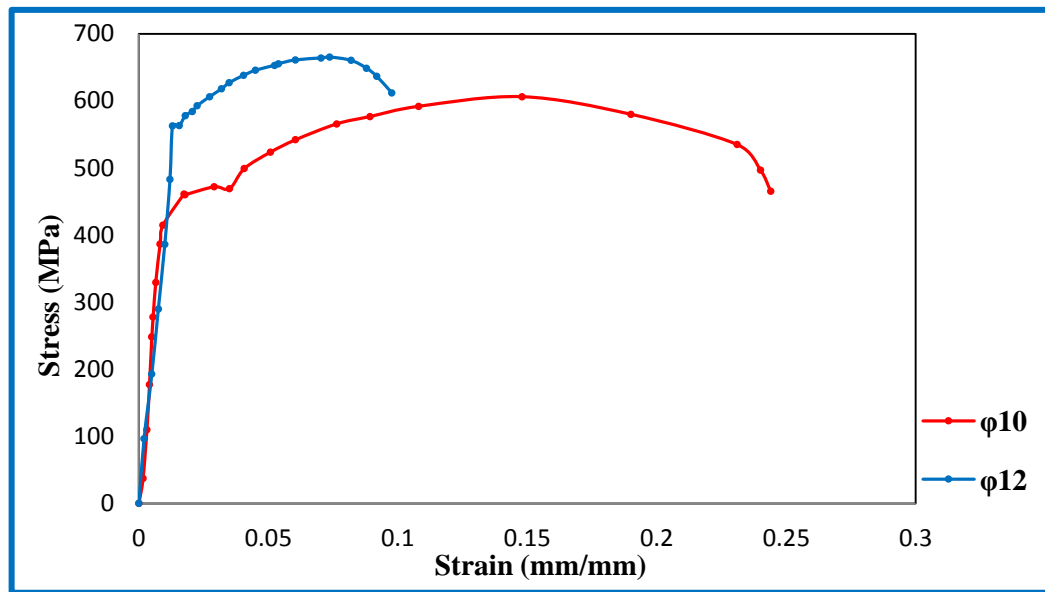


Figure 3.9 Stress-strain curve of steel bar

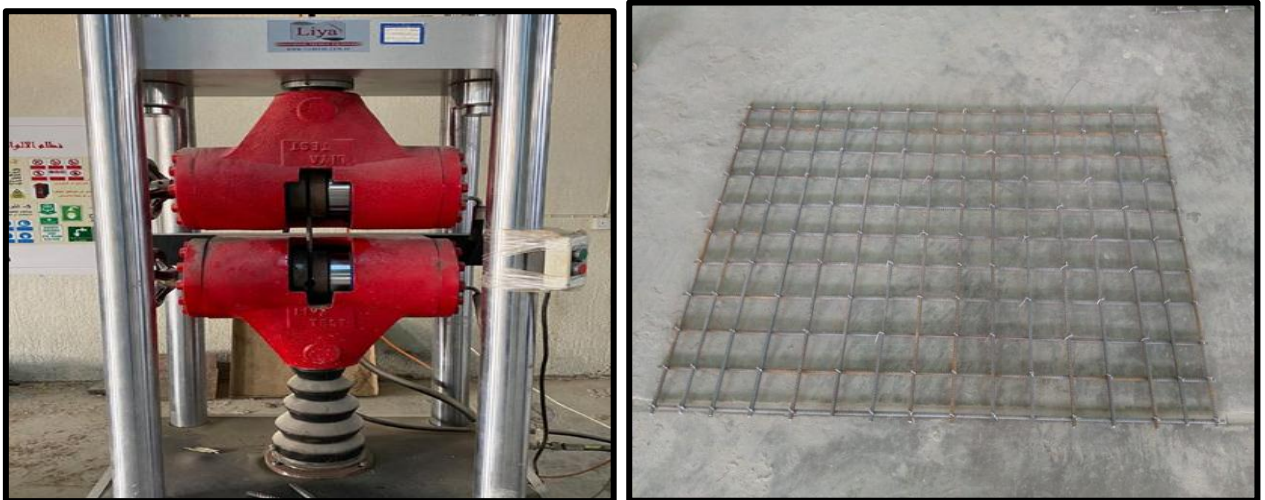


Figure 3.10 Testing machine of steel reinforcement.

3.6 Control Specimens

Control specimens were taken from mix used in casting the HPC slabs to investigate the mechanical properties of SFRC used, such as compressive strength, splitting tensile strength, modulus of rupture modulus of elasticity. The details of these specimens are shown in Table 3.15.

Table 3.15 Details of control specimens.

Type of test	Type of specimen	Specimen dimension(mm)
Compression	Cube and Cylinder	(100×100×100) and 100×200
Splitting tensile strength	Cylinder	100×200
Modulus of elasticity	Cylinder	100×200
Modulus of rupture	Prism	100×100×500

3.7 Moulds

Wooden formwork is used for casting all concrete panels (A, B). In this study twenty samples are taken. Each mold consists of a bed and four movable sides. The sides are fastened to the bed screws from the bottom face of the bed. These screws can be easily removed from the wooden profile to .Take out the side of the wooden Figure 3.11.The clear dimensions of the molds of group (A) were(1500×1100×100)mm, and also in this group a column with dimensions (150×150)mm of wood and the dimensions of group (B) were (1800x1100x100)mm.The openings was made by using wooden form with the size(200x100x100),(length ,width and thickness) and utilizing PVC pipes with diameter (Φ 100mm).The openings was fixed in their correct positions using bolts.Forms were sufficiently tight to prevent leakage of mortar.



(a)



(b)

Figure 3.11 Molds of slabs.

3.8 Concrete Mix Design

Four types of SFRC mixes were used in the present research so that the influence of the fibers on mechanical properties of the SFRC is investigated. The variables used in these mixes were the ratio of the volume ratio of steel fibers (four volume ratios were considered (0.5, 1, 1.5 and 2%), as shown in Table 3.16

were used to cast the slabs specimens as well as their control specimens. It was found that the used mixture produces high workability and uniform mixing of concrete without segregation.

Table 3.16 properties of different types of SFRC mixes.

Materials	Mix 1	Mix 2	Mix 3	Mix 4
Cement kg/m ³	600	600	600	600
Sand kg/m ³	875	875	875	875
Coarse aggregate kg/m ³	1050	1050	1050	1050
Silica fume %	20	20	20	20
Silica fume kg/m ³	120	120	120	120
w/b	0.25	0.25	0.25	0.25
Superplasticizer %	2	2	2	2
Superplasticizer kg/m ³	12	12	12	12
Steel fiber %	0.5	1	1.5	2
Steel fiber kg/m ³	39	78	117	156

3.9 Mixing Procedure

The concrete mixing process affects the quality of the concrete in the hardened phase, and the materials must be from mixture is homogeneous throughout the concrete to avoid weaknesses patterns the strength of the cohesion between the concrete depends on the correct mixing process. The concrete is mixed by using a horizontal rotary mixer with. The batching carried out in the laboratory of concrete of the technical institute of Amara. The steps of mix are following:

- 1- All required materials for each mixture are weighed and placed in a clean area.
- 2- Sand and gravel are washed by clean water and leave about to dry before mix.
- 3- The cement, silica fume and sand were mixed in dry state for 3minutes.

- 4- Add gravel and sand to the dry mixture and mix for 3 minutes.
- 5- Add 75% of the required water was added to the dry materials and mixed for 3 minutes.
- 6- Steel fibers were uniformly distributed into the mix slowly in 5 minutes.
- 7- Finally, mix the remainder water with superplasticizer (Sika ViscoCrete - 5930) and added to the mixture.
- 8- Continue the mixing process to obtain a homogeneous and thick paste mixture.
- 9- The total estimated time to finish the mixing process took 25-30 minutes.

3.10 Casting Procedure

Before casting, all specimen moulds were well cleaned thoroughly, tightened well and their internal surfaces were lightly oiled to avoid and prevent the adhesion of hardened concrete to the internal surface of the molds. Steel reinforcement was placed in the bottom face of the slabs mold and fixed at their correct position inside the slabs molds .The reinforcing steel bars were isotropically arranged along the two orthogonal directions of the mold and carefully placed in position by using tying wires then laid on the ground and leveled with small wood pieces at the bottom of the plywood die (for leveling purpose) and then the formwork is leveled with a manual bubble leveling tool as shown in Figure 3.12. In order to obtain a constant clear cover, small pieces of steel wires having 10-mm diameters were placed under the bottom layer of the reinforcement mesh then all specimens molds were filled with concrete mix and compacted by using external vibrating to remove the entrapped air voids as much as possible and to get well compacted concrete and consolidate the mix into the mold, the process of vibration was continued until no further air bubbles appeared on the surface and the slab surface was then carefully leveled. The time of vibration for each layer was limited. For cylinders, cubes and prisms, the

cylinders were filled with fresh concrete by means of scoop in three equal layers and prism moulds were filled with concrete in two equal layers, each layer was compacted using the same vibrating. The compaction was affected by means of a vibrating for a period of 15 seconds/ layer for (100mm cubes) and(100×200)mm cylinder and (100×100×500)mm prism [63]. For slabs, two layers were used to cast the slabs as shown in Figure 3.9. The top layer had been compacted, and the top surface of the specimen molds was leveled and well finished using a steel trowel. The duration of vibration for each layer was limited to the removal of entrapped air as much as possible and the surface of the concrete became relatively smooth and had a glazed appearance.



(a)

(b)



(c)

Figure 3.9 Casting of the specimens

3.11 Curing Procedure

All specimens were cast, cured and tested under laboratory conditions at the concrete lab of the laboratory of concrete of the technical institute of Amara casting stage, all specimens were covered with plastic nylon sheets and cover it by wet rib to prevent evaporation and loss of moisture from fresh concrete until final set had occurred and avoid cracks associated with water-loss shrinkage as shown in Figure 3.13. After 24 hours, the specimens (slabs and cubes, cylinders and prisms) are taken out of the molds, marked and then cured in water tank for 28 days, at the end of the curing period, all specimens were removed from water and kept in laboratory until date of testing.



(a)



(b)



(c)

Figure 3.13 Curing of the specimens.

3.12 Tests Concrete Mixtures

3.12.1 Fresh Concrete Tests (Slump Test)

Workability is one of the important properties defining the fresh properties of concrete and Concrete is said to be workable when it had appropriate consistency, handled without segregation, cast without loss inhomogeneity and compacted with less effort. This test is prescribed according to ASTM C143 [64], as shown in Figure 3.14 . The test results are presented in Table 3.17.

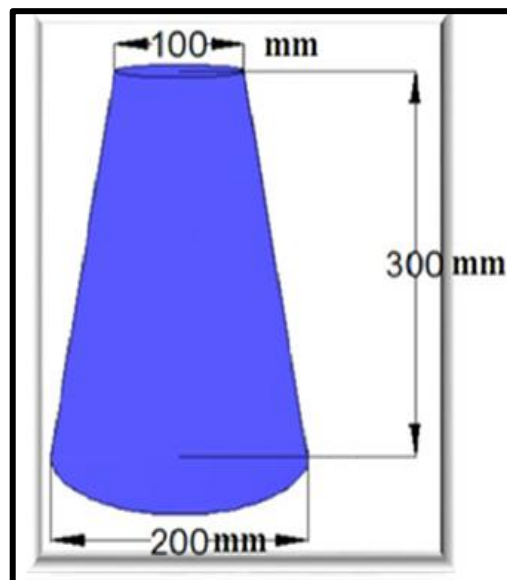


Figure 3.14 The slump cone used in the slump test.

Table 3.17 Results of slump test results of various types of SFRC mixes.

Mix Type	Mix 1	Mix 2	Mix 3	Mix 4
Slump Test (mm)	175	165	145	120

3.12. 2 Hardened Mechanical Tests

3.12.2.1 Compressive Strength

The compressive strength test was determined according to B.S-1881part 116 [65], (100x100 mm) cube and with ASTM C39 [66], (100x200 mm) cylindrical were used to determine compressive strength of SFRC using a hydraulic universal digital compression testing machine (ELE-Digital Elect 2000) of 2000 kN capacity available at the laboratory concrete of the technical institute Amara as shown in Figure 3.15 .The test results are presented in Table 3.18.



Figure 3.15 Compressive strength test.

Table 3.18 Average Compressive results of various types of SFRC mixes.

Mix Type		Mix 1	Mix 2	Mix 3	Mix 4
7 day	f'_c (MPa)	56.3	66.75	73.21	78.7
	f_{cu} MPa	59.3	68.5	77.6	81.94
28 day	f'_c	72.2	81.4	88.15	91.6
	f_{cu}	76	85.7	92.8	96.4

f'_c =Cylinder Compressive, MPa

f_{cu} =Cube Compressive ,MPa

3.12.2.2 Splitting Tensile Strength (F_{sp})

To test the tensile strength of the concrete, there are several methods of testing, but the most common and easiest method at the moment is the Brazilian method which is the indirect tensile strength test conforming to ASTM C496 [67]. Splitting tensile strength test was conducted on cylinders of (100×200)mm cylinders were tested at 28 days and the average of splitting tensile strength of three cylinders was adopted for every mix. The test results are presented in Table 3.19. The splitting tensile strength was determined using the same machine as for compressive strength as shown Figure 3.16. The splitting tensile strength of the specimens was calculated by using the following formula:

$$F_{sp} = \frac{2p}{\pi dl} \quad \text{.....3.1}$$

F_{sp} = Splitting Tensile Strength (MPa) p = Maximum applied load (N)

d = Diameter of cylinder (mm) L = Length of cylinder (mm)



Figure 3.16 Splitting tensile strength test.

Table 3.19 Average splitting results of various types of SFRC mixes.

Mix Type	Mix 1	Mix 2	Mix 3	Mix 4
F_{sp} (MPa)	4.86	6.8	8.54	10.21

3.12.2.3 Modulus of Rupture (F_r)

The flexural strength tests were carried out by using three (100 x 100 x 500) mm simple support prisms loaded at third points. Flexural strengths were determined by using three prisms for 28 days. The simply supported prisms were tested using one points load with clear span of 430 mm. Flexural strength tests were carried out on specimens in accordance with ASTM C78 [68]. The tests was done in the laboratory of concrete of the technical institute of Amara by using flexural machine as shown in Figure 3.17. The test results are presented in Table3.20. The results of tests are calculated by the mathematical formula below:

$$F_r = \frac{3pl}{2bd^2} \quad \dots 3.2$$

F_r = Modulus of rupture (MPa), p = Failure load (N), l = Length of span (mm)

b = Width of specimen (mm), d = Depth of specimen (mm)



Figure 3.17 Modulus of rupture test.

Table 3.20 Average flexural results of various types of SFRC mixes.

Mix Type	Mix 1	Mix 2	Mix 3	Mix 4
F_r (MPa)	6.4	9.54	11.32	13.65

3.12.2.4 Static Modulus of Elasticity (E_c)

Measurements of the static modulus of elasticity are made according to ASTM C469 [69]. This test was carried out on (100x200mm) cylindrical specimens. 40% of ultimate compressive strength was applied on the cylinders. The same testing machine used in to obtain the compressive strength was used to find the static modulus of elasticity as shown in Figure 3.18 . The specimens were tested at age of 28 days. The test results are presented in Table 3.21. The average of three specimens was taken every mix. Static modulus of elasticity is calculated by the following equation:

$$E_c = [(S_2 - S_1) / (e_2 - 0.00005)] \times 10^{-3} \quad \dots\dots 3.3$$

E_c = static modulus of elasticity of, GPa,

S_2 = stress corresponding to 40% of ultimate load MPa

S_1 = stress corresponding to a longitudinal strain (0.00005)

e_2 = longitudinal strain produced by stress S_2



Figure 3.18 Modulus of elasticity.

Table 3.21 Average modulus of elasticity of various types of SFRC mixes.

Mix Type	Mix 1	Mix 2	Mix 3	Mix 4
E_C (GPa)	33.16	36.63	40.52	43.72

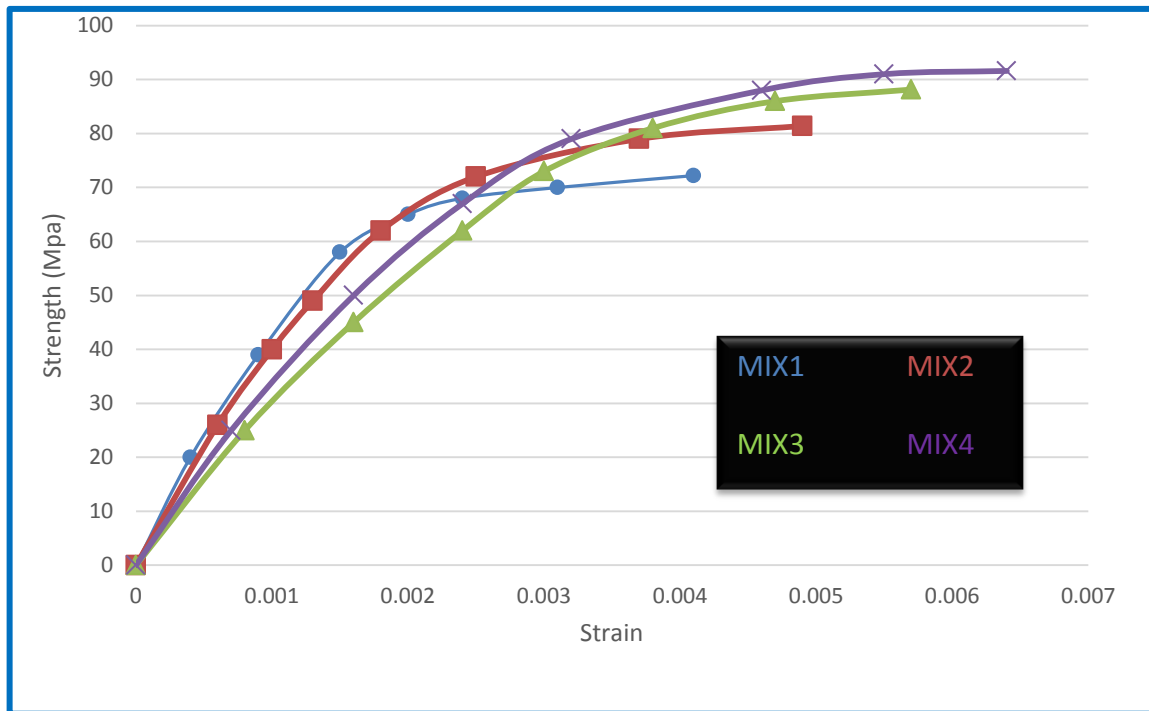


Figure 3.19 Experimental stress-strain curves for SFRC cylinders in compression the all mixes.

3.13 Test Measurement and Instrumentation

3.13.1 Load Measurement

All the specimens (A,B) of HPC two-way slabs are tested by using hydraulic jack with a maximum range capacity of 600 kN as shown in Figure 3.20. The tests was done in the laboratory of concrete of the technical institute of Amara.



Figure 3.20 Testing mechanism.

3.13.2 Supports and Loading Conditions

All slab group (A,B) specimens are tested using steel frame with hydraulic jack shown in Figure 3.16, with a maximum capacity of 600 kN. The slab group (A) was a rectangular with dimensions (1500 x 1100 x 100) mm (Knife edge), simply Supported along all four edges with a pronounced extension of (1350 × 950)mm for each direction .A special supporting frame was manufactured and used inside the testing machine, as shown in Figure 3.21.To provide the required span of the slab. This supporting frame was made using four steel beams welded and arranged to form a rectangular shape. Each of these four steel beams had a 25 mm dia. Steel bars are welded on its top face to provide a simple support for the slab edges, resting on rigid steel frame subjected to a central concentrated load over the area of column. All four support lines are 75 mm from the slab edges. Slab group (B) was a rectangular with dimensions (1800 x 1100 x 100) mm with their two edges simply supported, simply Supported along two edges with a clear span of (1650)mm. A special supporting

frame was manufactured and used inside the testing machine, as shown in Figure 3.22. To achieve a simply supported condition, steel beam (25mm) diameter was welded to the top flange resting on rigid steel frame subjected to a central concentrated load. Two edges support lines are 75 mm from the slab edges. The slabs are tested under static loads loaded in successive increments, up to failure. For each increment, the load is kept constant until the required readings are recorded.



Figure 3.21 Steel frames group (A).



Figure 3.22 Steel frames group (B).

3.13.3 Deflection Measurement

Dial gauge placed at mid of the bottom face of all slabs for measuring the deflection. At reading each load, deflection measured also by dial gauge. accuracy was 0.01mm and maximum measure was 5cm, as shown in Figure 3.23.



Figure 3.23 Dial gauge of deflection.

3.13.4 Crack Width Measurement

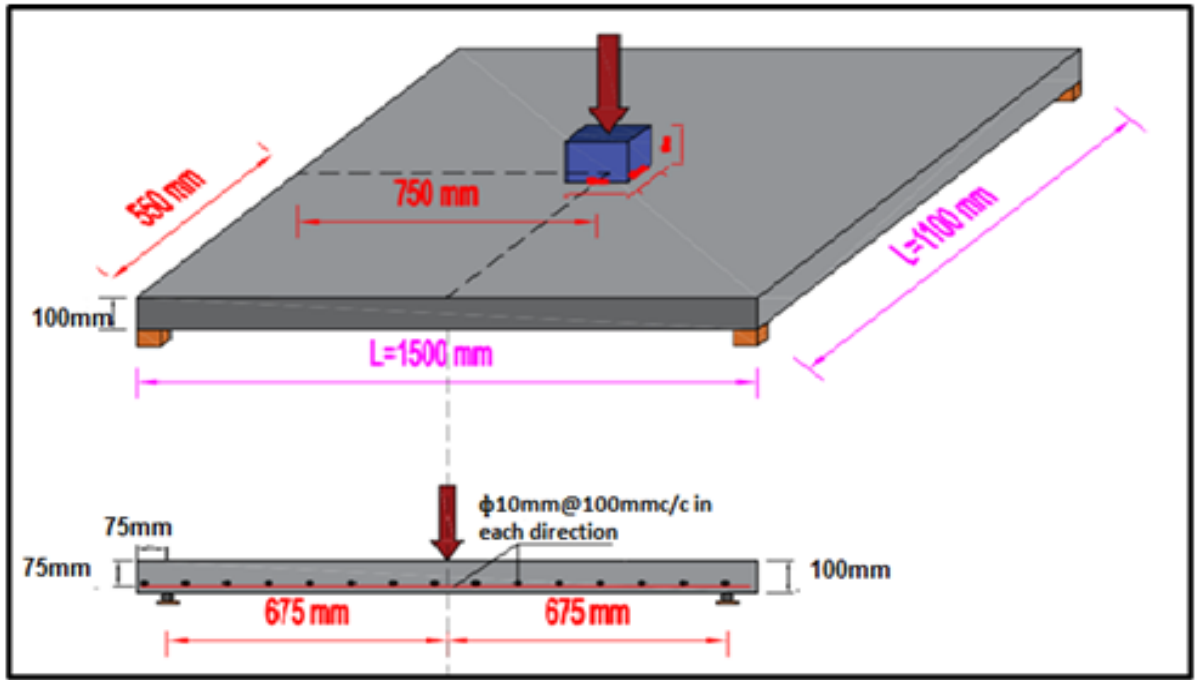
Crack propagation was mapped on the slab, and maximum crack widths were measured approximately with a microscope with 0.02 mm accuracy, as shown in Figure 3.24. The measurement point of crack was located on the first crack at and continued to determine the width of crack until failure occurs.



Figure 3.24 Cracks reader.

3.14 Testing Procedure

At the end of curing (28 days), all the specimens are kept dry in the laboratory for 24 hours before testing. During this time and before testing the slabs, the tension faces of the slabs were cleaned and painted white in order to help in locating the cracks and slabs were labeled. All the slab group(A) specimens are tested under monotonically increasing load up to failure. The load is applied vertically at the center of the top face of column over reinforced concrete slabs. Then the initial deflection is recorded and the specimens are loaded with constant rate of loading, and the load is increased gradually up to failure of the slab. Readings of central deflection are recorded at each load intervals. Also the crack formation and propagation are examined at each load step, as well as recording the first crack load and the failure load of the slab, Testing mechanism of slab specimens are shown in Figure 3.25. All the slab specimens of group (B) are tested under monotonically increasing load up to failure. The test specimen was laid on two edges simply supported rigid steel beams. The effective flexural span in direction was (1650) mm. A system of stiff steel beams was used tested under four points loading which applied on the slab by external frame in order to divide the total applied point load into four point loads applied on the slabs .The four load-application areas were at one-third position of the span. Forming a grid (320 × 550) within the effective flexural span as shown in Figure 3.26. Loading frame with four point part were then placed over the plate by which the load was transferred to the slabs from the loading frame bridge .To avoid concentration of high local stresses in these areas, square steel pads of dimensions (80× 80 ×30 mm), were placed in between the top of the slab and the stiff steel beams. The distance between the span loading points is (320mm) with moment arms of (550mm) at both sides of the four points loading.

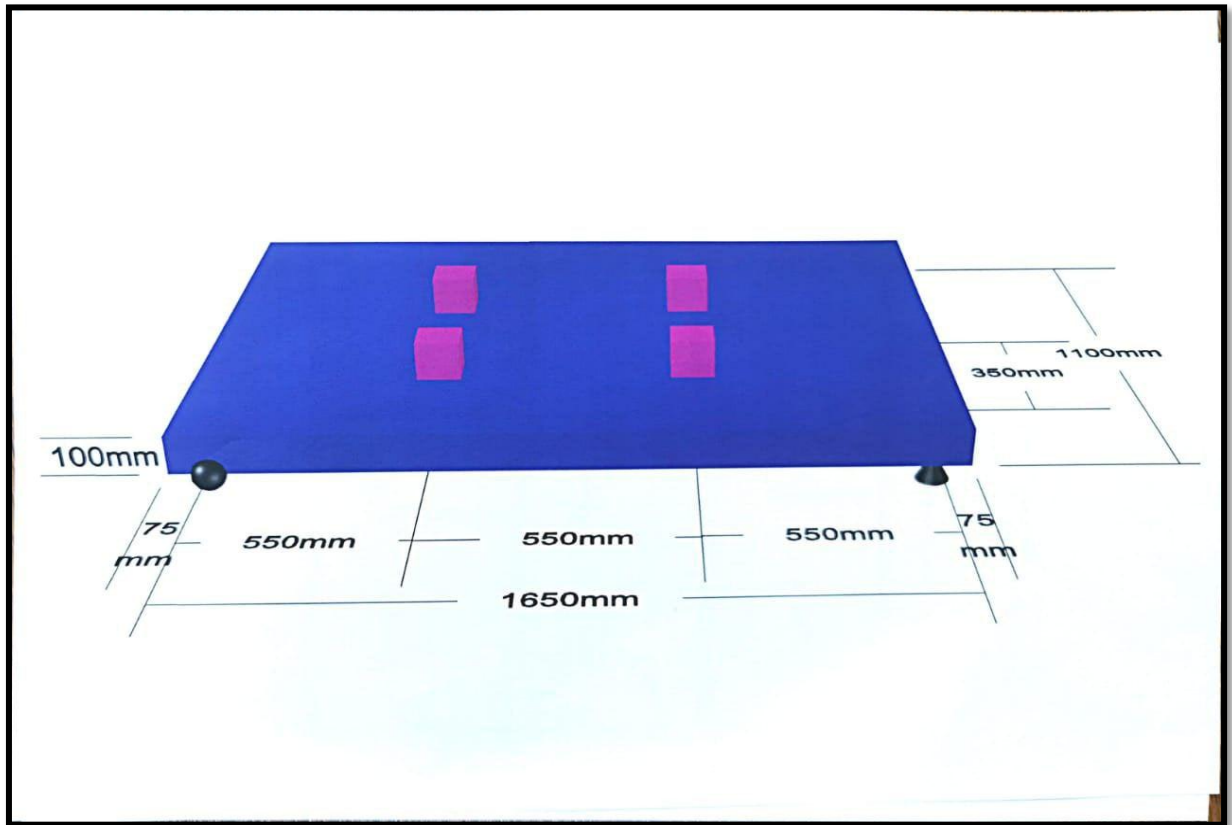


(a)



(b)

Figure 3.25 Test procurer group (A).



(a)



(b)

Figure 3.26 Test procurer group (B).

CHAPTER FOUR

RESULTS AND DISCUSSIONS

4.1 General

In this thesis, the reduced scale model are considered which included testing the concrete slabs with reduced dimensions of 1500 x 1100 x 100 mm for the first series of concrete slabs that designed to fail in punching shear. The second series were with dimensions of 1800 x 1100 x 100 mm which tested for the flexural failure conditions. The small scale of models is selected according to many considerations which must be enough to obtain a result which a near to the true behavior of the full model slab with real dimensions. Optimum scale factor was chosen according to feasibility study which carried out to satisfy the expected constraints for example the weight, dimensions, and cost and should be lab equipment compliant .The another one is the ultimate testing capacity of the machine which have a maximum load by 600 kN.

The section defines the obtained outcomes by an experimental study which included fabricating and testing of twenty slab specimens strengthened by steel fibers. The models are monotonically tested. The models were split into two sets, the first one consists of 10 models designed to fail in punching shear. The second series included ten slabs which designed to fail in flexure. Many parameters were chosen to investigate the outcome of these parameters on the general behavior, the scheme of load displacement relationship, energy absorption, ductility, and stiffness.

4.2 Testing Slab Specimens under Monotonic Loads

All slab specimens are tested under monotonic loads to attain an definitive load carrying capacity and explore the distribution of stresses at the failure stage.

4.3 Test Results

4.3.1 Series A (Punching Shear Models)

The first series of this study is punching shear models which denote the initial stage of this experimental work. This series includes ten specimens fabricated under several parameter such strengthening the slabs with steel fibers and in addition to the opening's existence with varied shape, location, and number.

4.3.2 Load- deflection Relationship

The obtained results of this series are presented in the Table 4.1. This series included testing of ten slab specimens under static loads which showed an ultimate load carrying capacity of (316) kN for the reference slab while the parametric slabs exposed an ultimate load variety between (320-350) kN by means of occurred displacement ranged between (22.1-44.34) mm as demonstrated in Table 4.1. The ultimate load carrying has affected due to several parameters such as the changes in the steel fibers ratios in addition to the openings effect. Expressing the obtained results with several calculations such as stiffness, energy absorptions, and ductility. Theses calculation provide a full understand to the behavior of such slabs. According to the obtained results and as exposed in Figures 4.1 and 4.2, is found that the slabs acted in a linear way until they achieve an average value of 32.6% of their ultimate strength. Each specimen's measured energy absorption (EAI), ductility index ($\mu\Delta$), and initial(K_i) and secant stiffness(K_s).

Table 4.1 Test results of punching shear series.

ID	Control	Group A1			Group A2			Group A3		
	SP1	SP2	SP3	SP4	SP5	SP6	SP7	SP8	SP9	SP10
$V_f\%$	0.5	1	1	1	1.5	1.5	1.5	2	2	2
$f'c$ (MPa)	72.2	81.4			88.15			91.6		
Openings Shapes	---	Rec*	Cir**	Rec	Rec	Cir	Rec	Rec	Cir	Rec
Size Openings (cm)	control	10×20	11	20×10	10×20	11	20×10	10×20	11	20×10
P_u (kN)	316	330	338	334	320	325	322	340	350	344
Δu (mm)	22.1	26.8	30.2	27.92	23.7	25.76	24.2	35.32	44.34	38.21
P_{cr} (kN)	47	61	71	52	56	48	43	78	94	82
P_y (kN)	65	73	80	75	62	58	53	100	120	107
Δy (mm)	7.06	5.9	5.7	5.43	6.6	6.2	5.81	5.23	5.63	5.35
$\mu\Delta$	3.13	4.53	5.3	5.14	3.55	4.14	4.3	6.75	7.93	7.1
K_i (kN/mm)	44.7	55.9	59.3	61.5	48.4	52.42	55.4	65.01	62.2	64.3
K_s (kN/mm)	9.21	12.4	14.04	13.82	9.45	9.32	9.10	14.82	15.14	20
EAI	9.75	14.32	18.14	16.58	10.65	12.35	11.47	19.8	26.8	21.21

*Rec=Rectangular

**Cir=Circler

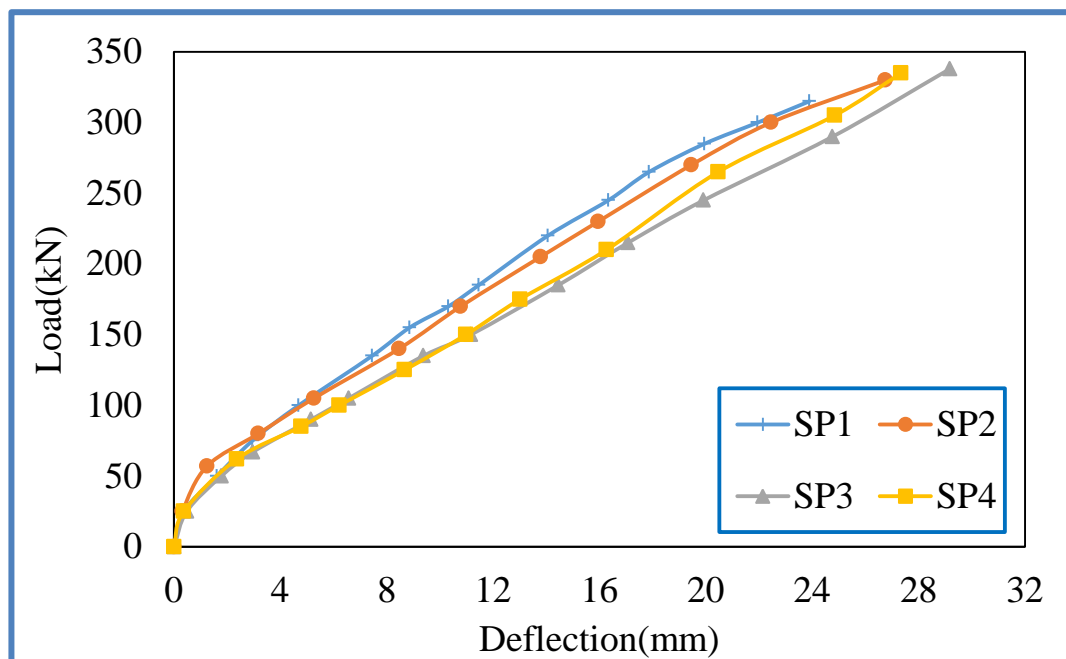
4.3.3 Openings Influence of on the Punching Shear Capacity

Table 4.1 exposes the results of the tested slab models in addition to with the energy absorption, stiffness, and ductility. The control solid slab with steel fibers of (0.5%) which demonstrated an ultimate load carrying capacity with (316) kN and (22.1) mm deflection .The parametric slabs created with opening near the corner and middle column. The parametric models are six slabs created with two openings with different locations and the remaining three fabricated with four openings in each slab. The influence of the opening's location, shape, and number were clear on the fiber reinforced slab behavior .It's should be noted that all slabs of this series faced a punching shear failure. Concerning the slab with openings (SP2) which have two openings with dimensions (100 x 200) mm near the slab corners in diagonal form. The opening presence affected the ultimate load carrying load capacity and displacement in addition to the remaining calculations.

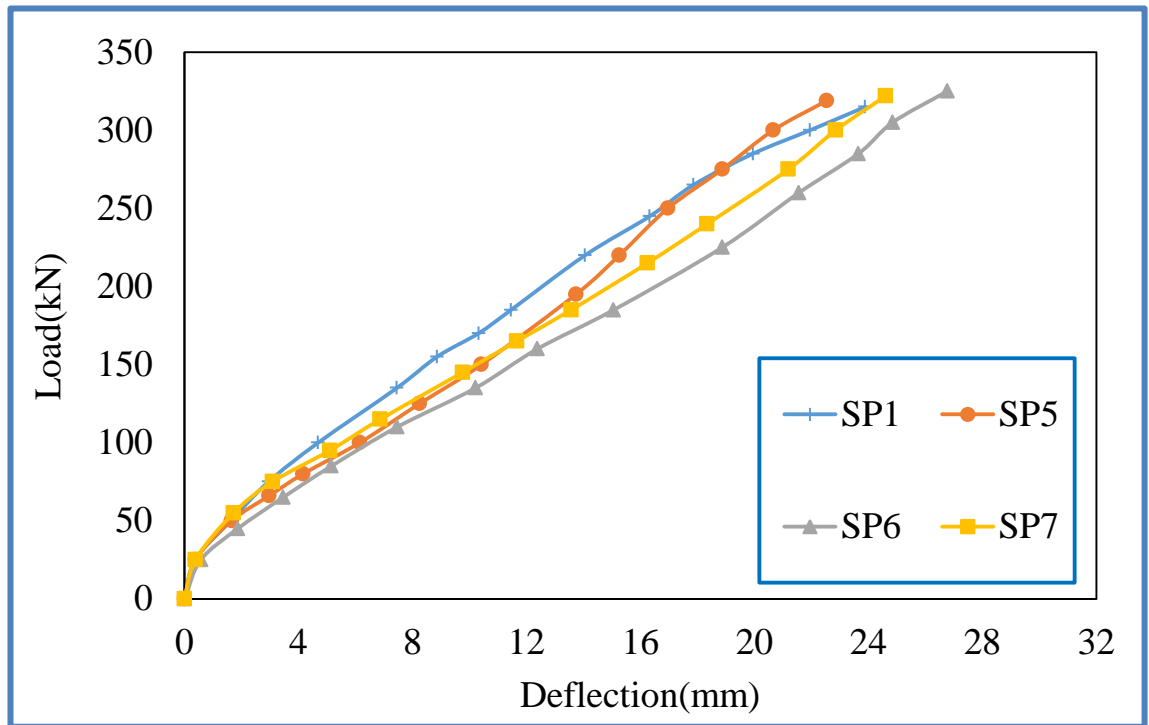
The opening existence redistribute the stresses which showed concentration in the corners of the opening and around the middle column. The opening existence affected the cracking load which decreased by (47.4%) which the cracks appeared at (27.3%) in the control solid slab when it decreased to (13%) after creating the two openings near the slab corners (SP2). This phenomenon occurred because the openings decrease the ability of the slab to resist the loads. The failure by punching shear occurred at (330) kN which is when compared with solid slab the results revealed that the difference was by (4.72%) for the first one due to the rise in the steel fiber proportion. The displacement is the most affected properties by the openings presence which the displacement increased by (21.3%) in comparison with solid slab.

Regarding the shape of the openings, other slabs were fabricated with two openings (rectangular and circular shapes). Creating rectangular openings with dimensions of (100 x 200) mm in the parallel direction to the slab width showed

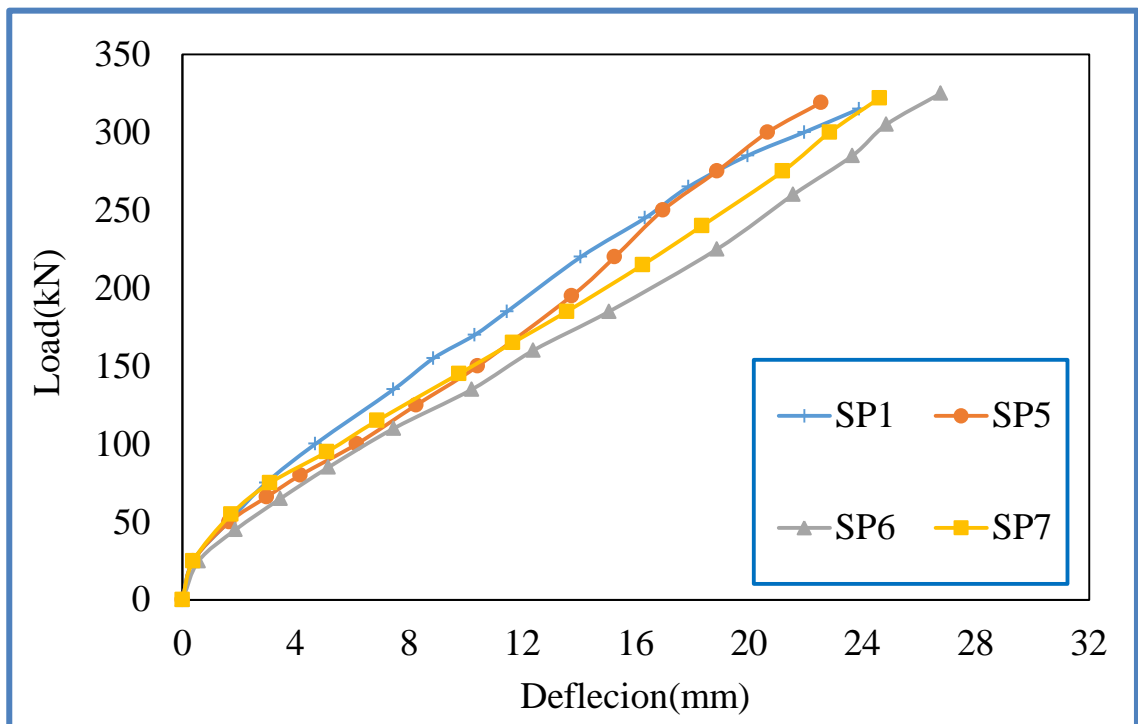
an ultimate load carrying capacity of (335) kN in which greater than the control slab (SP1) by (6%). The displacement is the most affected property by the openings which increased by (26.3%) when compared with the solid slab (SP1). The variance in the ultimate load between the slabs (SP2 and SP4) in term of the ultimate load and displacement was small (approximately 4.4% and 6 %). The effect of these openings was not significant because of the locations of the openings which is far from the critical region (near the middle column where the shear stresses concentrated). The cracking load also affected slightly by presence of the openings besides the load and displacement. The slabs with circular openings exposed a similar behavior of concrete slab with rectangular openings (SP2 and SP4) but with higher displacement which was by (17.23%) when compared with the control slab (36.6%) as appeared in Figure 4.1. In general, the shape of the openings didn't affect the behavior of the concrete slabs due to the locations of these openings which considered a suitable location to create the opening in slabs that fail in the slab with punching shear.



(a) Comparison between solid slab and slab with openings of group A1



(b) Comparison between solid slab and slab with openings of group A2

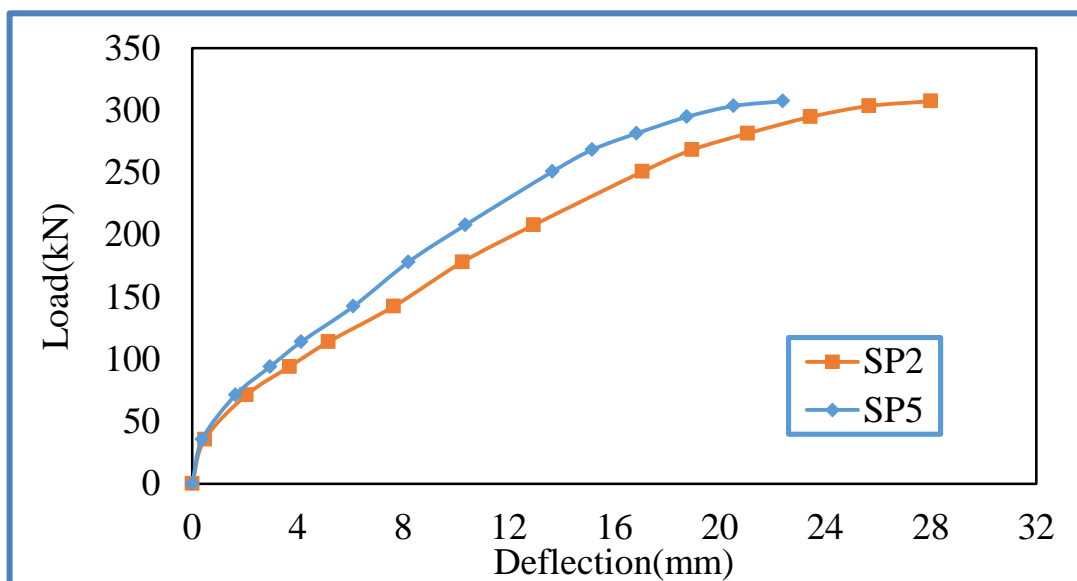


(c) Comparison between solid slab and slab with openings of group A3

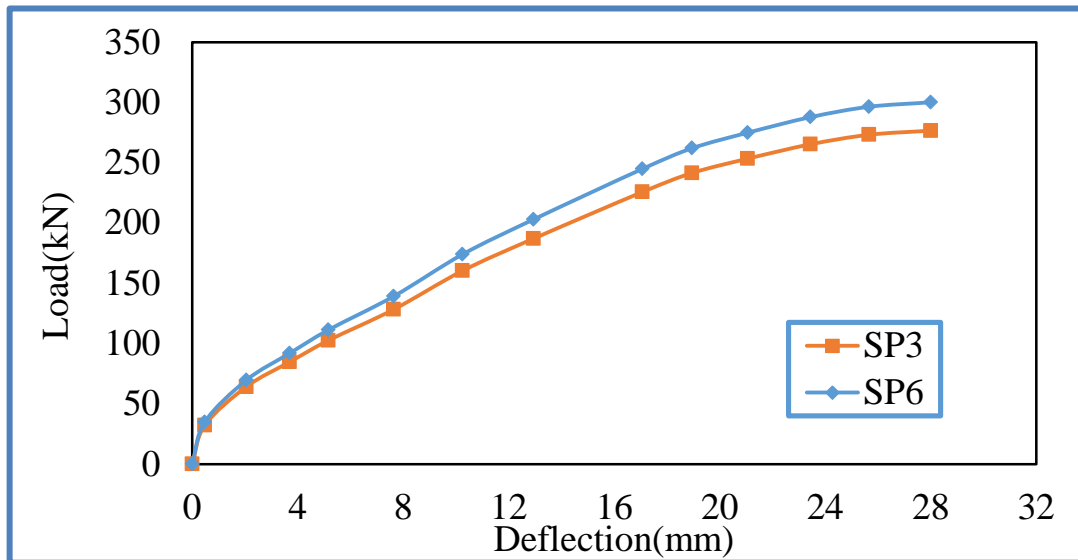
Figure 4.1 Load-deflection relationship of solid slab and slab with opening.

4.3.4 Influence of Steel Fibers

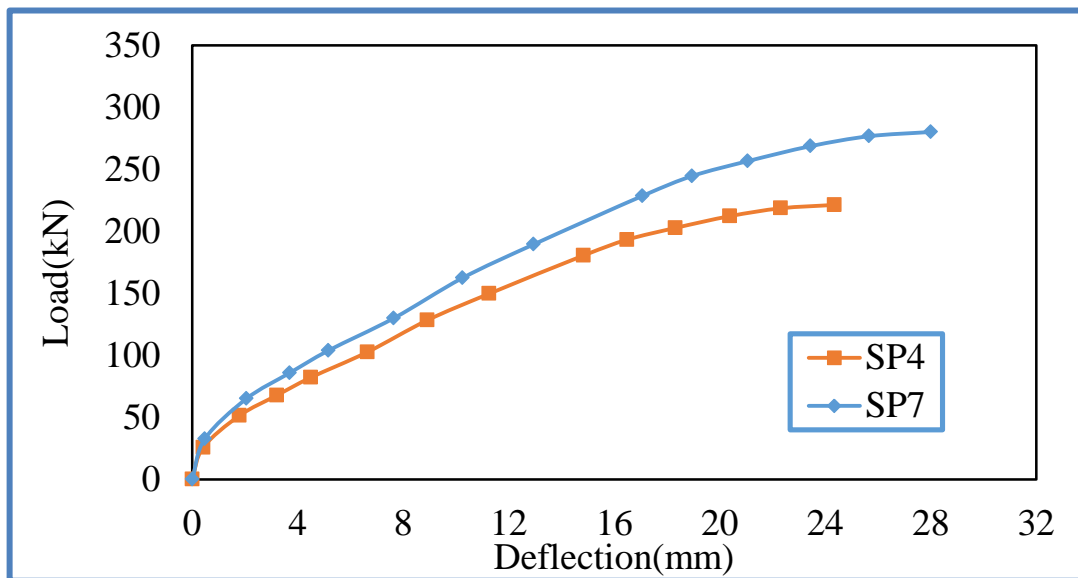
All Mechanical properties of the concrete slabs that failed in punching shear are affected by the presence of steel fibers. The ultimate load carrying capacity, maximum displacement, ductility, stiffness, energy absorption, and stress distribution are affected significantly. Increase of steel fibers from (0.5%, 1%, 1.5%, and 2%) of the slabs with openings increased the load carrying capacity and displacement. Concerning the slabs (SP2 - SP7) included increase of the steel fibers from (1%) to (1.5%) which exposed decreasing the average cracking load by (41.6%) approximately. The highest decrement in the cracking load happened in the slab with two circular openings (“SP6”) which was by (47.9%). The ultimate load carrying capacity is the most affected by change of steel fibers and shifting the openings to the critical region. The load capacity of the slabs (SP5, SP6, and SP7) exposed a little average decrement by less than (4%) besides the displacement dropping by average value of (11.2%) when compared with models (SP2 to SP4). Slab (SP5) has the maximum decrement which was by (16.2%) in comparison with the slab with two corner openings as exposed in Figure 4.2a . The variance in behavior between the models (SP2 to SP4) and (SP5 to SP7).



(a)



(b)



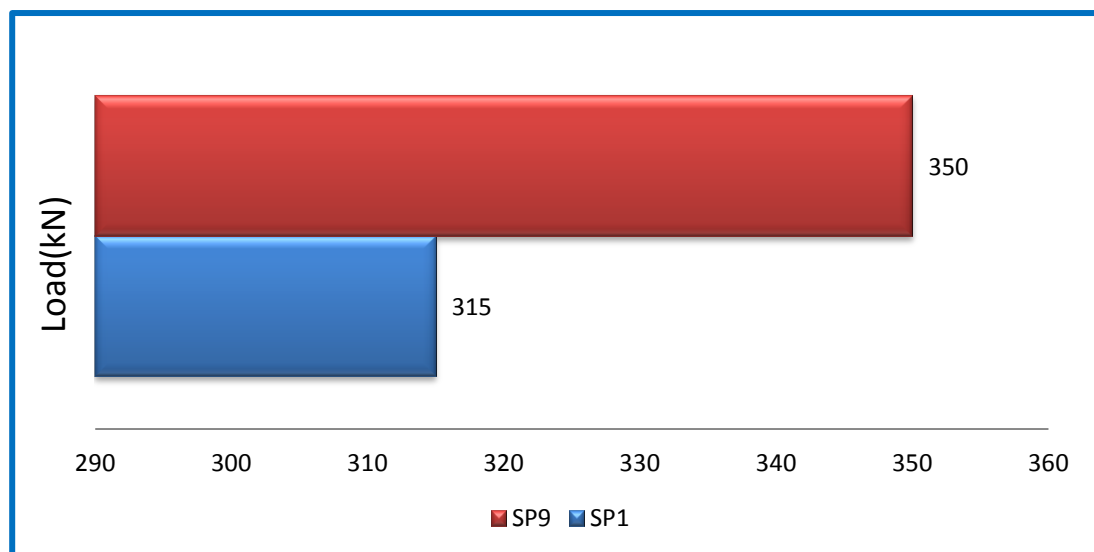
(c)

Figure 4.2 load-deflection relationship between group A1 and A2.

4.3.5 Number and Location of the openings

Concerning the openings' location and numbers, the effect of these two variables is the most effect on the general behavior of the concrete slab. Slabs (SP8 to SP10) fabricated with four openings and steel fibers of (2%). Ultimate load was obtained by model (SP9) was by (350) kN which is higher than (10.7%) and deflected by (100.62%) higher than the reference model as confirm

in Figure 4.3. The increment in steel fibers ratio from 0.5- 2% restored the expected strength loss due to the openings existence and gained additional strength improvement. The load carrying capacity didn't affect by the openings shape due to the smallness in the openings sizes which didn't exceeded the (2%). The increment in the displacement seemed significant with fabrication of more openings which the difference between the two openings slabs and four openings slab is quite simply a slight difference in strength and a high difference in displacement. As a comparison between the slabs with two and four openings (SP5 and SP8), the displacement increased by (49.1%) as exposed in Figure 4.4. The same comparison can be applied between the slabs with two and four circular openings (SP6 & SP9) which was by (72.4%) as revealed in Figure 4.5. The difference in general behavior between the models with two and four rectangular openings (SP7 and SP10) is quite simply a slight difference in strength and a high difference in displacement (about 57.8%) as revealed in Figure 4.6. The largest displacement happened in the slabs with four rectangular openings (100 x 200) mm than the remaining openings shape (rectangular 200 x 100 mm and circular 110 mm) as exposed in Figure 4.7.



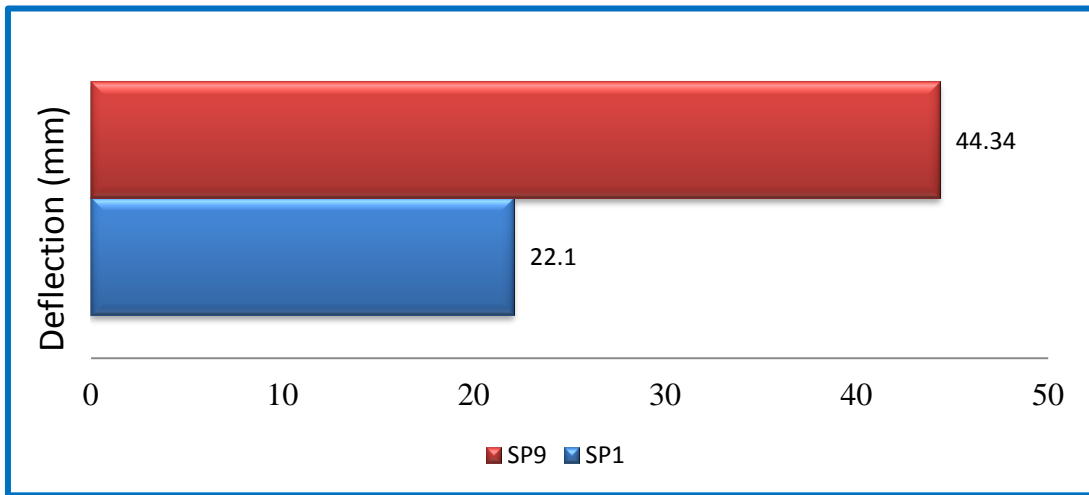


Figure 4.3 Comparison between SP1 and SP9 in term of the ultimate load deflection.

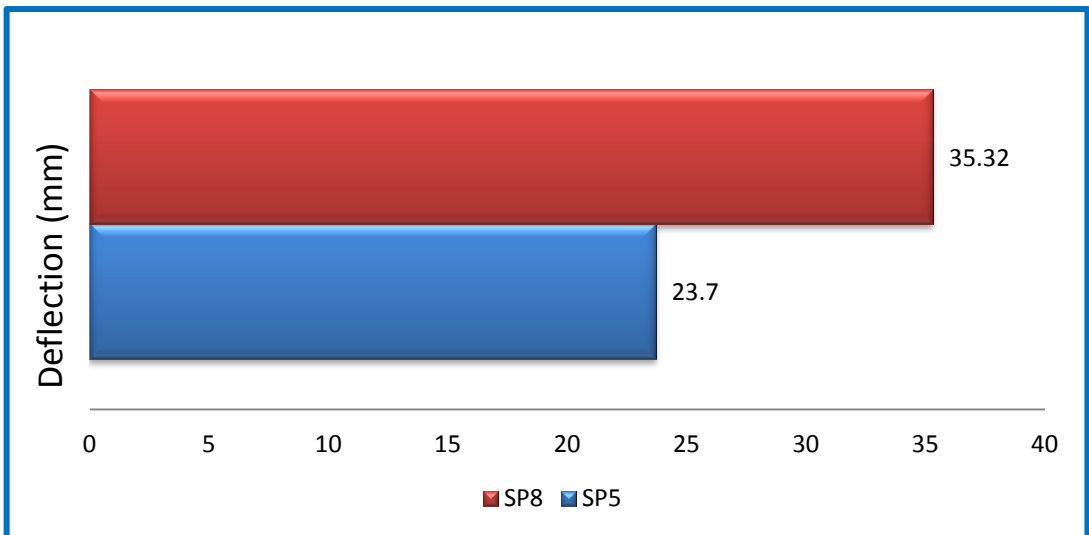


Figure 4.4 Comparison between SP5 and SP8 in term of the deflection.

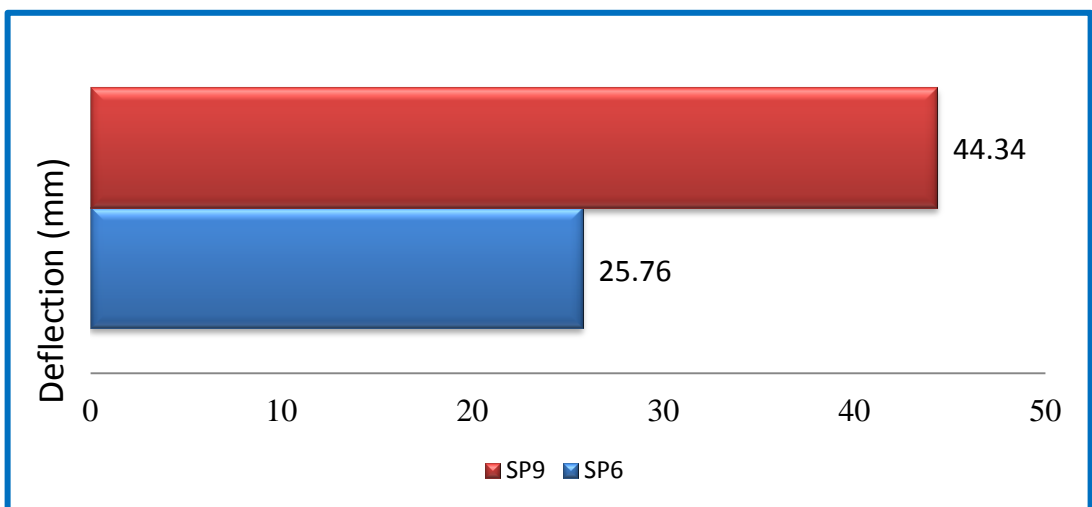


Figure 4.5 Comparison between SP6 and SP9 in term of the deflection.

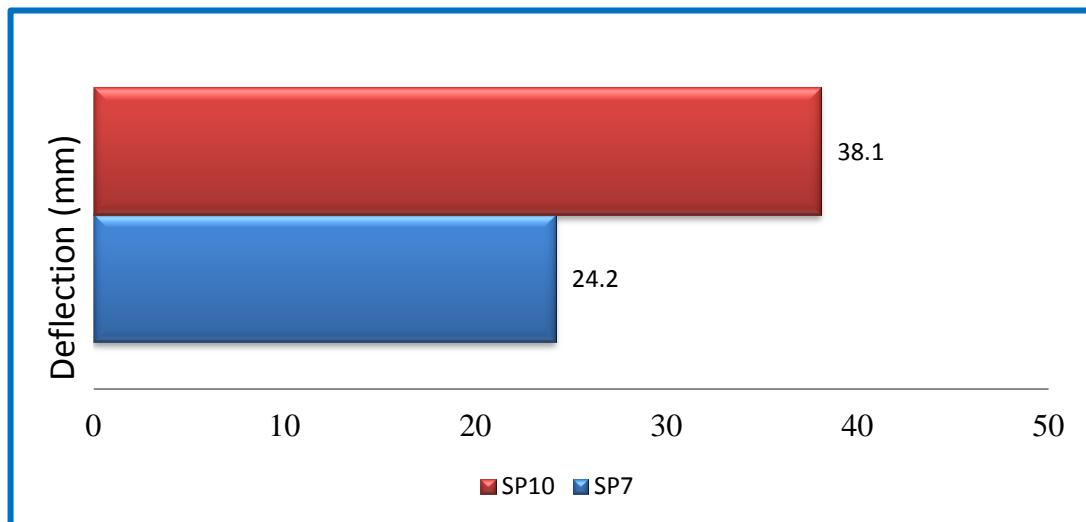


Figure 4.6 Comparison between SP7 and SP10 in term of the displacement.

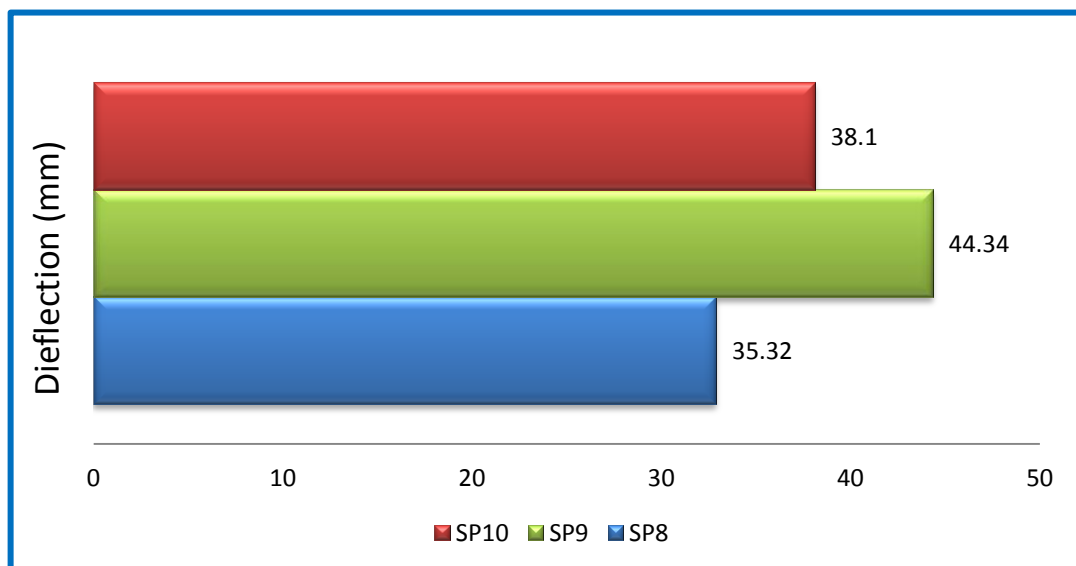


Figure 4.7 Comparison between SP8, SP9, and SP10 in term of the deflection.

4.3.6 Analyzed Slab Stiffness

As defined by the "Slab Stiffness" term is an index of the concrete's ability to resist deformation, i.e., the member stiffness that used to establish the necessary force to realize a certain deformation. The load-deflection curve slope can be used to measure stiffness [70]. Declared that "the load displacement relationship of most flat concrete slab that fail in punching shear denoted by two straight lines with distinct slopes" [71].

The plotted curve is indexed by two lines which the first one is the slab uncracked stiffness (initial stiffness K_i), and the other refers to the post-cracking rigidity (secant stiffness K_s), as publicized in Figure 4.8, initial stiffness as defined by the curve slope to the first slope transition (first cracking load), while the load-displacement curve slope is a definite steepness of load. While the load-displacement curve slope defines secant stiffness that extends to the flexural reinforcement yielding [72]. Therefore, it is very important to evaluate the yield displacement to show both original and secant steadiness [73].

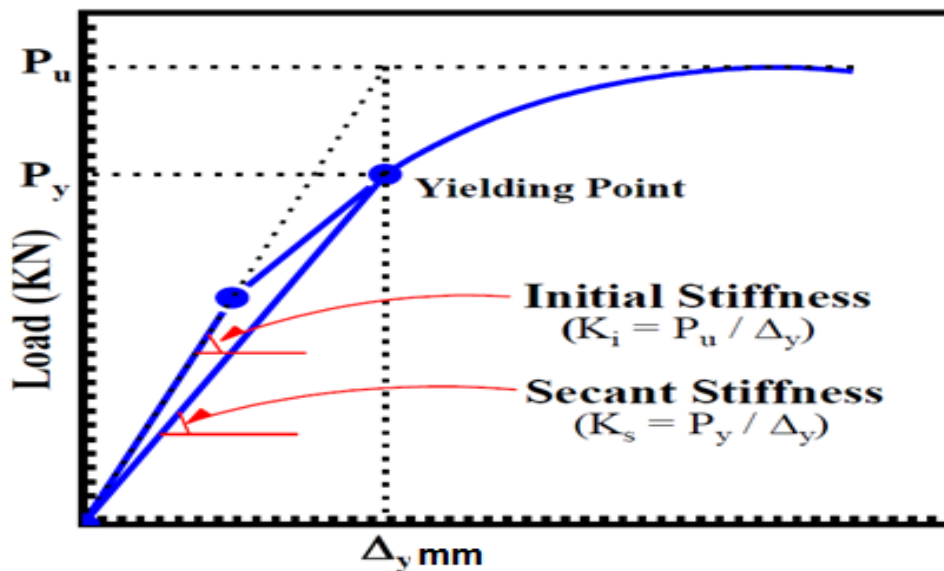


Figure 4.8 Determination of stiffness (evaluation of initial and secant stiffness)

(Husain et al.,2017).

Solid slab (SP1) has an initial stiffness of (44.7) kN/mm which degraded by (79.4%) when the concrete slab to the yield point to be (9.21) kN/mm. Regarding the slabs with two corner openings (SP2 to SP4), the initial and secant stiffness showed an increment due to the increase in steel fiber although of openings effect. The improvement of these two models in the initial stiffness by (25% and 37.5%) respectively. While the secant one, the enhancement were by (34.6% and 50%) respectively of these two models in comparison with control slab. The obtained results are considered a very good enhancement due

to the presence of steel fibers which can compensate the stiffness loss with gaining additional enhancement. The same mechanism occurred with the circular openings as illustrated in Figure 4.9.

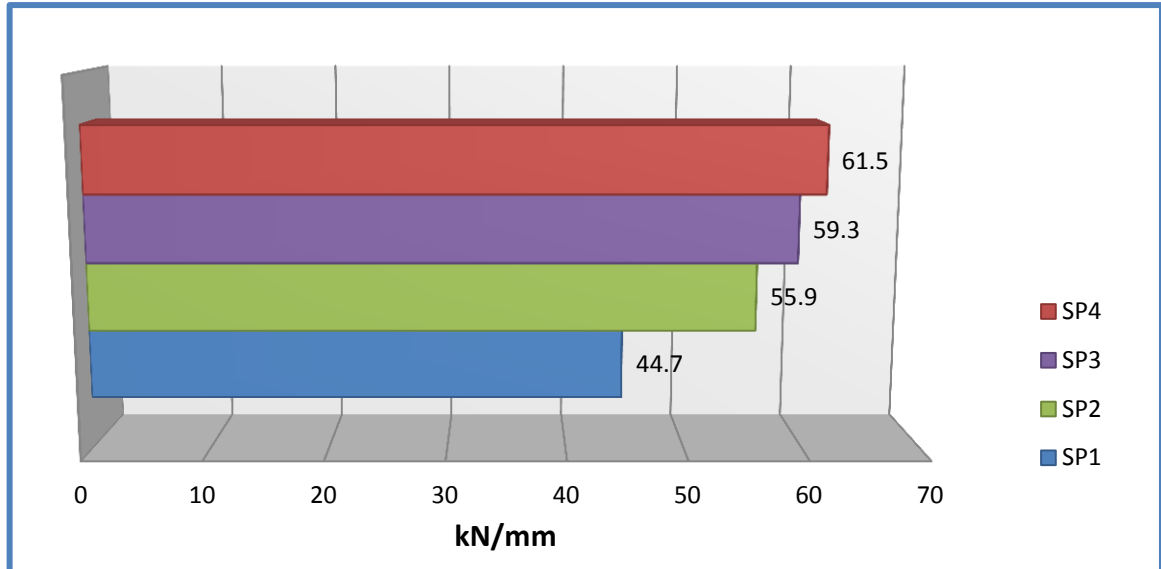


Figure 4.9 Comparison initial stiffness of the between SP1 and group(A1)

As compared to slabs of 1% steel fibers, changing the steel fibers (1-1.5%) increased the two stiffness components by an average of (13.4%). Last increase of the initial stiffness by (9%) about the model of (1%) steel fibers (SP2), as seen in Figure 4.10.

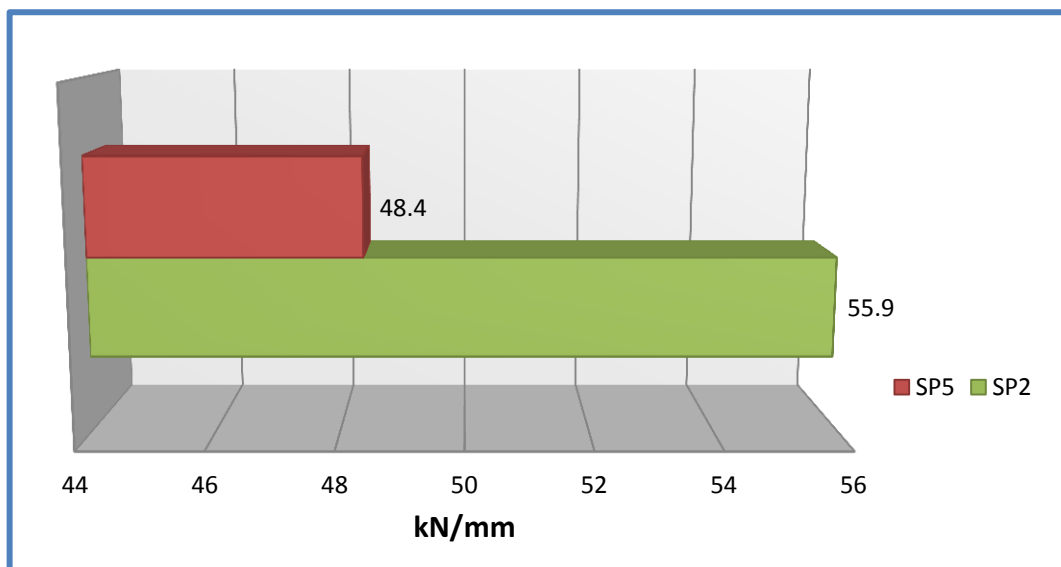


Figure 4.10 Comparison initial stiffness of the between SP1 and SP5.

Stiffness of the slabs with four openings has a significant decrement due to the existence of the opening although of changing of steel fibers to (2%) which could not compensate the loss in the stiffness. In contrast to the slab specimens (SP5, SP6, and SP7), the stiffness of the slab specimens (SP8, SP9, and SP10) increased by 45.4%, 39.5%, and 37.1 percent, respectively, as seen in Figure 4.11.

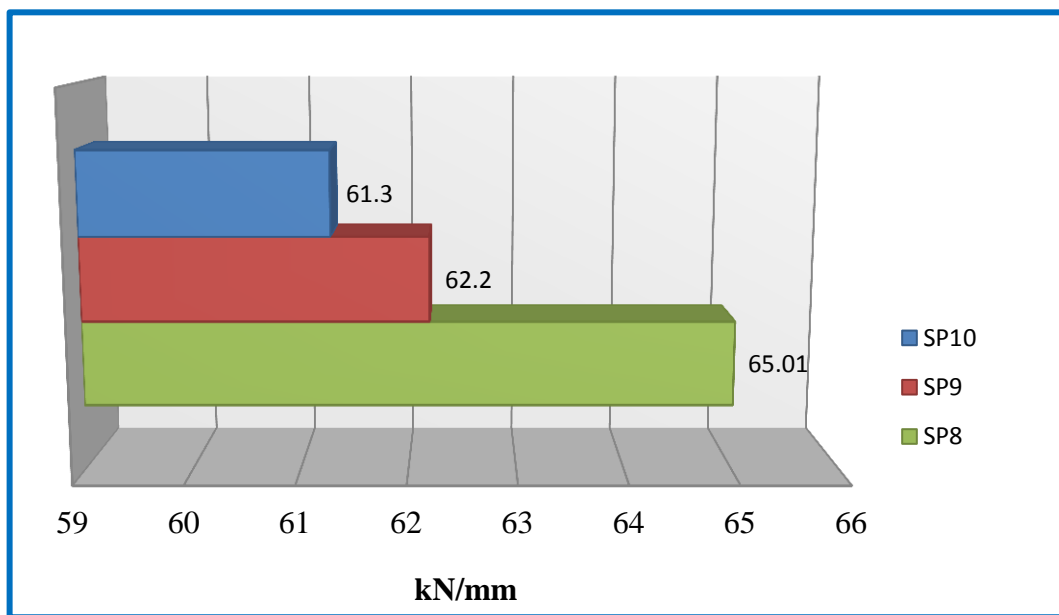


Figure 4.11 Comparison initial stiffness of the slabs with four openings.

4.3.7 Analyzed Slabs Ductility($\mu\Delta$)

The ratio between the displacement corresponding to the ultimate load (Δ_u) and the displacement corresponding to the first yielding of the flexure reinforcement (Δ_y) as can be shown in Figure 4.12,[71].The measured slabs' ductility was determined using a method suggested the researchers by [74] , and also proposed by [75]. The concept of yield displacement makes it difficult to calculate ductility factors from experimental data since the load-displacement relationship does not have a well-defined yield point. e.g., because of the material's non-linear behavior or the yield in a particular section of the system.

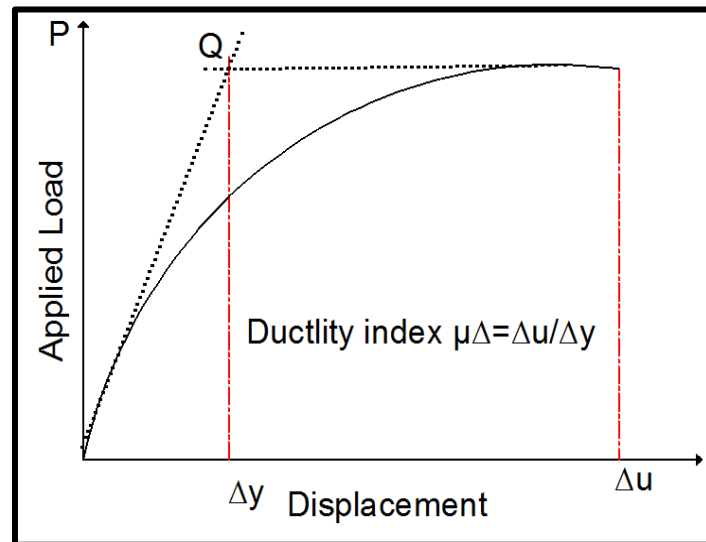


Figure 4.12 Show the ductility index calculation (Sullivan et al., 2004).

Opening's effect and as expected has a significant effect on the ductility of the concrete slabs which needed a solution to restore the strength loss and this solution is performed by increase of proportion of steel fibers to (1%) which gained an additional enhancement beside the compensation of the ductility loss. The average enhancement was by (59.7.3%) when compared with the control slab. The model with circular corner openings (SP3) gained the ultimate enhancement which was (69.3%) approximately in comparison with the solid slab (SP1) as revealed in Figure 4.13.

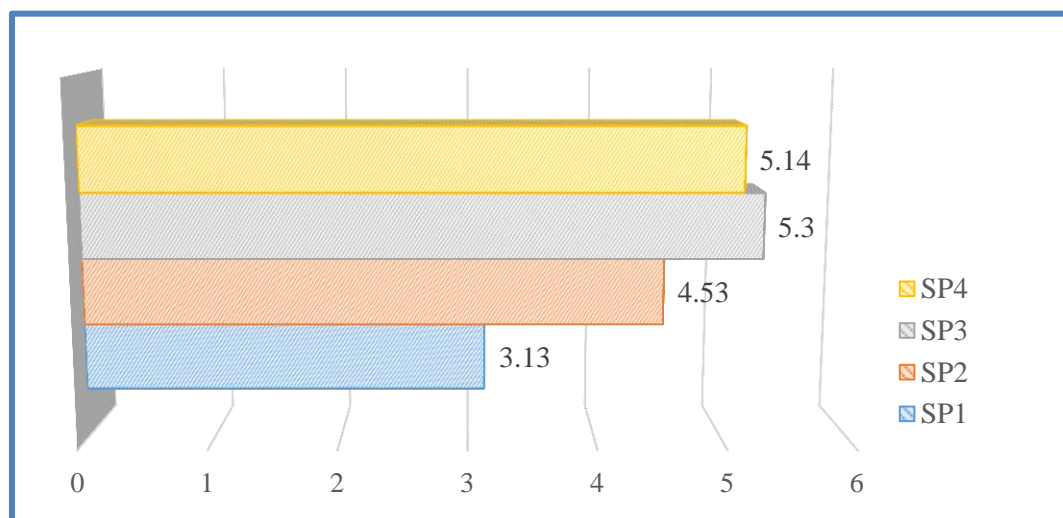


Figure 4.13 Comparison ductility index of the between SP1 and group(A1).

Regarding the models with central openings, the relationship between the ductility and openings' location showed a significant change which the openings' locations affected the ductility but with increasing of the steel fibers to (1.5%) could getting an additional average ductility which was by (27.8%) approximately when compared with the solid control model. As a comparison with the previous models with corner openings and steel fibers (1%) (SP2 to SP5), Due to the critical position of the openings (near the middle column), the improvement in steel fibers (1 percent -1.5 percent) has little effect on the ductility as indexed in Figure 4.14. In general, if there are a need to make opening in the slab, it should decrease the effect the of the openings by increasing the steel fibers to higher percentage.

Increase the steel fibers and number of openings has a big effect on the ductility value which demonstrated an enhancement by (90.9%) when simile with reference model (SP1). The slab model (SP9) has the maximum improvement in the ductility which reached to (154%) as revealed in Figure 4.15. It is important to point out an important point, which is that despite the presence of openings, the performance of the fiber reinforced slabs has improved greatly, and this is due to the presence of steel fibers, which gave high efficiency to withstand the slab to resist the punching shear loads and was able to recover the loss in the ductility of the concrete slab in addition to obtaining additional improvements developed the performance of the structural member. This is an excellent indicator of the possibility of making openings of various shapes even if they are in critical regions.

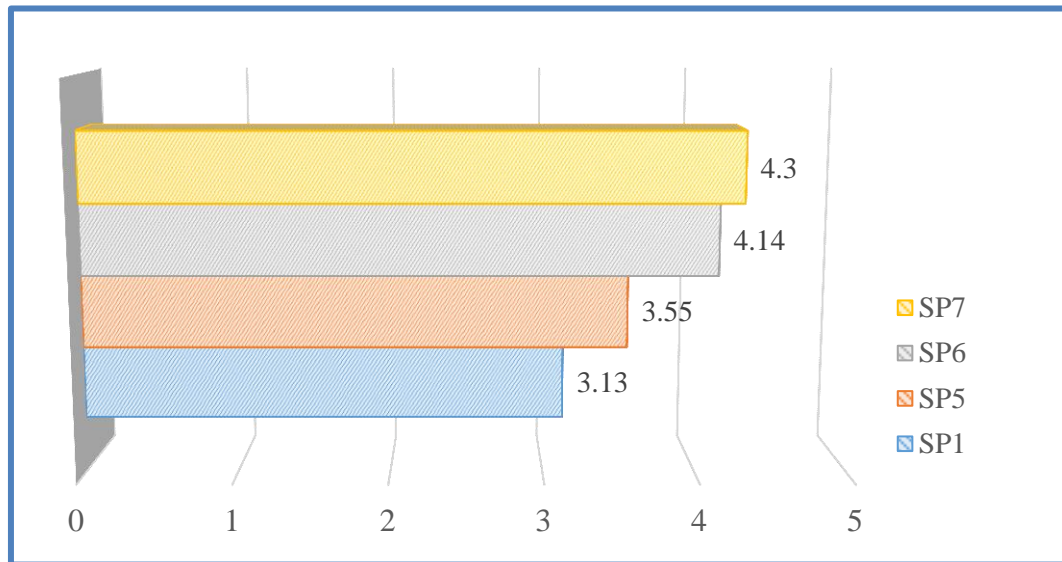


Figure 4.14 Comparison ductility index of the between SP1 and group(A2).

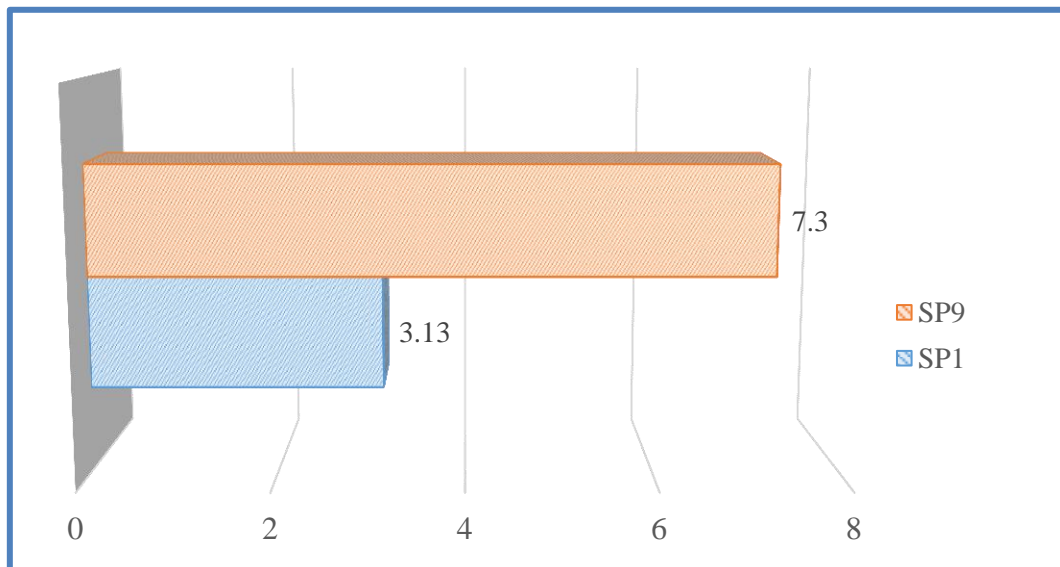


Figure 4.15 Comparison ductility index of the between SP1 and SP9.

4.3.8 Analyzed Slab Energy Absorption Index (EAI)

The region under the load-displacement diagram of the checked slabs can be described as energy absorption. This area was determined by numerical integration all the way up to the definitive load and displacement. The energy absorption of reinforced concrete members was defined by [76], as a measured of absorbed energy up to its ultimate state. According to the writers, the concrete status at the failure point represents the true behavior of the concrete member

expressed the energy absorption as a ratio of the total zone area under the load displacement [73], as explained in Figure 4.16.

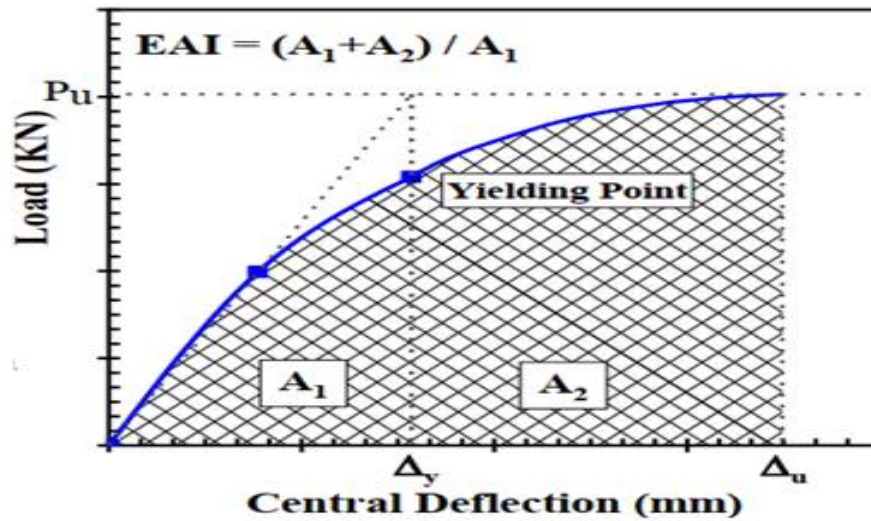


Figure 4.16 Determination of the energy absorption index (Husain et al, 2017).

Increasing the steel fibers could strengthen the slabs with openings and make a restitution to the expected loss in the energy absorption. The difference in the behavior seemed clear specially after increase the steel fibers to (1%) which exposed an increase in the energy absorption from (9.75) to the average value (16.34) which equal to more than (67.6%) in comparison with the solid slab. Maximum upgrading happened in the slab model (SP2) that was by double times as exposed in Figure 4.17.

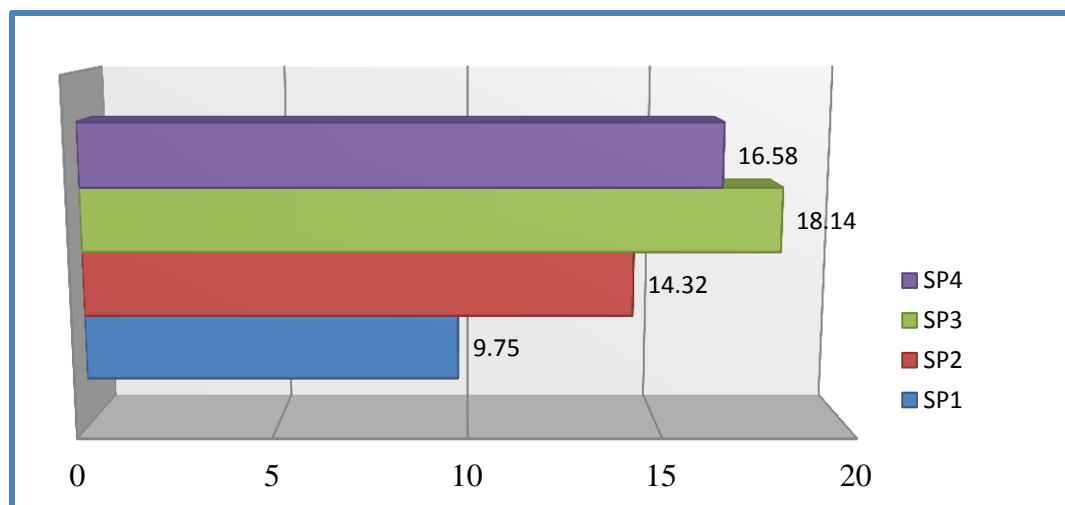


Figure 4.17 Comparison energy absorption of the between SP1 and group(A1).

Presence of openings near the middle column can be considered as the most critical parameter due to the weakness of this region although of increase of steel fibers which appeared a decrement in the energy absorption by more than (32%) which as occurred in the model with two central openings (SP6) in comparison with the slab model (SP3) as illustrated in Figure 4.18. Regarding the number of openings, also addition of another two openings beside (SP8) it contains steel ratio 2%, the existed ones affected the energy absorption by increasing it with more than (38.2%) in comparison with the two opening corner slabs (SP2) it contains steel ratio 2% as showing in Figure 4.19.

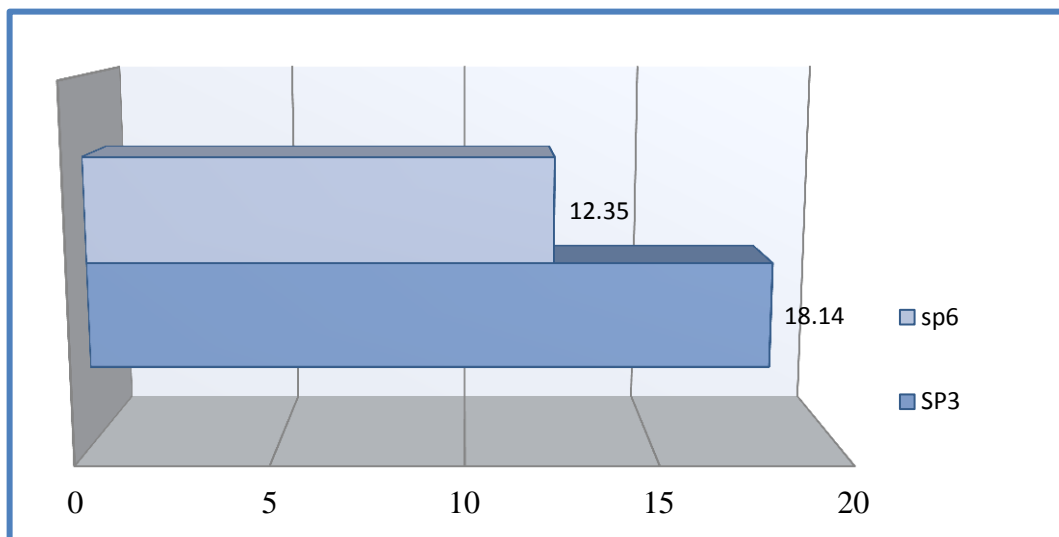


Figure 4.18 Comparison energy absorption of the between SP3 and SP6.

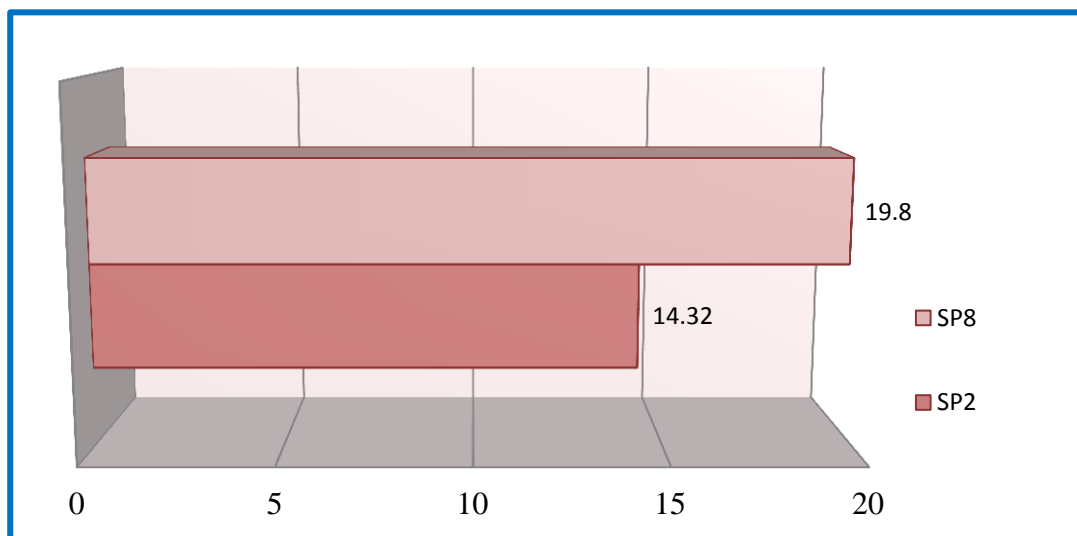


Figure 4.19 Comparison energy absorption of the between SP2 and SP8.

4.3.9 Failure Mode and Crack width

Table 4.2 and Figure 4.20 illustrated the failure details such as the crack width at several loading stages, failure angle, deformed area, in addition to the crack pattern and failure mode. This should be remembered that all of the slab specimens in this collection had a punching shear failure. For the first model (SP1), the failure of this slabs was in a ductile manner because of the steel fibers presence which provided a higher cohesion between the concrete particles. In comparison between the solid and hollow slabs and although of increase of steel fibers, the solid slab has the highest failure angle by (19.53%) greater than the parametric models. The failure mechanism started by generating the cracks horizontally which for a circle around the middle column. The deformation amount in the solid model was the smallest in comparison with the slabs with slabs with openings because the openings generate a weak region. Add more steel fibers increase the cracks amount which increase the ductility and provide an additional resistance against the loads. Concerning the specimens with openings specially the concrete slabs with two opening (SP2 to SP4), the failure mechanism started by generating the cracks horizontally which for a circle around the middle column. The mentions slabs showed a crack width smaller than the solid slab by about (8.6%). The openings presence in slabs caused increase in the deformed area. Slab with circular openings (SP3) showed the larger deformed area which was by more than (35%) when compared with (SP1). Regarding the angle of cracks, existence of circular openings decreased the size and angle of the cracks.

Transmitting the openings to the critical zone (near the middle column) accompanied with the increase of steel fibers to (1.5%) reduced the crack width and increased the area of deformation. The deformed zone increased by more than (23.6%) when compared with two openings model.

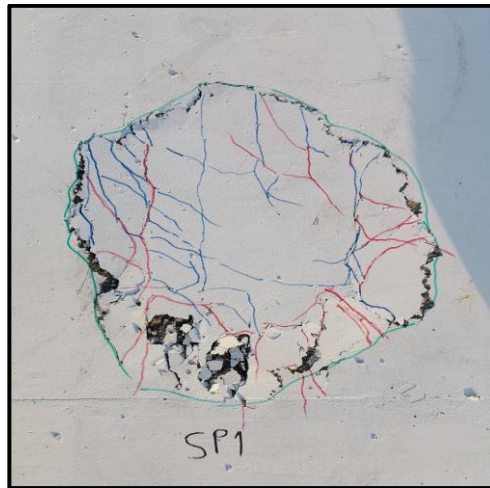
Add of more openings beside the existed ones with addition of more steel fibers (2%) upgrade the deformation zone with reducing the width and angle of cracks. The deformation area upgraded by more than (26%) as happened in the comparison (between the models SP5 and SP8).

Table 4.2 Crack width, failure angle, and failure area of punching models

ID	$W_{cr}(mm)$	$W_u(mm)$	Failure Angle(θ)	Failure Area(mm^2)
SP1	0.042	0.9	18.35	268468
SP2	0.032	0.85	14.71	311371
SP3	0.028	0.80	13.14	362954
SP4	0.030	0.82	14.1	330790
SP5	0.041	0.74	15.01	380287
SP6	0.05	0.7	14.4	420791
SP7	0.037	0.72	14.91	440825
SP8	0.035	0.64	11.25	480670
SP9	0.024	0.53	10.62	550433
SP10	0.038	0.61	12.1	478469



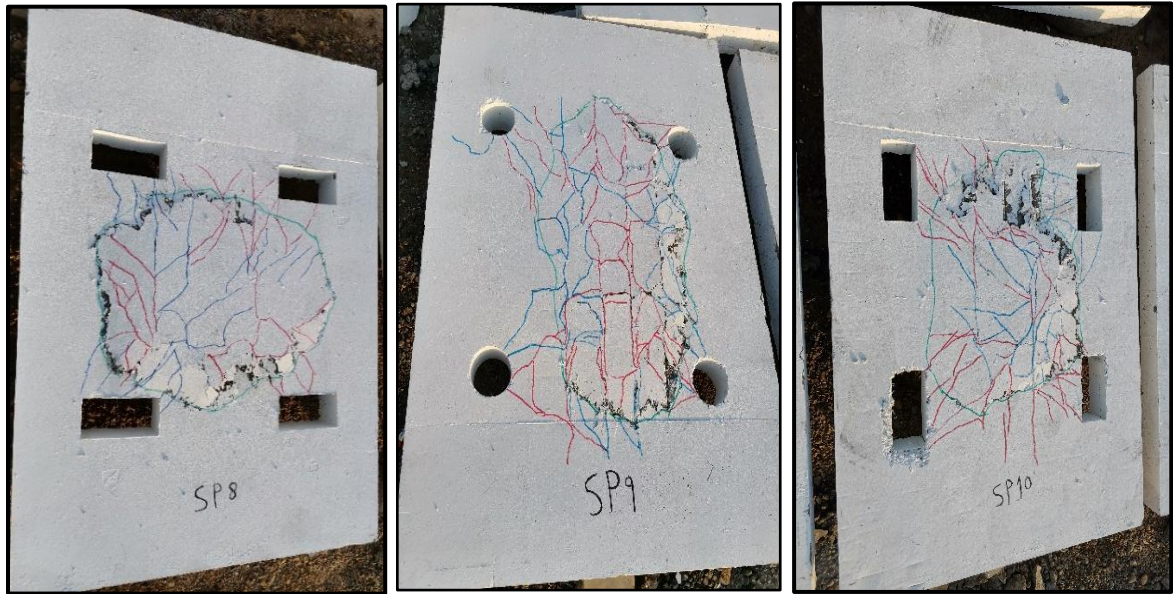
(a) Crack patterns for tested slabs group A1



(b) Crack patterns for tested control slabs



(c) Crack patterns for tested slabs group A2



(d) Crack patterns for tested slabs group A3

Figure 4.20 Crack pattern and failure mode of series one models (Punching Shear).

4.4 Analyzing and Results Discussion

4.4.1 Flexural Models Results

The second series is the flexural series specimens which consists of ten slabs designed to fail in flexure. These slabs strengthened with several ratios of steel fibers in addition to fabricate many openings with different shapes, location, and number. The first model was solid slab while the remaining ones are divided into three groups which each group has three slabs. First group included three slabs with two openings with different shapes located at the corners of slab. The second one consisted of three slabs with two openings with different shapes located at the mid-span of slab. The third three specimens were slabs with four openings with different shapes located at the corners of slab.

4.4.2 Load-Displacement Relationship

Table 4.3 and Figures 4.21 to 22 demonstrations that the concrete strengthened solid and opening slabs behaves linearly until (35%) of the ultimate load. The results of this series was dissimilar in comparison with the slabs that failed in punching shear according the failure loads, displacement, stress distribution, mechanical properties such as the energy absorption, stiffness, ductility, in addition to the failure mode and crack pattern. The outcomes illustrated that the solid slab failed in flexure at (173) kN while the hollow slabs failed at failure load ranged between (180-255) kN with deflection range (30.3-55.42) mm as revealed in Table 4.3. The difference in steel fibers ratios and presence of openings varied the ultimate loads values. Expressing the slabs results was illustrated by use of several calculation such as energy absorption, stiffness, and ductility. Expressing these calculations beside the load-deflection curves and failure mode explanations provide a full understand to slab behavior.

Table 4.3 Test results of Flexural series B.

ID	Control	Group B1			Group B2			Group B3		
	SF1	SF2	SF3	SF4	SF5	SF6	SF7	SF8	SF9	SF10
V_f %	0.5	1	1	1	1.5	1.5	1.5	2	2	2
$f'c$ (MPa)	72.2	81.4			88.15			91.6		
Openings Shapes	---	Rec*	Cir**	Rec	Rec	Cir	Rec	Rec	Cir	Rec
Size Openings (cm)	control	10×20	11	20×10	10×20	11	20×10	10×20	11	20×10
P_{cr} (kN)	50.4	70	95	82	48	64	56	101	120	107
P_y (kN)	74	84	108	97	57	79	76	115	145	123
P_u (kN)	173	200	215	195	180	189	185	235	255	247
Δy (mm)	9.2	10.4	9.7	10.2	7.9	11.3	11.38	9.8	9.2	10.7
Δu (mm)	33.2	37.14	43.4	39.87	30.3	34.2	32.92	51.3	55.42	48.35
$\mu\Delta$	3.65	5.58	6.75	6.2	5.02	5.62	5.23	8.2	9.1	8.53
K_i (kN/mm)	17.8	20.3	21.82	20.78	18.1	19.02	18.65	24.1	27.7	23.08
K_s (kN/mm)	6.4	8.07	11.13	9.51	7.3	7.04	6.8	11.75	15.74	11.95
EAI	4.85	6.9	7.85	7.2	5.12	6.4	5.54	9.82	11.43	10.13

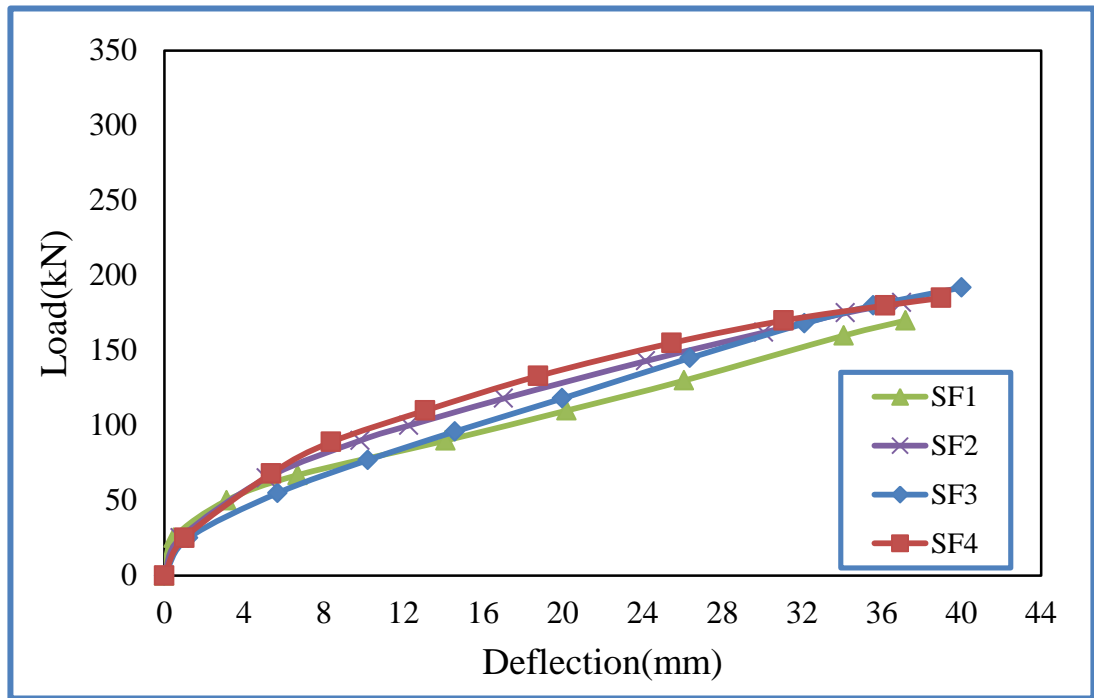
*Rec=Rectangular

**Cir=Circler

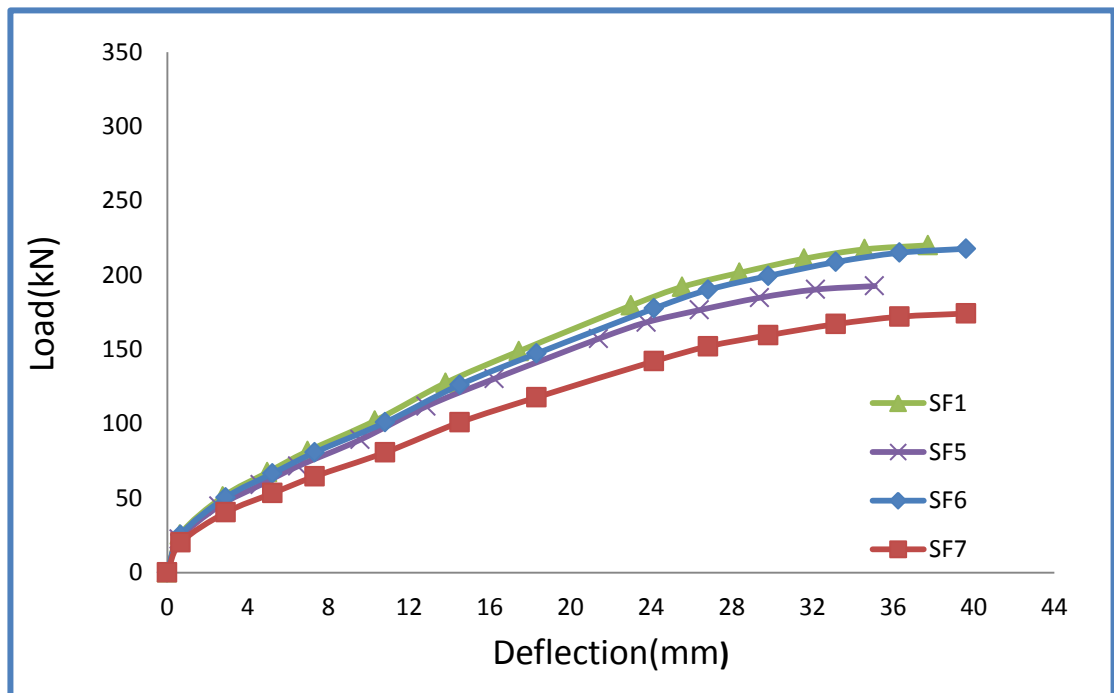
4.4.3 Influence of Opening on the Flexural Behavior

The flexural behavior affected by use of steel fibers with several ratio and with existence of openings. The solid slab that strengthened with (0.5%) showed strength of (173) kN and displaced by (33.2) mm approximately. The influence of opening existence was seemed on the behavior but this effect ranged from medium to high according the location and number of openings. According to the obtained results, it is found that all specimens of this series failed in flexure, regarding the slabs with openings, rectangular openings (100 x 200) and (200 x 100 mm) and circular ones (110 mm) were fabricated with different locations which affected the ultimate flexural loads.

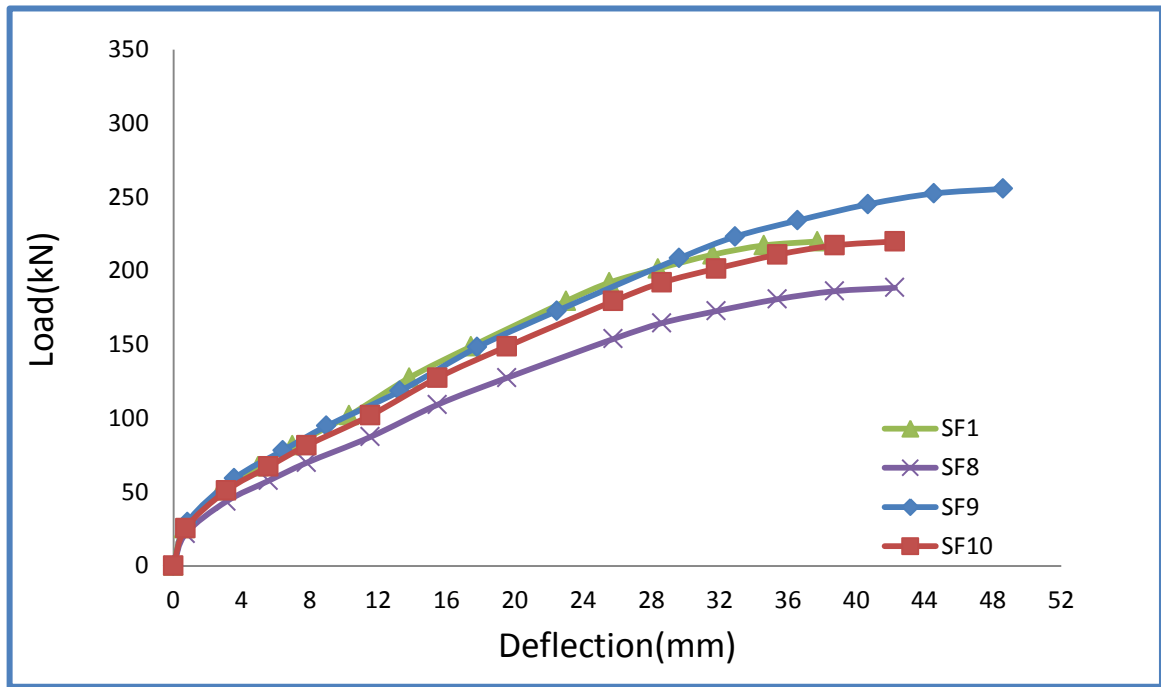
The openings redistributed the stresses along the slab. The load at cracking stage appeared at (30.7%) approximately which raised to (88%) after increasing the steel fibers with making openings such as (SF3). The failure of the model (SF2) happened at a value larger than the solid slab (SF1) by (30.5%) and deflection a value similar to the solid one approximately. Flexural strength of the slab specimens that fabricated with openings was higher than the solid one because of the steel fibers presence which these fibers recover the strength loss due to the presence of the openings. Creation of another shapes of openings in the slabs such as models (SF3 and SF4) affected the general behavior of the slabs in comparison with reference model. The difference between the opening's shapes in term of the load and deflection was not large due to the small size of the opening beside the location which placed far from the critical region as exposed in Figures 4.21 and 4.22.



(a) Comparison between solid slab and slab with openings of group B1



(b) Comparison between solid slab and slab with openings of group B2



(c) Comparison between solid slab and slab with openings of group B3

Figure 4.21 Load-deflection relationship of flexural slabs.

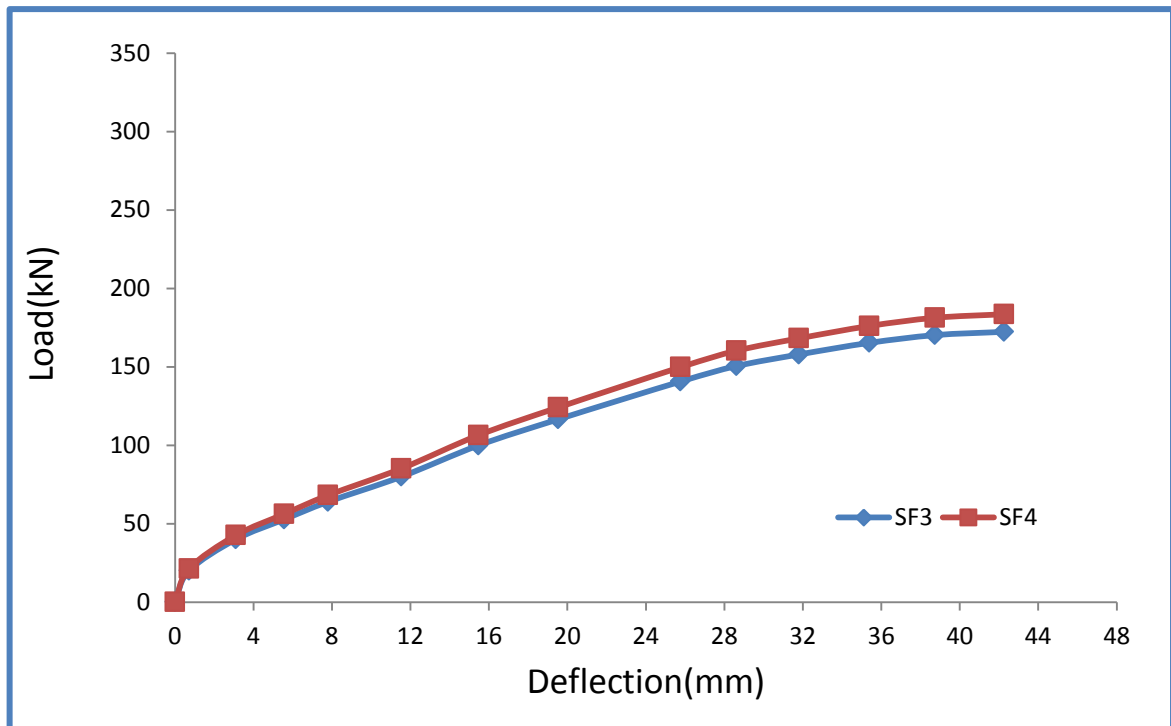


Figure 4.22 Comparison load-deflection between SF3 and SF4.

4.4.4 Effect of Steel Fibers

All Mechanical properties of the concrete slabs that failed in flexure are affected by the presence of steel fibers. The ultimate load carrying capacity, maximum displacement, ductility, stiffness, energy absorption, and stress distribution are affected significantly. Increase of steel fibers from (0.5%, 1%, 1.5%, and 2%) of the slabs with openings increased the load carrying capacity and displacement.

Models (SF5 to SF7) included change of the steel fibers to (1.5%) after it was (1%) which the addition of more steel fibers could compensate the strength loss with get of more upgrading in the load carrying capacity. More steel fibers of (1.5%) upgrade the performance by (9%) with little raising in the deflection. Model with (100 x 200) mm middle rectangular openings got the maximum upgrade in the performance which was by (4%) approximately. It should be noted the higher stiffness appeared at the slabs with rectangular openings as illustrated in Figure 4.23.

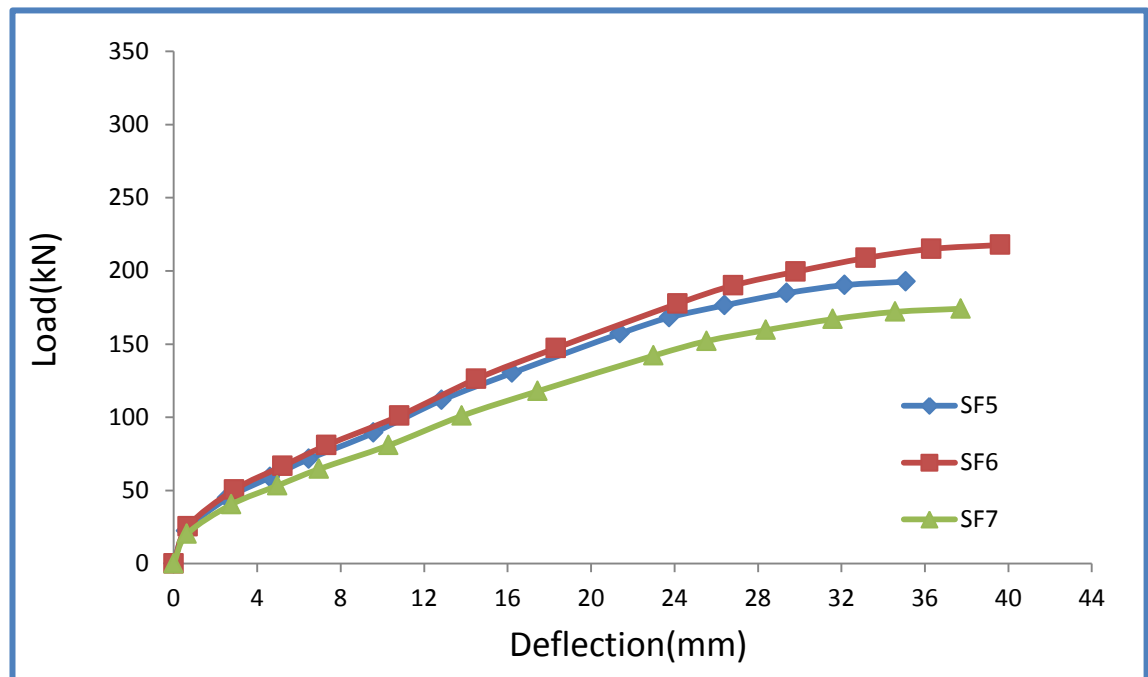


Figure 4.23 Comparison load-deflection between group B2.

4.4.5 Location and Numbers of the Openings

Concerning the openings' location and numbers, the effect of these two variables is the most effect on the flexural behavior of the concrete slab. Slabs (SF8 to SF10) fabricated with four openings and steel fibers of (2%). Ultimate load was obtained by model (SF9) was by (255) kN which is higher than (47.4%) and deflected by (67%) higher than the control slab as verified in Figure 4.24. The increment in steel fibers ratio from 0.5% to 2% compensated the expected strength loss due to the openings existence and gained additional strength enhancement. The load carrying capacity didn't affect by the openings shape due to the smallness in the openings sizes which didn't exceeded the (2%). The increment in the displacement seemed significant with fabrication of more openings which the difference between the two openings slabs and four openings slab is quite simply a medium differences in strength and a high difference in displacement.

More of steel fibers repay the happened loss with achieving of more upgrade in the flexural capacity. It should be noted that the variance in the shape of the openings has a small effect on the flexural capacity which was by (30.5%) but affected the displacement significantly. The most affected parameter is the number and location of openings which transmitting the two openings to the middle zone of the slab reduced the cracking load with average of (35.5%) approximately when compared with models of corner openings (SF2, SF3, and SF4).

Regarding the comparison aspect, it is possible to compare the two models (one has two openings and the other have four), which showed that the increase of openings causes more deflection. The first comparison in this section is between the models (SF6 and SF9) which both of them have a circular opening but with different openings number which appeared that the addition of another two openings deflection the slab by more than (62%) when compared

with the model with two corner openings as illustrated in Figure 4.24. The same thing occurred with the remaining slabs (SF7 & SF10) which upgrade the deflected by (46.8%) as illustrated in Figure 4.25. Largest displaced slab was the slab with circular openings (SF9) which displaced by (55.42) mm greater than the two slabs (SF8 & SF10) by (8% and 14.6%) respectively as verified in Figure 4.26.

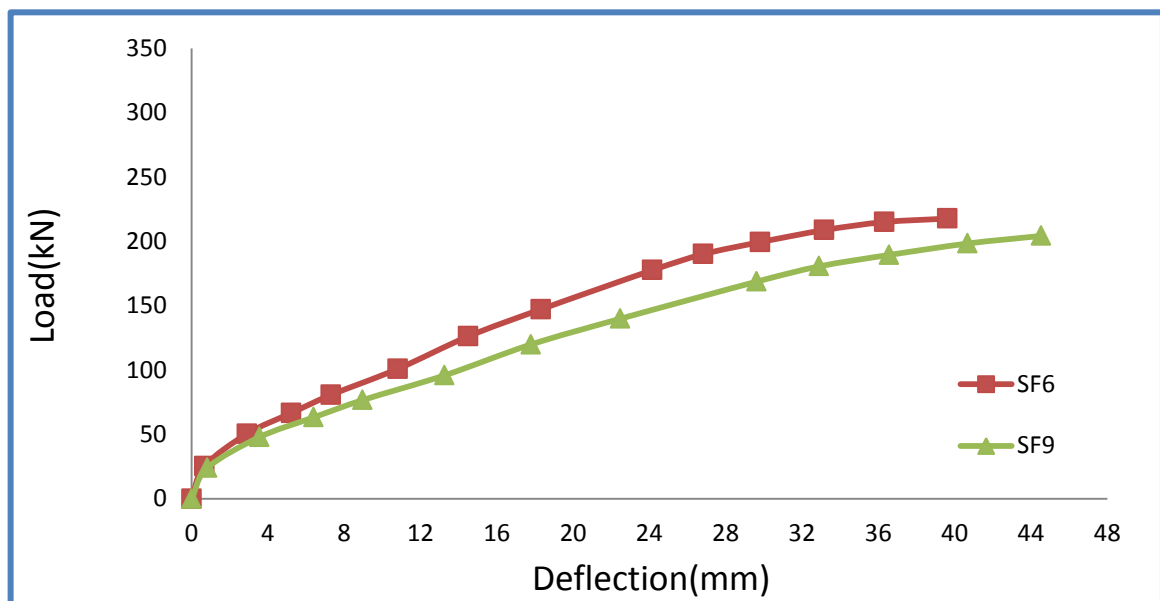


Figure 4.24 SF6 and SF9 Load-deflection curve.

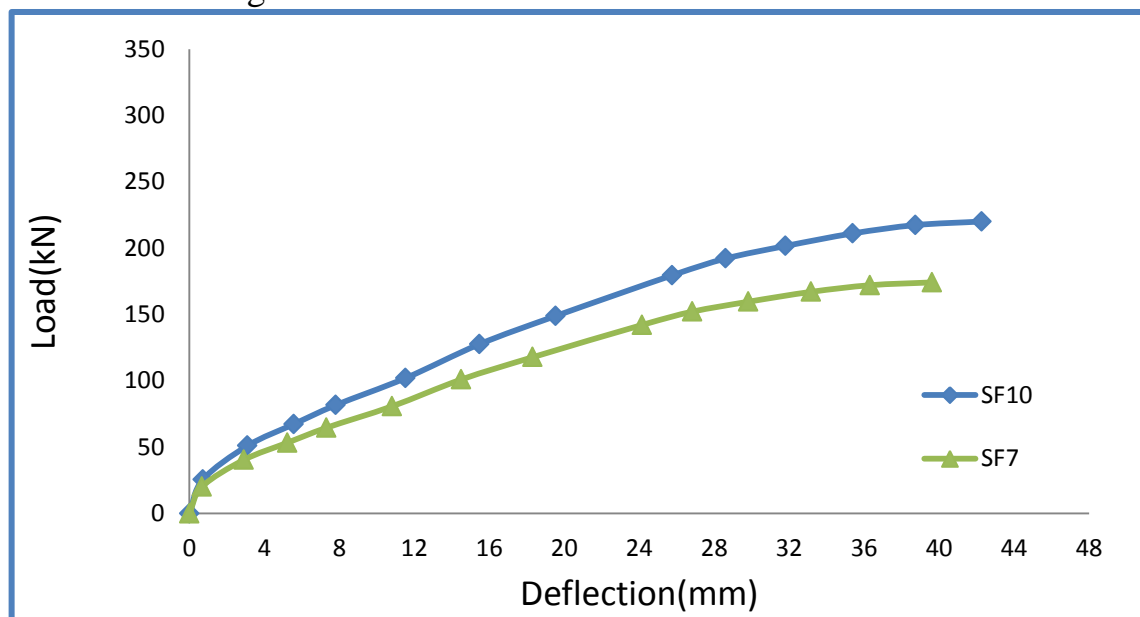


Figure 4.25 SF7 and SF10 Load- deflection curve.

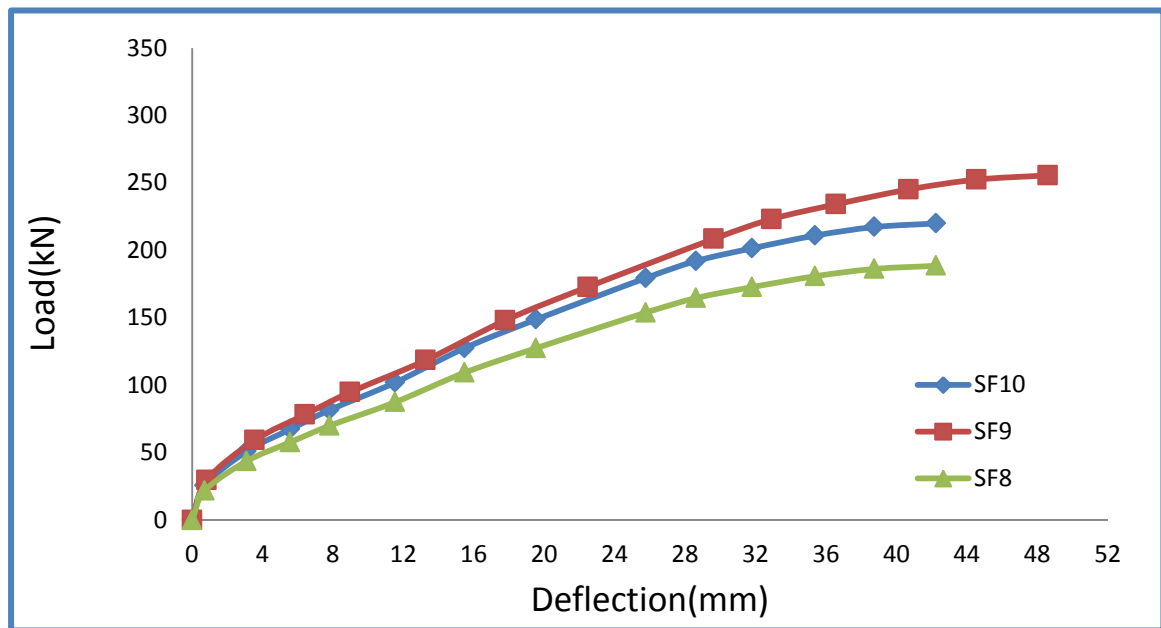


Figure 4.26 SF8, SF9, and SF10 Load- deflection curve

4.4.6 Stiffness of the Flexural Slabs

The term stiffness is considered an indicator and intended by many engineers as it represents the strength of the origin against external loads. The stiffness of flexural slabs was less than the stiffness of the punching shear because the stiffness is a results of contributing resisting forces such as concrete and steel reinforcement and fibers. The punching shear have a higher stiffness because the concrete has a high strength a against the shear forced beside the strengthening by steel fibers and steel reinforcement while the flexural slabs depend on the steel reinforcement and steel fibers only. The punching shear slabs stiffness was larger than flexural ones by (300%) because of the mentioned reasons above. Concerning the degradation in stiffness, the flexural specimens suffer from high degradation in initial stiffness larger than the punching slabs by about (3.5%) and according to these outcomes it is found that the flexural slabs need to strengthening more than punching ones. The solid slab (SF1) exposed a stiffness (17.7) kN/mm which suffers a degradation by about (173.2%) once the concrete member reached to the yield. The stiffness of the slabs with openings exposed an upgrade in the stiffness although of the openings' effect which it is

due the increase in steel fibers. The first three models with circular and rectangular openings showed an upgrade in the initial stiffness but these enhancements are varying according to the variation in shape of the opening which affected directly on the stiffness of flexural slabs. The slab with circular openings (SF3) got higher upgrade in the initial and final stiffness by (22.5% & 71.2%) respectively as exposed in Figure 4.27. Otherwise, the slab with rectangular openings which showed an upgrade less than the above model (SF3) which got enhancement by (11.5% and 8%) approximately in the initial stiffness for both slabs (SF2 and SF4) respectively. The secant stiffness upgraded by (38% & 18%) approximately for the both models respectively.

Change of steel fibers ration from (1%) to (1.5%) accompanied by transmitting the openings to the mid-region of the slab which affected the upgrade of the stiffness due to the increase in steel fibers. The upgrade in the stiffness values were little and not effective when compared with the previous models (SF2 to SF4). The upgrade in the slab (SF6) was (13%) only when compared with the model with less steel fibers ratio (1%) (SF3) as illustrated in Figure 4.28. The transmitting caused weakening to the concrete slab which affected negatively on the performance in general. The fabrication of more openings was accompanied by increase the steel fibers to higher ratio to compensate the effect of the openings and this is what happened in the slab specimens (SF8; SF9 and SF10) but the large effect of these openings was clear. The outcomes of addition of another two openings beside the existed ones affected the stiffness significantly which decreased the initial stiffness by rate of (14%) in comparison with the slabs with two openings (SF2; SF3 and SF4) respectively. The variance in the steel fibers which is (1%) could not repay all the loss in stiffness due to the weakening of the slab by the openings.

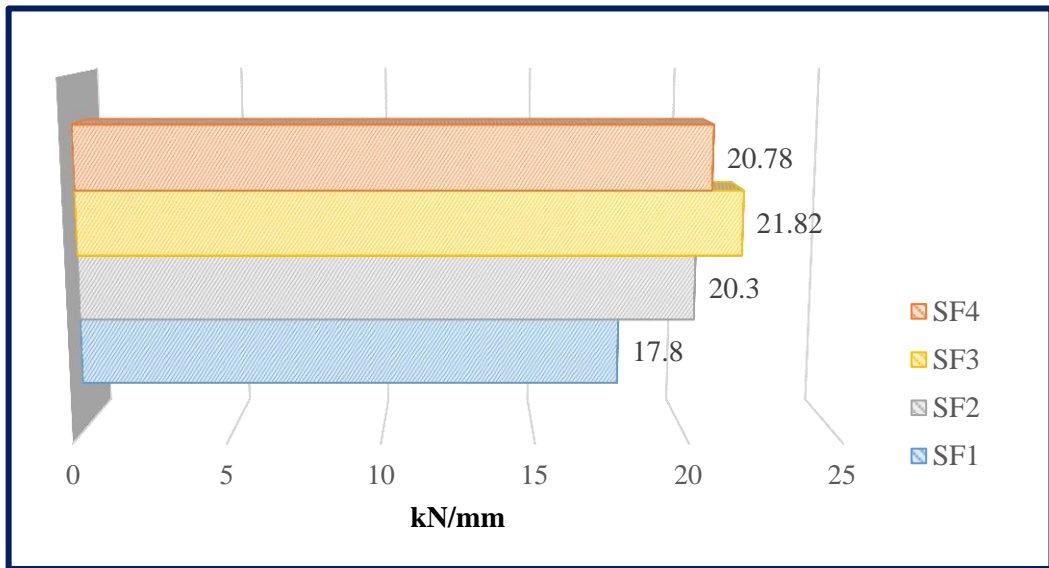


Figure 4.27 Comparison stiffness between of the SF1 and group B1.

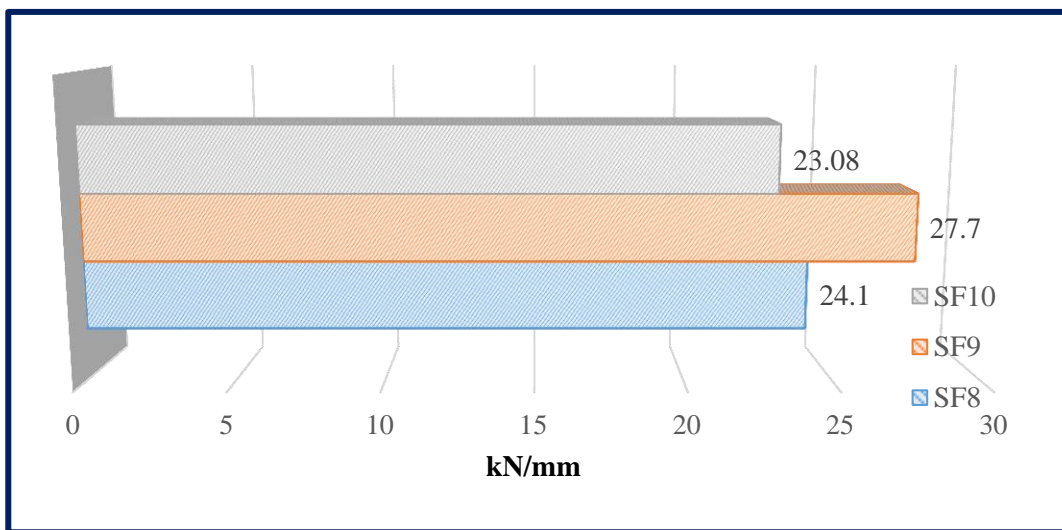
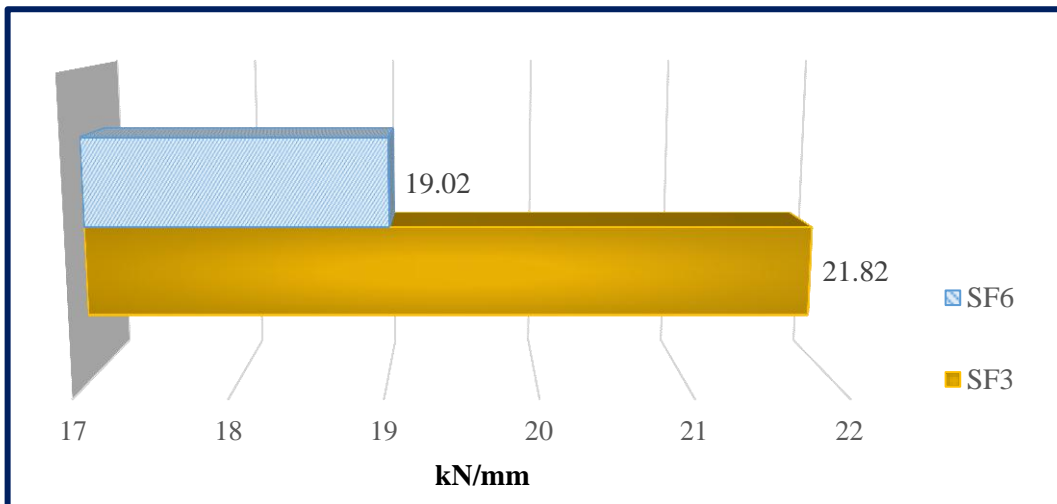
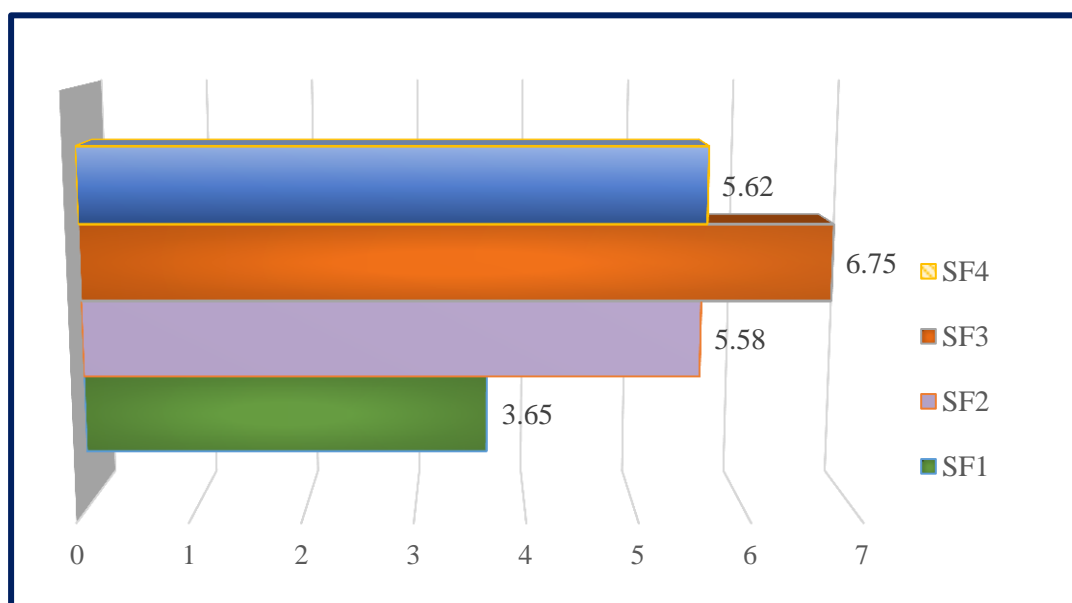


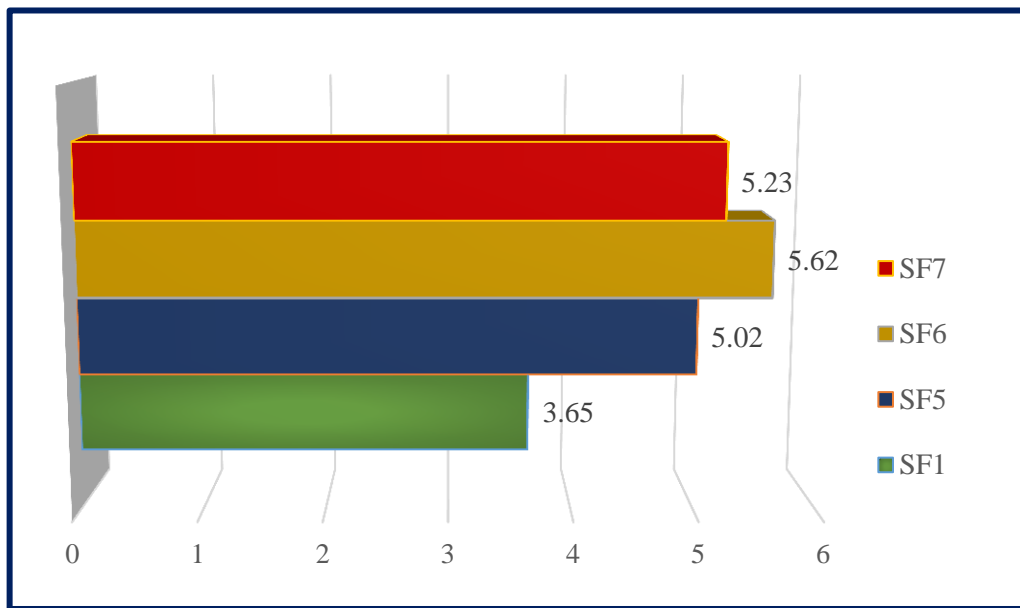
Figure 4.28 Comparison stiffness between of the solid and opening slabs.

4.4.7 Ductility of the tested slabs

Opening's effect and as expected has a significant effect on the ductility of the concrete slabs but with increase steel fibers to (1%) could gain an additional enhancement beside the compensation of the ductility loss. The average enhancement was by (34%) when compared with the control slab. The model with two circular corner openings (SF3) gained the ultimate enhancement which was (85%) approximately in comparison with the solid slab (SF1) as revealed in Figure 4.29a. Regarding the models with central openings, the relationship between the ductility and openings' location showed a significant change which the openings' locations affected the ductility but with increasing of the steel fibers to (1.5%) could getting an additional average ductility which was by (16%) approximately when compared with the solid control model. As a comparison with the previous models with corner openings and steel fibers (1%) (SP2 to SP5), it is found that the change of steel fibers (1%-1.5%) was un effected on the ductility index due to the critical location of the openings (near the middle column) as exposed in Figure 4.29b. In general, if there are a need to make opening in the slab, it should decrease the effect the of the openings by increasing the steel fibers to higher percentage.



(a) Comparison ductility index between of the SF1 and group (B1).



(b) Comparison ductility index between of the SF1 and group (B2).

Figure 4.29 Comparison ductility index between of the solid and slab with openings.

Increase the steel fibers and number of openings has a big effect on the ductility value which demonstrated an enhancement by (41.5%) approximately when simile with reference model (SF1). The slab model (SF9) has the maximum improvement in the ductility which reached to (140%) as revealed in Figure 4.30. It should be noted that the variance between the ductility of the models of (1.5% and 2%) was little due to the opening's effect.

It is important to point out an important fact, which is that despite the presence of openings, the performance of the fiber reinforced slabs has improved greatly, and this is due to the presence of steel fibers, which gave high efficiency to withstand the slab to resist the flexural stresses and able to recover the loss in the ductility of the concrete slab in addition to obtaining additional improvements developed the performance of the structural member. This thing can consider an excellent indicator of the possibility of construction of openings in critical regions.

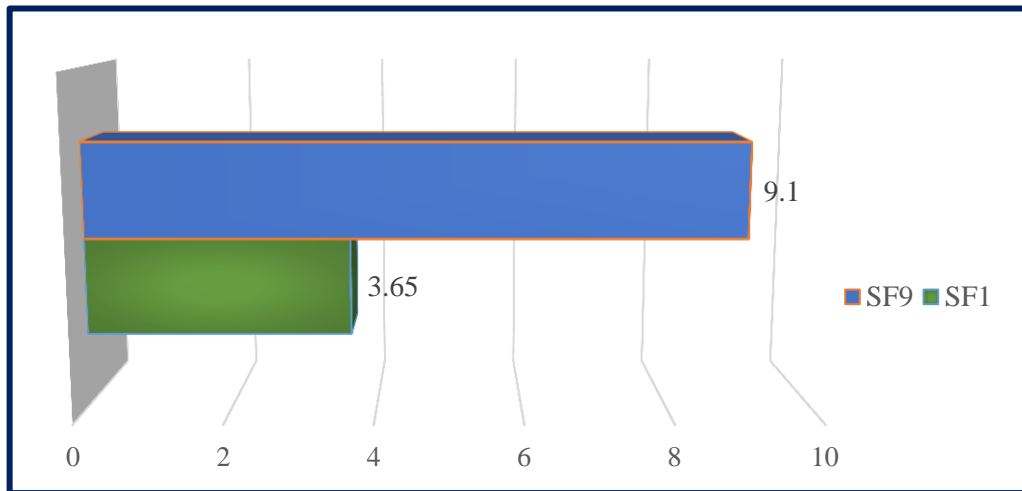


Figure 4.30 Ductility index of the solid and slab with four openings.

4.4.8 Energy Absorption

The energy absorption behavior of the flexural slabs was different to the scenario of the punching shear slabs which the flexural ones affected too much otherwise the punching slabs. The energy absorption suffered a highest dropping due to the openings existence when compared with the reference model although of steel fibers presence. The average absorption value dropped by (68%) in comparison with the solid slab (SF1). Larger decrement occurred in the model (SF4) which was (69%) as illustrated in Figure 4.29. Increase the ratio of fibers to (1.5%) could recover a part of the energy absorption although of shifting the openings to the middle zone of the concrete slab as exposed in Figure 4.31.

Reaching to the original capacity of energy absorption of the solid slab can be possible by increase the steel fibers ratio. The ratio of (2%) steel fibers increased the energy absorption by (71%) when compared with the two corner openings (SF2; SF3 and SF4). Regarding the number of openings, also addition of another two openings beside the existed ones affected the energy absorption by decreasing it but with addition of more steel fibers could compensate about (45%) of the happened loss in absorption value as showing in Figure 4.32, comparing the four and two openings slabs, it is found that energy absorption upgraded by up to (112%).

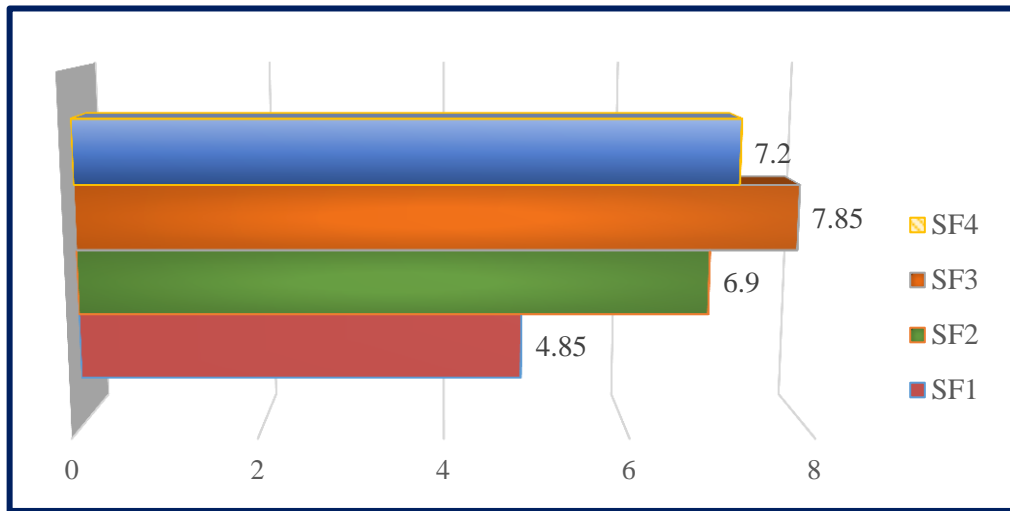


Figure 4.31 Comparison energy absorption between of the SF1and group B1.

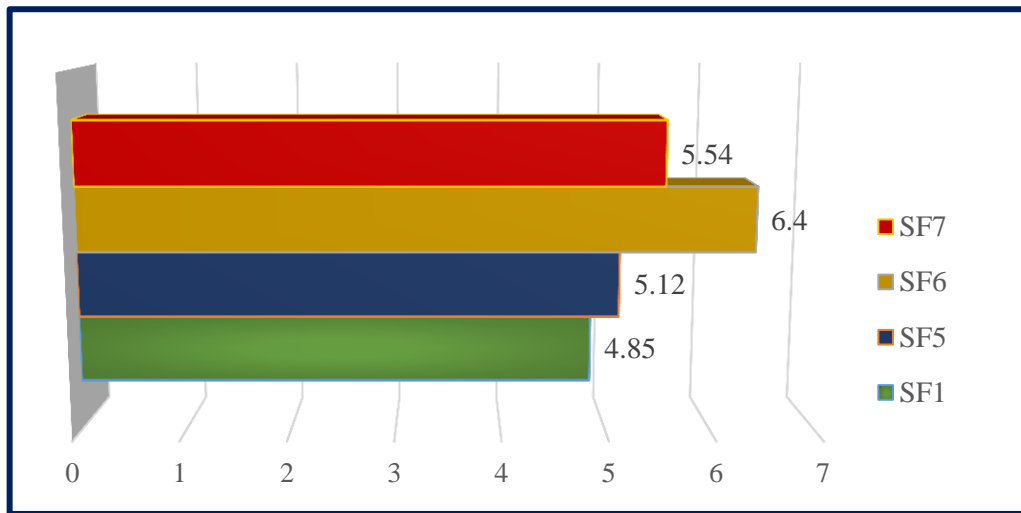


Figure 4.32Comparison energy absorption between of the SF1and group B2.

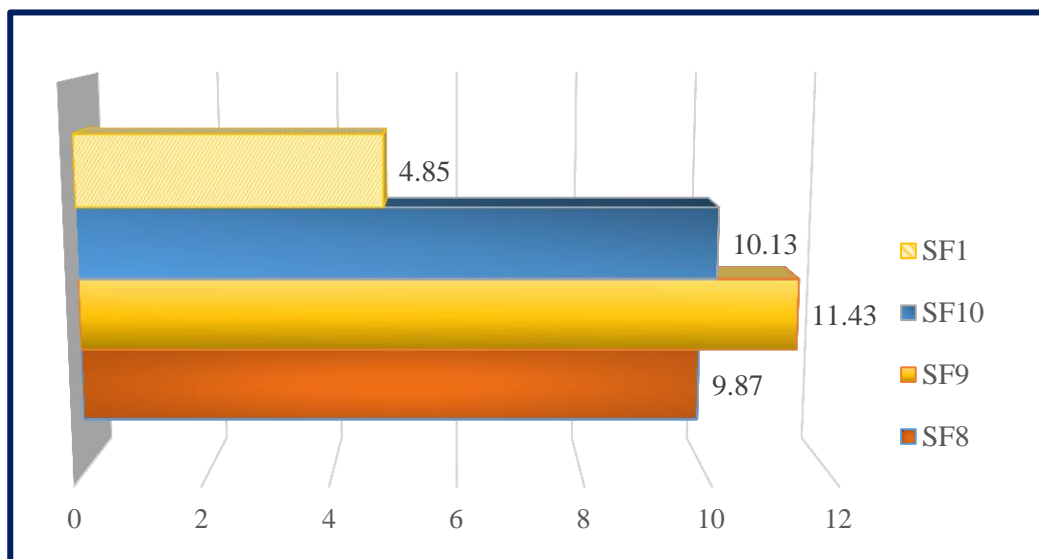


Figure 4.33 Comparison energy absorption between of the SF1and group B3.

4.4.9 Failure Mode and Crack Width

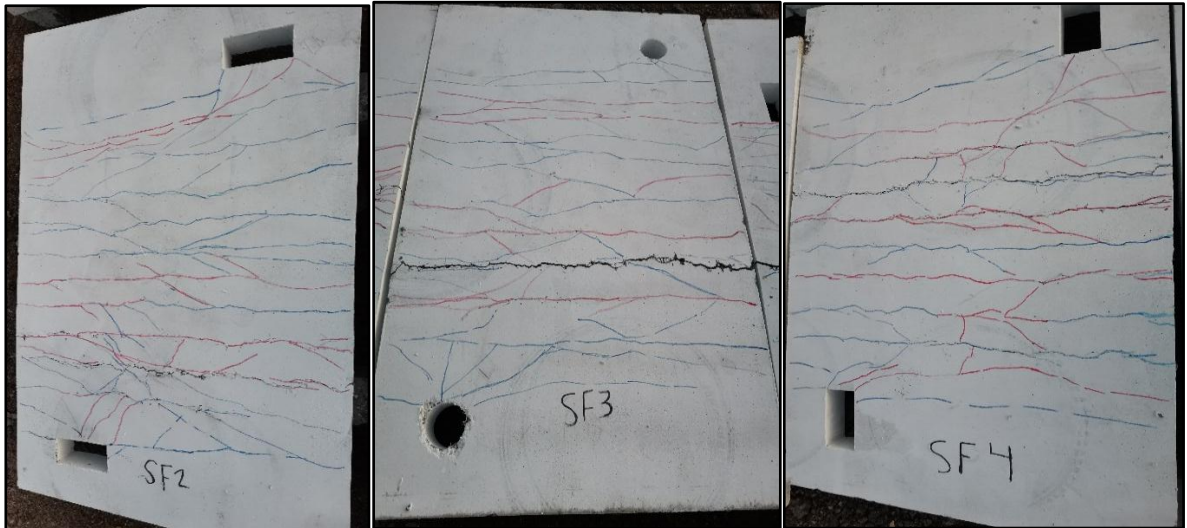
Table 4.4, illustrated the failure details such as the crack width at several loading stages, in addition to the crack pattern and failure mode. It's worth noting that this series' slab specimens all had flexure failures. The failure mode of control slab failure started by initiating the crack in a horizontal zigzag line parallel to the width of slab. The cracks appeared at the yield point then widened and extended reaching to the failure load. Area of the deformation in the control model was less than the occurred in the slabs with openings due to the steel fibers increment and the existence of the opening. The models (SF2; SF3 and SF4) showed an appearance of cracks in the perpendicular direction to the slab's length and extended towards the corner of the openings.

The crack width of each slab varied according to the geometry and mix of the concrete member. The slab specimens with two openings has a crack width larger than existed in the solid slab by (8.7%). The deformation amount in the solid model was the smallest in comparison with the slabs with slabs with openings because the openings generate a weak region. Add more steel fibers increase the cracks amount which increase the ductility and provide an additional resistance against the loads.

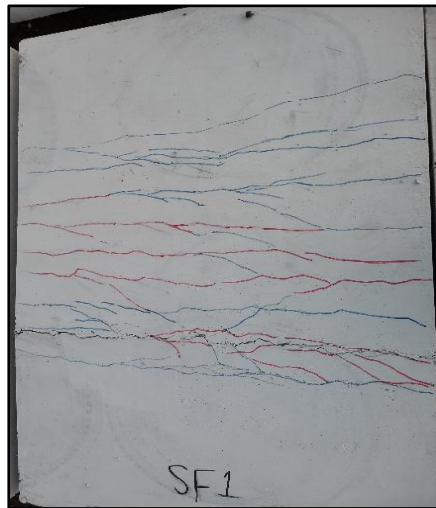
Transmitting the openings to the critical zone accompanied with the steel fibers increase to (1.5 percent) crack width was narrowed and increased the area of deformation. Comparing between the slabs (SF5 & SF7) and (SF2 & SF4) revealed an increment in the crack width by (38%) and (75%) when the openings transmitted to the mid-span. Regarding the circular opening's effect on the crack width, (SF6) had a crack width larger than once in the (SF3) by (20.1%). Add of more openings beside the existed ones with addition of more steel fibers (2%) upgrade the deformation zone with reducing the width. The crack width widened by (37%) as happened in the comparison (between the models SF2 and SF8).

Table 4.4 Crack width at the cracking and ultimate load of series two

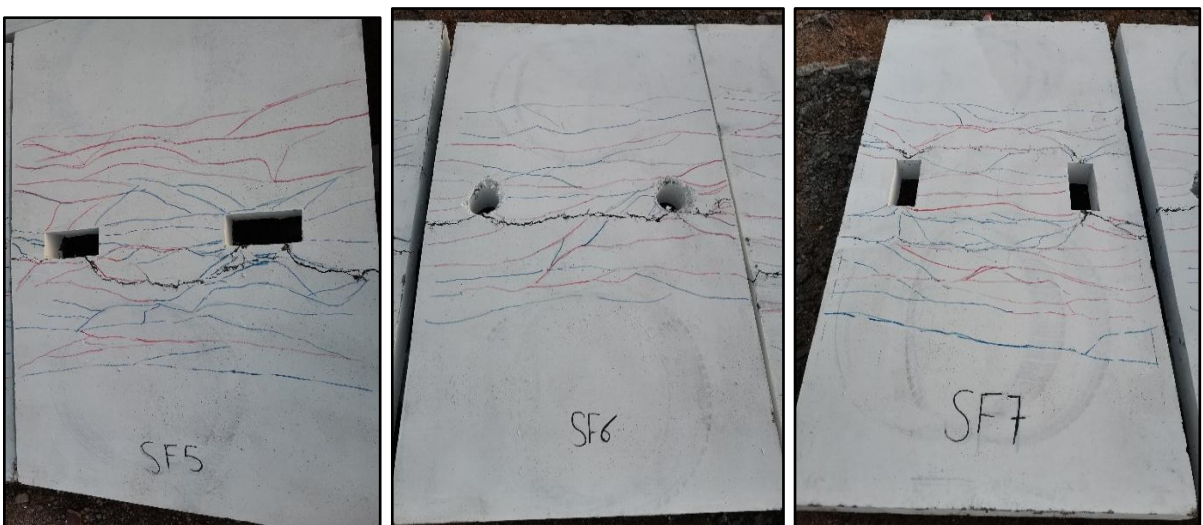
ID	W_{cr}(mm)	W_u(mm)
SF1	0.032	0.92
SF2	0.042	1.02
SF3	0.044	1.1
SF4	0.038	0.88
SF5	0.055	1.41
SF6	0.061	1.32
SF7	0.048	1.54
SF8	0.051	1.4
SF9	0.033	0.8
SF10	0.043	1.1



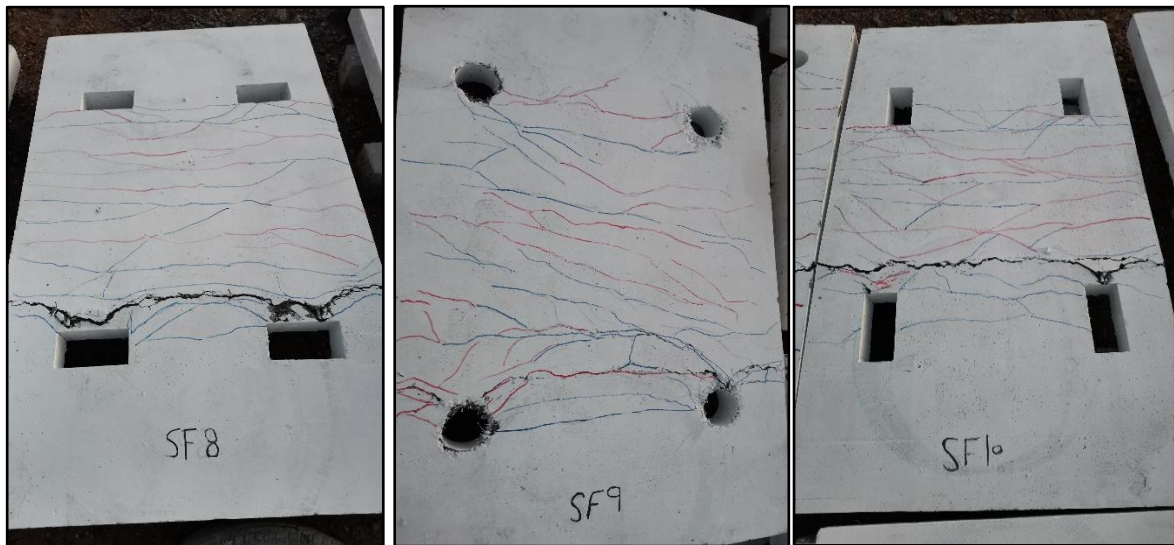
(a) Crack patterns for tested slabs group B1



(b) Crack patterns for tested control slabs



(c) Crack patterns for tested slabs group B2



(d) Crack patterns for tested slabs group B3

Figure 4.34 Crack pattern and failure mode of flexural slabs.

4.5 Effect of Steel Fibers

As expected, the steel fibers affect the mechanical properties which increase the strength capacity of the concrete member against the applied loads but these effects varied according to the condition of the member. Effect of increase the steel fibers look clear on the strength of both punching and flexural slabs but the increment was dissimilar. The increment in the fiber's ratio revealed a compensation to the loss in load with gaining an average upgrade by (6%) in the flexural slabs and (12%) in the punching models. This thing refers to the need of the flexural member to strengthening and their sensitivity against the construction of openings inside the concrete body. Additional effects accompanied the increase in fiber ratios, including its effect on the initial and secant stiffness, in addition to energy absorption and ductility. As for the spread of cracks, it was greatly affected by the increase of fibers, and concrete slabs became more deformed as a result of providing the steel fibers higher efficiency to the slabs to resist external loads.

4.6 The Impact of Opening

The presence of openings in general, affects the general performance of the concrete member, but the effect of the presence of the opening varies according to the design followed for the concrete member. It was noticed that the presence of openings in the slabs designed to fail in flexure were more affected and weaker due to the presence of the openings, as they suffered from reduced strength, stiffness, and absorption of energy in large proportions than slabs that designed to fail by punching shear. The cracking load decreased after creating the openings but the decrement values varied between the flexural and punching shear slabs, which decreased by (55.3%) for the punching shear slabs. The flexural slabs suffered a decrement by (27%) in the cracking load after creating the openings.

The presence of the openings had an effect even on the percentage of upgrade in the strength as a result of the addition of steel fiber, as the presence of the openings reduced the possibility of obtaining large upgrade due to weaken the concrete member. The effect of the openings not only reduced the load capacity and weaken its strength, but also extended to the reduction of stiffness, energy absorption and ductility of concrete slabs, but increasing the proportion of steel fibers was able to recover a large part of the loss. It should be noted that the concrete properties most affected by the presence of openings are the properties of slabs that have failed in flexure.

4.7 The Openings' location, Shape, and Number

The location and shape of the opening, as well as its number, had a direct effect on the properties of the concrete slab. For example, when moving the opening to the middle of the slab, the strength of the slabs decreased, but this ratio differs between the two types of slabs (flexural and punching shear slabs). After transmitting the openings of the flexural slabs, the strength decreased by average of (4.3%) and the displacement decreased by average of (2.7%) approximately. While the punching slabs, the strength decreased by average of (3.7%) and the displacement decreased by average of (11.3%) approximately. The number of openings is directly proportional to the decrease in the strength of the concrete slab, as it was found that the effect of increasing the number affects the displacement of the slab and this descent, its value varies according to the concrete slab type. Increase the openings number in the flexural slabs increased the displacement by (17.4%) approximately while the punching ones included reducing the displacement by average of (8%) approximately.

CHAPTER FIVE**CONCLUSIONS AND RECOMMENDATIONS****5.1 Conclusions**

The experimental study is focuses on the behavior of the slab with opening strengthened by steel fiber reinforced concrete under monotonic loading. Based on the results obtained experimentally, many factors have significant effect on the behavior of flat slab at failure, and these effects can be summarized as follows:

- 1) The addition of steel fibers redistributed the internal stresses and enhanced the ultimate strength, load-carrying capacity, stiffness, ductility, and energy absorption of the concrete slab
- 2) Increase of hooked steel fibers ratio (0.5%, 1%, 1.5%, and 2%) exposed different load capacities which revealed a compensation to the loss in load with gaining an average upgrade by (21.2%) in comparison with control slab. An increase in steel fibers does not mean a permanent increase in ultimate load capacity, Therefore, the unnecessary increase in the number of steel fibers causes more cost without large benefit. The optimum value for hooked steel fibers in the punching shear case is (1.0%) and (1.5%) for the flexural case.
- 3) The steel fibers presence redistributed the flexural stresses and affected the cracking load. Cracks appeared in the solid punching slab at (27.2%) and in the flexural specimens at (34.5%) of the ultimate load which increased after increasing the steel fibers.
- 4) The increase of openings number caused less displacement and decrease the ultimate strength which the strength decreased by average of (5.7%) and the displacement decreased by average of (11.13%) approximately.

- 5) The difference in the opening shape has an effect on the ultimate flexural strength which exceeded (43.5%).
- 6) The variance in the opening numbers and locations causing increasing the occurred displacement beside the decreasing in the cracking load. The cracking load decreased when the openings when transmitted from the corner to the critical zone near the center of the slab.
- 7) Increase the openings number causes decrease in the occurred displacement in the punching shear slabs but increased the displacement for the flexural slabs.
- 8) The variance in the opening numbers and locations affected the flexural behavior which caused increasing the occurred displacement beside the decreasing in the cracking load. The cracking load decreased when the openings when transmitted from the corner to the critical zone near the center of the slab which decreased by average value equal to (62%) in comparison with slabs with corner openings.

5.2 Recommendation for Future Works

Extra investigation to understand the basic behavior of RC Flat slabs is required. The following suggestions are recommended:

- 1) Investigation of flat slab with opening by ultra-high strength concrete.
- 2) Study of the behavior of SFRC slab under cyclic loading (experimentally and numerically).
- 3) Experimental and numerical study of retrofitting damaged slabs by CFRP.
- 4) Punching shear behavior of fibrous concrete flat slab with openings subjected eccentric loading.
- 5) Behavior of Reinforced Concrete Slabs with Openings under Impact Loads.

References

- [1] Wight, J. K., & MacGregor, J. G. " Reinforced concrete mechanics and design",2011.
- [2] Fürst, A., & Marti, P. "Robert Maillart's design approach for flat slabs", Journal of Structural Engineering, 123(8), 1102-1110,1997.
- [3] Gasparini, D. A. "Contributions of CAP Turner to development of reinforced concrete flat slabs" , 1905–1909. Journal of Structural Engineering, 128(10), 1243-1252,2002.
- [4] Kierdorf. "Early Mushroom Slab Construction in Switzerland, Russia and the .S.A. – A Study in Parallel Technological Development". Proc. Second Int. Congr. Constr. Hist, pp. 1793–1807,2006.
- [5] Bartolac, M., Damjanović, D., & Duvnjak, I. " Punching strength of flat slabs with and without shear reinforcement". 67(08.), 771-786,2015.
- [6] Park, R., & Gamble, W. L. " Reinforced concrete slabs". John Wiley & Sons,2006.
- [7] Nilson.A.D, Darwin.D, &. DolanC.W."Design of concrete structures". McGraw-Hill Higher Education, 2010.
- [8] Halvonik, J., & Fillo, L. " The maximum punching shear resistance of flat slabs",Procedia Engineering, 65, 376-381.2013.
- [9] A. Sayed, "Punching shear behaviour of FRP-reinforced concrete interior slab-column connections", 2015.
- [9] Muttoni, A., & Fernández Ruiz, M. "Shear strength of members without transverse reinforcement as function of critical shear crack width", ACI Structural Journal, 105(ARTICLE), 163-172,2008.
- [10] Chiang, C. L. "Punching shear strength of reinforced and post-tensioned concrete flat plates with spandrel beams",1994.
- [11] Fernández Ruiz, M., Mirzaei, Y., & Muttoni, A. " Post-punching behavior of flat slabs", ACI Structural Journal, 110(ARTICLE), 801-812,2013.
- [12] Krüger, G. " Resistance to eccentric punching of floors-slabs",1999.
- [13] Pantazopoulou, S. J., & Moehle, J. P. " The Effect of Slabs on the Flexural Behavior of Beams", Earthquake Engineering Research Center, College of Engineering, University of California at Berkeley,1987.
- [14] Rusinowski, P. "Two-way concrete slabs with openings: experiments, finite element analyses and design",2005.

REFERENCES

- [15] Ali.A.H . "Nonlinear Behavior of Self -Compacting Reinforced Concrete Two-Way Slabs with Central Square Opening under Uniformly Distributed Loads", Journal of Engineering , No.(7) vol.(22),2016.
- [16] Standard, B., 1997. "Structural Use of Concrete: Code of Practice for Design and Construction", Part 1, BS 8110. British Standard Institution, UK
- [17] ACI Committee 318 (2014). "Building Code Requirements for Structural Concrete (ACI 318-14) and Commentary (ACI 318R-14)", American Concrete Institute", Farmington Hills, MI, 519 pp.
- [18] Abrishami, H. H. and Mitchell, D., "Influence of Steel Fibers on Tension Stiffening", ACI Structural Journal, November-December, 1997, pp.769-776
- [19] ACI 544.1 R-96, "State of the Art Report on Fiber Reinforced Concrete", ACI Manual, 1999, 66p.
- [20] ACI Committee 544, "Measurement of Properties of Fiber Reinforced Concrete", (ACI544.2R)
- [21] Muslim K. Al-kanoon , "Studying of Compressive, Tensile and Flexural Strength of Concrete by Using Steel Fibers", Journal of Babylon University/Engineering Sciences, Vol.24, 2016.
- [22] Shah, S. P., Stroeven, P., Dalhuisen, D., Van Stekelenburg, P. " Complete Stress-Strain Curves for Steel Fibre Reinforced Concrete in Uniaxial Tension and Compression", Construction Press, Lancaster, p.p. 399–408.1987.
- [23] ACI 544.1 R-96, "State of the Art Report on Fiber Reinforced Concrete", ACI Manual, 1999, 66p
- [24] ACI 544 .5R-1 0"Report on the Physical Properties and Durability of Fiber -Reinforced Concrete, 2010.
- [25] Pilakoutas, K., & Li, X. " Alternative shear reinforcement for reinforced concrete flat slabs", Journal of Structural Engineering, 129(9), 1164-1172,2003.
- [26] Oliveira, M. H. D., Pereira Filho, M. J. M., Oliveira, D. R. C. D., Ferreira, M. D. P., & Melo, G. S. S. D. A. (2013). Punching resistance of internal slab-column connections with double-headed shear studs. Revista IBRACON de Estruturas e Materiais, 6(5), 681-714.
- [27] Bu, W., & Polak, M. A. "Seismic Retrofit of Reinforced Concrete Slab-Column Connections Using Shear Bolts". ACI Structural Journal, 106(4),2009.

REFERENCES

- [28] Fernández Ruiz, M., & Muttoni, A. " Applications of the critical shear crack theory to punching of R/C slabs with transverse reinforcement", ACI Structural Journal, 106(ARTICLE), 485-494,2009.
- [29] Polak, M. A., El-Salakawy, E., & Hammill, N. L. " Shear reinforcement for concrete flat slabs", Special Publication, 232, 75-96,2005.
- [30] Broms, C. E. " Elimination of flat plate punching failure mode", ACI Structural Journal, 97(1), 94-101,2000.
- [31] Hoang, L. C. "Punching shear tests on RC slabs with different initial crack patterns". Procedia engineering, 14, 1183-1189,2011.
- [32] Gouveia, N. D., Fernandes, N. A., Faria, D. M., Ramos, A. M., & Lúcio, V. J. " SFRC flat slabs punching behaviour–Experimental research", Composites Part B: Engineering, 63, 161-171,2014.
- [33] Ha, T., Lee, M. H., Park, J., & Kim, D. J. " Effects of openings on the punching shear strength of RC flat-plate slabs without shear reinforcement", The structural design of tall and special buildings, 24(15), 895-911,2015. Structures, 203, 109872,2020.
- [34] Silva, J. A., Marques, M. G., Trautwein, L. M., Gomes, R. B., & Guimarães, G. N. "Punching of reinforced concrete flat slabs with holes and shear reinforcement", REM-International Engineering Journal, 70(4), 407-413,2017.
- [35] Musse, T. H., Liberati, E. A. P., Trautwein, L. M., Gomes, R. B., & Guimarães, G. N. ()" Punching shear in concrete reinforced flat slabs with steel fibers and shear reinforcement", Revista IBRACON de Estruturas e Materiais, 11(5), 1110-1121, 2018.
- [36] Ismail, E. S. I. M. " Non-linear finite element analysis of reinforced concrete flat plates with opening adjacent to column under eccentric punching loads", HBRC journal, 14(3), 438-449,2018.
- [37] Liberati, E. A., Marques, M. G., Leonel, E. D., Almeida, L. C., & Trautwein, L. M. "Failure analysis of punching in reinforced concrete flat slabs with openings adjacent to the column", Engineering Structures, 182, 331-343,2019.
- [38] Abdel-Rahman, A. M., Hassan, N. Z., & Soliman, A. M. " Punching shear behavior of reinforced concrete slabs using steel fibers in the mix", HBRC journal, 14(3), 272-281,2018.

REFERENCES

- [39] Mostofinejad, D., Jafarian, N., Naderi, A., Mostofinejad, A., & Salehi, M. "Effects of openings on the punching shear strength of reinforced concrete slabs", In Structures (Vol. 25, pp. 760-773). Elsevier,2020, June.
- [40] Schmidt, P., Kueres, D., & Hegger, J. " Contribution of concrete and shear reinforcement to the punching shear resistance of flat slabs", Engineering,203.109872, 2020.
- [41] Kumari, T. G., Puttappa, C. G., Shashidar, C., & Muthu, K. U. "Flexural Characteristics of SFRSCC and SFRNC one way slabs",IJRET: International Journal of Research in Engineering and Technology, 2321-7308,2013.
- [42] Al-hafiz, A. M., Chiad, S. S., & Farhan, M. S. " Flexural Strength of Reinforced Concrete One-Way Opened Slabs with and without Strengthenin", Australian Journal of Basic and Applied Sciences, 7(6): 642-651, 2013 ISSN 1991-8178,2013.
- [43] Baarimah, A. O., & Mohsin, S. S. " Behaviour of reinforced concrete slabs with steel fibers. In IOP Conference Series", Materials Science and Engineering (Vol. 271, No. 1, p. 012099). IOP Publishing,2017 November.
- [44] Shaheen, Y., Hekal, G., & Khalid, A. " Behavior of Reinforced Concrete Slabs with Openings under Impact Loads",2017.
- [45] Chkheiw, A. H., & Abdullah, M. D. " Flexural behavior of high strength RC slabs with opening strengthening with wire mesh and steel fibers", Kufa Journal of Engineering, 8(3),2017.
- [46] McMahan, J. A., & Birely, A. C. " Service performance of steel fiber reinforced concrete (SFRC) slabs". Engineering Structures, 168, 58-68,2018.
- [47] Holý, M., Čítek, D., Tej, P., & Vráblík, L. " Flexural Strength of Thin Slabs Made of UHPFRC", In Solid State Phenomena (Vol. 292, pp. 224-229). Trans Tech Publications Ltd,2019.
- [48] Qasim, O. A. " Behavior of reinforced reactive powder concrete two-way slabs with openings", In IOP Conference Series: Materials Science and Engineering (Vol. 518, No. 2, p. 022077). IOP Publishing,2019May
- [49] Sadowska-Buraczewska, B., Szafraniec, M., Barnat-Hunek, D., & Łagód, G. "Flexural behavior of composite concrete slabs made with steel and polypropylene fibers reinforced concrete in the compression zone". Materials, 13(16), 3616, 2020.

REFERENCES

- [50] Triantafillou. T. "Externally bonded FRP reinforcement for RC structures". Bulletin FIB, vol. 14. International Federation for Structural Concrete (fib), 2001
- [51] Iraqi Standard 5/1984. Portland cement central organization for standardization and quality control Iraq. (in Arabic) .
- [52] ASTM C150. Standard Specification for Portland Cement, 2012.
- [53] Iraqi standard 45/1984. Aggregates from natural sources for concrete and building construction. central organization for standardization and quality control. Iraq (in Arabic).
- [54] ASTM C33. Standard Specification for Concrete Aggregates. (Vol. 4.2, PP. 1–11),2003.
- [55] Dahake, A. G., & Charkha, K. S. " Effect of steel fibers on strength of concrete". Journal of Engineering, Science & Management Education, 9(I), 45-51, 2016.
- [56] ASTM A820/A 820M. Standard Specification for Steel Fiber for Fiber-Reinforced Concrete. pp.1-4,2016.
- [57] Hannant D. J. " Fiber Cements and Fiber Concretes". John Wiley and sons, Wiley International Publication, 218p, Department of Civil Engineering University of Surrey, John Wiley & Sons. pp 52-6,1978.
- [58] American Specification for Testing and Materials. Standard Specification for Chemical Admixtures for Concrete, C – 494.
- [59] ASTM C1240. Standard Specification for Silica Fume used in Cementations mixtures. ,USA: ASTM International,2005.
- [60] Aldred, J. M., Holland, T. C., Morgan, D. R., Roy, D. M., Bury, M. A., Hooton, R. D., & Zhang, M. H. " Guide for the use of silica fume in concrete". ACI–American Concrete Institute–Committee: Farmington Hills, MI, USA, 234,1996.
- [61] Panesar, D. K. " Developments in the Formulation and Reinforcement of Concrete", (Second Edition). Woodhead Publishing Series in Civil and Structural Engineering, 2019.
- [62] ASTM A615 / A615M. Standard Specification for Deformed and Plain Carbon-Steel Bars for Concrete Reinforcement. ASTM International, West Conshohocken, PA,2020.

REFERENCES

- [63] Al-Wahili A.A. " Mechanical Properties of Steel Fiber Reinforced Reactive Powder concrete", M.Sc Thesis, Building and Construction Engineering Department, University of Technology, Baghdad, 123p,2015.
- [64] ASTM C143. Standard Test Method for Slump of Hydraulic Cement Concrete,2000
- [65] B.S.1881, Part 116. Method for Determination of Compressive Strength of Concrete Cubes. British Standards Institution,1989.
- [66] ASTM C39/C39M. Standard Test Method for Compressive Strength of Cylindrical Test Specimens. Vol. 04.02,2019.
- [67] ASTM C496/C496M-18. Standard Test Method for Splitting Tensile Strength of Cylindrical Concrete Specimens. Vol. 4.2, PP. 1-5,2018.
- [68] ASTM C78/C78M. Standard Test Method for Flexural Strength of Concrete. (Using Simple Beam with Third-Point Loading), USA: ASTM International, pp.1-4,2015.
- [69] ASTM C469/C469M. Standard Test Method for Static Modulus of Elasticity and Poisson's Ratio of Concrete in Compression. USA: ASTM International, pp.1-5,2014.
- [70] Baumgart, F. "Stiffness-an unknown world of mechanical science",Injury-International Journal for the Care of the Injured, 31(2), 14-23,2000.
- [71] Marzouk, H., & Hussein, A. "Experimental investigation on the behavior of high-strength concrete slabs". ACI Structural Journal, 88(6), 701-713, 1991.
- [72] Husain, M., Eisa, A. S., & Roshdy, R. "Alternatives to enhance flat slab ductility. International Journal of Concrete Structures and Materials, 11(1), 161-169, 2017.
- [73] Sullivan, T. J., Calvi, G. M., & Priestley, M. J. N. "Initial stiffness versus secant stiffness in displacement based design". In 13th World Conference of Earthquake Engineering (WCEE) (No. 2888),2004 August.
- [74] Priestley, M. J. N., & Park, R. "Strength and ductility of concrete bridge columns under seismic loading". Structural Journal, 84(1), 61-76,1987.
- [75] Robertson, I. N., & Durrani, A. J. " Gravity load effect on seismic behavior of exterior slab-column connections". Structural Journal, 88(3), 255-267,1991.
- [76] Ohno, T., & Nishioka, T. " An experimental study on energy absorption capacity of columns in reinforced concrete structures". Doboku Gakkai Ronbunshu, 1984(350), 23-33,1984.



河北宇森网类制品有限公司
Hebei YuSen Metal Wire Mesh Co., Ltd.

钢纤维质量证明书
Steel fibre quality certificate

地址 (ADDRESS): 河北省安平丝网大世界开发区
Wire Mesh World Anping, Hengshui, Hebei,
P. R. China
电话 (TEL): +86-318-7758858
传真 (FAX): +86-318-5288858
网址 (WEB): www.china-steelfiber.com.cn
邮箱 (EMAIL): yusen01@metalmesh.com.cn

名称: Description	端勾钢纤维(Hooked End Steel Fiber)				订单号: Order No.	20180326
规格: DIMENSIONS	0.5*30mm				质量证明书号: Certificate ID	YS-GQW18032701
执行标准: Executive Standard	YB/T151-1999, ASTM A820-96, ASTM1116				签发日期: Date Of Issue	2018.03.27
检测项目 Detected items	等效直径 Diameter	长度 Length	抗拉强度 Tensile Strength	长径比 L/D	弯曲性能, 变芯 3mm Bending Properties ,Bend Core 3mm	外观质量 Quality of Soating
标准值 Standard values	0.5±10%	30±10%	≥1100	30~100	冷弯 90°, 9/10 不断 Cold bend 90°, 9/10 have not broken	OK
检测值 Detected value	0.51mm	30.2	1200	60	10/10 不断 10/10 have not broken	OK
综合判定 Final Result	合格 OK	1、质量证明书复印件不作有效证明文件。 The copy of this certificate is invalid. 2、用户验货使用有异常及时告知编号、并保留实物及标志。 The no. will be sent to ours in time by the customer,if the complain would happened after in section.Keep in the material and the marking card.				质量印章 SEAL 质检专用章 签证人 Inspector 刘勤力

Product Data Sheet
Edition 2, 2015
Version no. 12.2014

Sika ViscoCrete® -5930L

High Performance Superplasticiser Concrete Admixture

Product Description Sika ViscoCrete® -5930L is a third generation super plasticizer for concrete and mortar. It meets the requirements for super plasticizer according to ASTM-C- 494 Types G and F and BS EN 934 part 2: 2001.

Uses Sika ViscoCrete® -5930L is suitable for the production of concrete.
Sika ViscoCrete® -5930L facilitates extreme water reduction, excellent flowability at the same time optimal cohesion and highest self compacting behaviour.

Sika ViscoCrete® -5930L is used for the following types of concrete:

- Precast concrete.
- Ready Mix Concretes.
- Concrete with highest water reduction (up to 30%).
- High strength concrete.
- Hot weather Concrete.
- Self compacting concretes.

High water reduction, excellent flowability, coupled with high early strengths, have a positive influence on the above mentioned applications.

Advantages Sika ViscoCrete® -5930L acts by different mechanisms. Through surfaces adsorption and sterical separation effect on the cement particles, in parallel to the hydration process, the following properties are obtained:

- Strong self compacting behaviour. Therefore suitable for the production of self compacting concrete.
- Extremely high water reduction (resulting in high density and strengths).
- Excellent flowability (resulting in highly reduced placing - and compacting efforts)
- Increase high early strengths development.
- Improved shrinkage- and creep behaviour.
- Reduced rate of carbonation of the concrete.
- Improved Water Impermeability.

Sika ViscoCrete® -5930L does not contain chloride or other, steel corrosion promoting ingredients. It may therefore be used without any restrictions for reinforced and prestressed concrete construction.

Technical Data

Basis	Aqueous solution of modified Polycarboxylate
Appearance	Turbid liquid
Density	1.1 kg/lit. (ASTM C494)
Packaging	5 Kg, 20 Kg pails 200 kg drums Bulk Tanks are available upon request.

Storage/ Shelf Life In unopened, undamaged original container, protected from direct sunlight and frost at temperatures between + 5 °C and + 35°C. Shelf life at least 12 months from date of production.



Application	
Dosage	<p>Recommended dosage:</p> <ul style="list-style-type: none"> ■ For soft plastic concrete: 0.2 - 0.8 % litre by weight of cement ■ For flowing and self compacting concrete (S.C.C.) 0.8 - 2 % litre by weight of cement
Addition	<p>Sika ViscoCrete® -5930L is added to the gauging water or simultaneously with it poured into the concrete mixer. For optimum utilisation of the high water reduction we recommend through mixing at a minimal wet mixing time of 60 seconds.</p> <p>The addition of the remaining gauging water - to fine tune concrete consistency - may only be started after 2/3 of wet mixing time, to avoid surplus water in the concrete.</p>
Concrete Placing	<p>With the use of Sika ViscoCrete® -5930L concrete of highest quality is being produced. The standard rules of good concreting practice (production as well as placing) must also be observed with Sika ViscoCrete® -5930L concrete.</p> <p>Fresh concrete must be cured properly.</p>
Frozen Sika ViscoCrete® -5930	<p>Frozen Sika ViscoCrete® -5930L may be used after It has been slowly thawed at room temperature and intensively mixed.</p>
Combinations	<p>Sika ViscoCrete® -5930L may be combined with the following Sika products:</p> <ul style="list-style-type: none"> ■ Sika Pump®. ■ Sika Rapid®. ■ Sika Ferrogard®-901. ■ Sikafume®. ■ Sika Fro® -V5A ■ Sika Retarder® <p>Pre-trials are recommended if combinations with the above products are being made. Please consult our technical service.</p>
Important Flowing Concrete S.C.C	<p>Sika ViscoCrete® -5930L is also used to produce flowing and self compacting concrete (S.C.C.) For these, special mix designs are required, contact our Technical Service division.</p>
Safety Instructions	
Ecology	<p>Do not dispose of into water or soil, but according to local regulations.</p>
Transport	<p>Non-hazardous.</p>
Safety Precautions	<p>In contact with skin, wash off with soap & water. In contact with eyes or mucous membrane, rinse immediately with clean warm water and seek medical attention without delay.</p>
Toxicity	<p>Non-Toxic under relevant health and safety codes.</p>
Legal notes	<p>The information and in particular the recommendations relating to the application and end-use of Sika products, are given in good faith based on Sika's current knowledge and experience of products when properly stored, handled and applied under normal conditions. In practice, the differences in materials, substrates and actual site conditions are such that no warranty in respect of merchantability or of fitness for a particular purpose, nor any liability arising out of any legal relationship whatsoever, can be inferred either from this information, or from any written recommendations, or from any other advice offered. The proprietary rights of third parties must be observed. All orders are accepted subject to our current terms of sale and delivery. Users should always refer to the most recent issue of the technical data sheet for the product concerned, copies of which will be supplied on request.</p> <p>For further technical information, please consult our technical service department.</p>



Sika Egypt for Construction Chemicals
 El About City
 1st Industrial zone (A)
 Section # 10 Block 13035,
 Egypt

Tel :+202- 4481 0580
 Fax :+202- 4481 0459
 Mob :+2012- 2390 8822/55
 www.sika.com.eg





MegaAdd MS(D)

Densified Microsilica

DESCRIPTION	<p>MegaAdd MS(D) is a very fine pozzolanic, ready to use high performance mineral additive for use in concrete. It acts physically to optimize particle packing of the concrete or mortar mixture and chemically as a highly reactive pozzolan.</p> <p>MegaAdd MS(D) in contact with water, goes into solution within an hour. The silica in solution forms an amorphous silica rich, calcium poor gel on the surface of the silica fume particles and agglomerates. After time the silica rich calcium poor coating dissolves and the agglomerates of silica fume react with free lime (CaOH_2) to form calcium silicate hydrates (CSH). This is the pozzolanic reaction in cementitious system.</p>
STANDARDS	ASTM C1240
USES	MegaAdd MS(D) can be used in a variety of applications such as concrete, grouts, mortars, fibre cement products, refractory, oil/gas well cements, ceramics, elastomer, polymer applications and all cement related products.
ADVANTAGES	<ul style="list-style-type: none"> • High to ultra high strength • High resistance to chlorides and sulfates • Protection against corrosion • Increased durability, longer service life for structures • Enhanced rheology, control of mixture segregation and bleed • Greater resistance to chemicals

TYPICAL PROPERTIES at 25°C

PROPERTY	TEST METHOD	VALUE
State	Amorphous	Sub-micron powder
Colour	-	Grey to medium grey powder
Specific Gravity	-	2.10 to 2.40
Bulk Density	-	500 to 700 kg/m ³
Chemical Requirements		
Silicon Dioxide (SiO ₂)	-	Minimum 85%
Moisture Content (H ₂ O)	-	Maximum 3%
Loss on Ignition (LOI)	-	Maximum 6%
Physical Requirements		
Specific Surface Area	-	Minimum 15 m ² /g
Pozzolanic Activity Index, 7 days	-	Maximum 105% of control
Over size particles retained on 45 micron sieve	-	Maximum 10%

COMPATIBILITY	<p>MegaAdd MS(D) is suitable for use with all types of cement and cementitious materials.</p> <p>With Admixtures :</p> <p>MegaAdd MS(D) is compatible to use with all types of water reducing plasticisers / superplasticisers and poly carboxylate based superplasticiser.</p>
DOSAGE	The normal dosage of MegaAdd MS(D) is 5 - 8% by weight of cement, but it can be used up to 10%. Site trials should be carried out to establish the optimum dosage for the mix to be used as the dosage varies depending on application.

Construction Chemicals



MegaAdd MS(D)

BATCHING	Batch MegaAdd MS(D) into the concrete mixer and mix thoroughly with the other mixture ingredients, adopting a procedure that ensures full dispersion of the product.	
PACK SIZE	600 Kgs and 1200 Kgs Jumbo bags	
GENERAL INFORMATION	Shelf Life	12 months from date of manufacture when stored under warehouse conditions in original unopened packing. Extreme temperature / humidity may reduce shelf life.
	Cleaning	Clean all equipments and tools with water immediately after use.
HEALTH and SAFETY	PPE's	Gloves, goggles and suitable mask must be worn.
	Precautions	Contact with skin, eyes, etc. must be avoided.
	Hazard	Regarded as non-hazardous for transportation.
	Disposal	Do not reuse bags. To be disposed off as per local rules and regulations.
	Additional Information	Refer MSDS. (Available on request.)
TECHNICAL SERVICE	CONMIX Technical Services are available on request for onsite support to assist in the correct use of its products.	



IMSASA
Construction Solutions for Africa

CAPE TOWN
Tel: +27 (0)87 231 0253
Unit 5 | M5 Freeway Park
Upper Camp Rd | Maitland | 7405
Cape Town | South Africa

JOHANNESBURG
Tel: +27 (0)82 785 8529
64 Maple Street | Pomona
Kempton Park | Johannesburg | 1619
South Africa

Email: info@msasa.co.za | www.msasa.co.za

Manufacturer:
CONMIX LTD.
P.O. Box 5936, Sharjah
United Arab Emirates
Tel: +971 6 5314155
Fax: +971 6 5314332
Email: conmix@conmix.com

Sales Office:
Tel: +971 6 5682422
Fax: +971 6 5681442
www.conmix.com



It is the customer's responsibility to satisfy themselves by checking with the company whether information is still current at the time of use. The customer must be satisfied that the product is suitable for the use intended. All products comply with the properties shown on current data sheets. However, Conmix does not warrant or guarantee the installation of the products as it does not have any control over installation or end use of the product. All information and particularly the recommendations relating to application and end use are given in good faith. The products are guaranteed against any manufacturing defects and are sold subject to Conmix standard terms and conditions of sale.

APPENDIX - C

Data

$$f_y = 495 \text{ MPa} \quad f'_{c_{\text{avg}}} = 84 \text{ MPa}$$

$$\text{Column dimension (C)} = 150 \times 150 \text{ mm}$$

$$t_s(h) = 100 \text{ mm} \quad \text{L.L} = 4.5 \text{ kN/m}^2 \quad \text{F.C} = 1.5 \text{ kN/m}^2$$

$$A_s \text{ bar} = \frac{\pi}{4} d^2 = \frac{\pi \times 100}{4} = 78.5 \text{ mm}^2$$

$$d = h - \text{cover} - \frac{db}{2} = 100 - 20 - \frac{10}{2} = 75 \text{ mm}$$

$$\rho_{\text{max}} = 0.75 \times \rho_b = 0.75 \times 0.06403 = 0.048$$

$$\rho_b = 0.85 \times \beta_1 \times \frac{f'_c}{f_y} \times \frac{600}{600 + f_y} = 0.06403$$

$$f'_c > 28 \text{ MPa} \rightarrow \beta_1 = 0.85 - 0.005 \times \frac{f'_c - 28}{7} = 0.81 > 0.65 \text{ ok}$$

$$\rho_{\text{min}} = \frac{0.0018 \times 420}{f_y} \text{ for } f_y > 420 \text{ MPa}$$

$$\rho_{\text{min}} = \frac{0.0018 \times 420}{495} = 0.00153$$

Long span:

$$A_s \text{ total} = \frac{A_s \text{ bar} \times 1500}{\text{spacing}} = \frac{78.5 \times 1500}{100} = 1177.5 \text{ mm}^2$$

$$\rho = \frac{A_s \text{ total}}{b \times d} = \frac{1177.5}{1500 \times 75} = 0.0105$$

$\rho > \rho_{\text{min}}$ and $\rho < \rho_{\text{max}}$ ok

$$a = \frac{A_s \times f_y}{0.85 \times f'_c \times b} = \frac{1177.5 \times 495}{0.85 \times 84 \times 1500} = 5.44 \text{ mm}$$

$$\text{No. of bars} = \frac{A_s \text{ required}}{A_s \text{ one bar}} = \frac{1177.5}{78.5} = 15 \text{ bars}$$

In this long span (15 \emptyset 10) bars will be used

$$\text{Spacing (S)} = \frac{A_s \text{ total}}{\text{No. of bars}} = \frac{1177.5}{15} = 100 \text{ mm ok}$$

$$M_n = A_s \times f_y \left(d - \frac{a}{2}\right) \times 10^{-6} = 1177.5 \times 495 (75 - 2.72) \times 10^{-6} = 42.1 \text{ kN.m}$$

Short span:

$$A_s \text{ total} = \frac{AS \text{ bar} \times 1100}{\text{spacing}} = \frac{78.5 \times 1100}{100} = 863.5 \text{ mm}^2$$

$$\rho = \frac{AS \text{ total}}{b \times d} = \frac{863.5}{1100 \times 75} = 0.0105$$

$\rho > \rho \text{ min}$ and $\rho < \rho \text{ max}$ ok

$$a = \frac{As \times fy}{0.85 \times f'c \times b} = \frac{863.5 \times 495}{0.85 \times 84 \times 1100} = 5.44 \text{ mm}$$

$$\text{No. of bars} = \frac{As \text{ required}}{As \text{ one bar}} = \frac{863.5}{78.5} = 11 \text{ bars}$$

In this short span (11Ø10)bars will be used

$$\text{Spacing (S)} = \frac{As \text{ total}}{\text{No. of bars}} = \frac{863.5}{11} = 80 \text{ mm use } 100 \text{ mm}$$

$$M_n = As \times fy \left(d - \frac{a}{2}\right) \times 10^{-6} = 863.5 \times 495 (75 - 2.72) \times 10^{-6} = 30.9 \text{ kN. m}$$

Now, finding the relation between P and M by using yield line theory:

$$\text{External work} = P \times \delta \times \theta$$

$$\text{Internal work} = m \times a \times \theta \quad b = \text{long direction}$$

$$\sum \text{Internal work} = m^+ \times b \times \frac{\delta}{2} = 2m^+ \times \delta$$

$$\sum \text{Internal work} = 4 \times 2 \times m^+ \times \delta$$

$$\sum \text{Internal work} = \sum \text{External work}$$

$$8m^+ \times \delta = P \times \delta \rightarrow P = 8m^+$$

$$\text{Long span} = 8 \times 42.1 = 337.8 \text{ kN}$$

$$\text{Short span} = 8 \times 30.9 = 247.2 \text{ kN}$$

Punching Shear Calculations

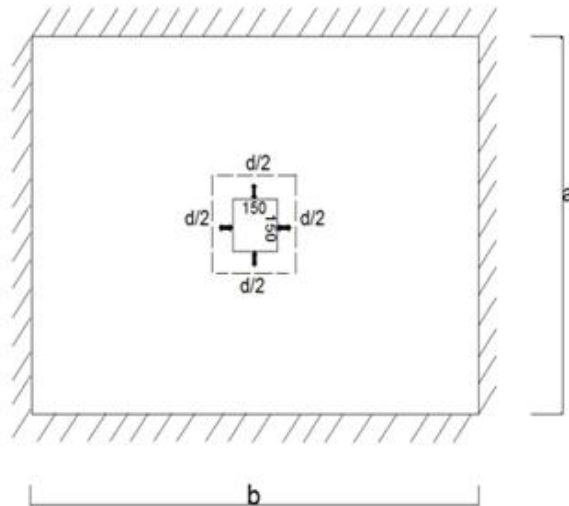
$$V_c = \frac{1}{3} \times \sqrt{f'c} \times b_o \times d \times 10^{-3}$$

$$b_o = 4 \times (c+d) = 4 \times (150+75) = 900 \text{ mm}$$

$$V_c = 0.333 \times \sqrt{84} \times 900 \times 75 \times 10^{-3} = 206 \text{ kN}$$

$$V_c = 206 \text{ kN} < P = 337.8 \text{ kN and } P = 247.2 \text{ kN}$$

∗Punching shear failure occurs before flexural failure



Shear Reinforcement calculation

$$V_c = 0.33 \times \lambda \times \sqrt{f_c} \quad \lambda = 1$$

$$V_c = 0.33 \times 1 \times \sqrt{84} = 3.03 \text{ MPa}$$

$$V_u = W_u \times A_p$$

$$W_u = 1.4DL + 1.7LL = 1.4(\gamma \times t_s + F.L) + 1.7 \times LL = 1.4(25 \times 0.1 + 1.5) + 1.7 \times 4.5$$

$$W_u = 13.5 \text{ kN/m}^2$$

$$V_u = 13.5 \times (1.5 \times 1.1 - 0.225 \times 0.225) = 21.6 \text{ kN}$$

$$V_{ug} = \frac{V_u \times 1000}{b \times d} = \frac{21.6 \times 1000}{900 \times 75} = 0.32 \text{ MPa}$$

$$\phi V_c > V_{ug} \quad V_c = 0.75 \times 3.03 = 2.3$$

Ok safe $2.3 > 0.32$ * Without shear reinforcement

Design Group B

$$A_s \text{ bar} = \frac{\pi}{4} d^2 = \frac{\pi \times 100}{4} = 78.5 \text{ mm}^2$$

$$d = h - \text{cover} - \frac{db}{2} = 100 - 20 - \frac{10}{2} = 75 \text{ mm}$$

$$\rho_{\max} = 0.75 \times \rho_b = 0.75 \times 0.06403 = 0.048$$

$$\rho_b = 0.85 \times \beta_1 \times \frac{f'_c}{f_y} \times \frac{600}{600 + f_y} = 0.06403$$

$$f'_c > 28 \text{ MPa} \rightarrow \beta_1 = 0.85 - 0.005 \times \frac{f'_c - 28}{7} = 0.81 > 0.65 \text{ ok}$$

$$\rho_{\min} = \frac{0.0018 \times 420}{f_y} \text{ for } f_y > 420 \text{ MPa}$$

$$\rho_{\min} = \frac{0.0018 \times 420}{495} = 0.00153$$

Long span:

$$A_s \text{ total} = \frac{A_s \text{ bar} \times 1800}{\text{spacing}} = \frac{78.5 \times 1800}{100} = 1413 \text{ mm}^2$$

$$\rho = \frac{A_s \text{ total}}{b \times d} = \frac{1413}{1800 \times 75} = 0.0105$$

$\rho > \rho_{\min}$ and $\rho < \rho_{\max}$ ok

$$a = \frac{A_s \times f_y}{0.85 \times f'_c \times b} = \frac{1413 \times 495}{0.85 \times 84 \times 1800} = 5.44 \text{ mm}$$

$$\text{No. of bars} = \frac{A_s \text{ required}}{A_s \text{ one bar}} = \frac{1413}{78.5} = 18 \text{ bars}$$

In this long span (18Ø10) bars will be used

$$\text{Spacing (S)} = \frac{A_s \text{ total}}{\text{No. of bars}} = \frac{1413}{15} = 100 \text{ mm ok}$$

Short span:

$$A_s \text{ total} = \frac{A_s \text{ bar} \times 1100}{\text{spacing}} = \frac{78.5 \times 1100}{100} = 863.5 \text{ mm}^2$$

$$\rho = \frac{A_s \text{ total}}{b \times d} = \frac{863.5}{1100 \times 75} = 0.0105$$

$\rho > \rho_{\min}$ and $\rho < \rho_{\max}$ ok

$$a = \frac{A_s \times f_y}{0.85 \times f'_c \times b} = \frac{863.5 \times 495}{0.85 \times 84 \times 1100} = 5.44 \text{ mm}$$

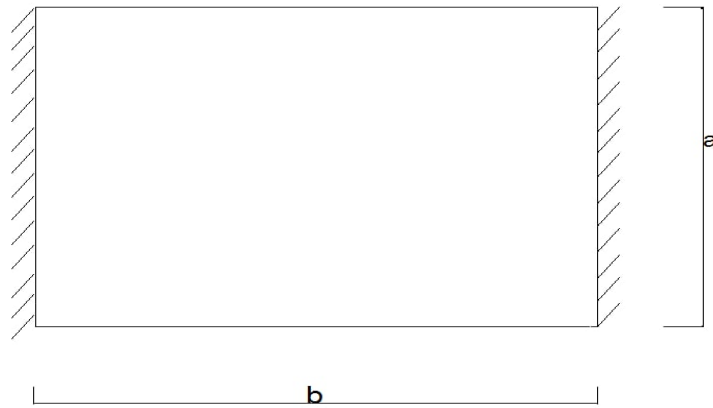
$$\text{No. of bars} = \frac{A_s \text{ required}}{A_s \text{ one bar}} = \frac{863.5}{78.5} = 11 \text{ bars}$$

APPENDIX - C

In this short span (11Ø10)bars will be used

$$\text{Spacing } (S) = \frac{A_s \text{ total}}{\text{No. of bars}} = \frac{863.5}{11} = 80 \text{ mm use 100 mm}$$

$$M_n = A_s \times f_y \left(d - \frac{a}{2}\right) \times 10^{-6} = 863.5 \times 495 (75 - 2.72) \times 10^{-6} = 30.9 \text{ kN. m}$$





جمهورية العراق
وزارة التعليم العالي والبحث العلمي
جامعة ميسان / كلية الهندسة
قسم الهندسة المدنية



سلوك البلاطات الخرسانية المسلحة بالألياف الفولاذية ذات الفتحات

رسالة

مقدمة الى كلية الهندسة في جامعه ميسان

كجزء من متطلبات الحصول على درجة الماجستير في علوم الهندسة المدنية / الإنشاءات

من قبل

مرتضى دفار عبدالرضا

بكالوريوس هندسة مدنية ٢٠١٤

بإشراف

الاستاذ المساعد الدكتور

سامر محمد جاسب

ايار ٢٠٢١

الخلاصة

أحد المتطلبات الرئيسية لتعزيز الهياكل الخرسانية المسلحة الحالية هو زيادة قدرات أعضائها على تحمل الأحمال المتوقعة الأكبر. هناك تقنيات مختلفة لزيادة سعة الألواح الموجودة ؛ ومع ذلك ، تختلف هذه التقنيات في المزايا والعيوب. الهدف الرئيسي من هذه الدراسة هو فحص كفاءة خرسانة المسلحة بالألياف الفولاذية لتقوية المسطح الخرساني ذات فتحات قريبه عن الدعامة.

كانت المتغيرات الرئيسية التي تم أخذها في الاعتبار في الدراسة التجريبية هي نسبة ألياف الصلب ، موقع الفتحات ، شكل الفتحات ، عدد الفتحات. أثرت زيادة نسبة الألياف الفولاذية المعقوفة (0.5 ، 1 ، 1.5 ، و 2%) وتأثير الفتحات على قدرة تحمل الحمولة لكل من قص التقيب وألواح الانحناء. فيما يتعلق بألواح القص المسطحة ، فإن وجود الفتح يعيد توزيع الضغوط التي أظهرت التركيز في زوايا الفتحة وحول العمود الأوسط. أثر وجود الفتح على حمل التكسير الذي انخفض بنسبة (47.4%) حيث ظهرت التشققات بنسبة (27.35%) بلاطة التحكم الصلبة عندما انخفضت إلى (13%) للمجموعة (A1) التي تحتوي على نسبة الالياف فولاذية 1% ($f'c=81.4$ MPa) هذه المجموعة تحتوي على فتحتين زوايا البلاطة. فيما يتعلق بشكل الفتحات ، لم يكن تأثير أشكال الفتحات مهماً بسبب مواقع الفتحات البعيدة عن المنطقة الحرجة. فيما يتعلق بموقع الفتحات وأرقامها ، فإن تأثير هذين المتغيرين هو التأثير الأكبر على السلوك العام للبلاطة الخرسانية خاصة على الإزاحة. المجموعة (A3)، التي تحتوي على نسبة الالياف فولاذية 2% ($f'c=91.7$ MPa). مصنعة بأربع فتحات أقصى إزاحة و حمل أعلى من لوح التحكم بنسبة (61.42% و 11.13%). بدت الزيادة في الإزاحة كبيرة مع تصنيع المزيد من الفتحات التي يكون الفرق بين لوحتي الفتحتين (A1) وأربع فتحات (A3) هو ببساطة اختلاف بسيط في القوة وفرق كبير في الإزاحة. التي تضمنت زيادة ألياف الصلب من (0.5%) إلى (2%) والتي كشفت عن التعويض في الخسارة التي حدثت في الصلابة وامتصاص الطاقة والليونة وسعة الحمل القصوى .

فيما يتعلق بعينات الانحناء ، يتأثر سلوك الانحناء باستخدام ألياف فولاذية بنسب متعددة ووجود فتحات. ظهر تأثير الوجود الفتحات على السلوك لكن هذا التأثير تراوح من متوسط إلى مرتفع حسب الموقع وعدد الفتحات. ظهر الحمل عند مرحلة التكسير عند (30.5%) تقريباً وارتفع إلى (88%) بعد زيادة الألياف الفولاذية مع عمل فتحات بالقرب لوح الزاوية المجموعة (B1) الالياف فولاذية 1% ($f'c=81.4$ MPa). كانت مقاومة الانحناء لعينات الألواح التي تم تصنيعها بالفتحات أعلى من تلك المصممة بسبب وجود الألياف الفولاذية التي تستعيد هذه الألياف فقدان القوة بسبب وجود الفتحات. لم يكن الفرق بين أشكال الفتحة من حيث الحمل والانحراف كبيراً نظراً لصغر حجم الفتحة بجانب الموقع الذي تم وضعه بعيداً عن المنطقة الحرجة. فيما يتعلق بموقع الفتحات وأرقامها ، فإن تأثير هذين المتغيرين هو التأثير الأكبر على سلوك الانحناء للبلاطة الخرسانية. المجموعة (B3)، التي تحتوي على نسبة الالياف فولاذية 2% ($f'c=91.7$ Mpa). مصنعة بأربع فتحات وألياف فولاذية بنسبة (2%). تم الحصول على الحمل النهائي بمقدار 255) وهو أعلى من

(48%) وانحرف بنسبة 61%) أعلى من لوح التحكم. الزيادة في نسبة ألياف الصلب من 0.5% إلى 2% عوضت خسارة القوة المتوقعة بسبب وجود الفتحات واكتسبت تعزيزاً إضافياً للقوة. بدت الزيادة في الإزاحة. المزيد من الألياف الفولاذية تسدد الخسارة التي حدثت مع تحقيق المزيد من الترقية في السعة الانحناء. وتجدر الإشارة إلى أن التباين في شكل الفتحات له تأثير ضئيل على قدرة الانثناء التي كانت بنسبة (43.3%) لكنها أثرت على الإزاحة بشكل كبير. العامل الأكثر تأثيراً هو عدد الفتحات وموقعها حيث أدى نقل الفتحتين إلى المنطقة الوسطى من البلاطة إلى تقليل حمل التكسير بمتوسط (35.5%) تقريباً عند مقارنته بنماذج فتحات الزاوية.